Order Number 9136076

Diode laser kinetic spectroscopy

Unfried, Kenneth Gary, Ph.D.

Rice University, 1991

U·M·I
300 N. Zeeb Rd.
Ann Arbor, MI 48106

RICE UNIVERSITY

DIODE LASER KINETIC SPECTROSCOPY

by

KENNETH GARY UNFRIED

A THESIS SUBMITTED IN PARTIAL FULFILLMENT OF THE REQUIREMENTS FOR THE DEGREE

DOCTOR OF PHILOSOPHY

APPROVED, THESIS COMMITTEE

Robert Curl

Dr. R. F. Curl, Professor of Chemistry, Chairman

G. P. Glass

Dr. G. P. Glass, Professor of Chemistry

F. B. Dunning

Dr. F. B. Dunning, Professor of Space Physics

Houston Texas

April 1991

ABSTRACT

High resolution infrared diode laser kinetic spectroscopy has been used to study reaction kinetics and spectroscopy of short-lived species. These unstable molecules were produced in a flowing system by excimer laser photolysis of suitable precursors. Their concentrations were monitored using an infrared diode laser with fast InSb detectors. Time resolution of better than 1μs was achieved.

HNO production is predicted by the reaction sequence $NH_2 + NO \rightarrow HN_2 + OH$, $HN_2 + NO \rightarrow HNO + N_2$ in the Miller mechanism for the thermal deNOx process. A search was made for the HNO molecule in the reaction system NH_2+NO at room temperature using diode laser infrared kinetic spectroscopy to search for NH stretch absorptions of HNO. No HNO attributable to the deNOx process was observed. Sensitivity calibration measurements using known amounts of HNO produced from the reaction of HCO with NO were used to set an upper bound of 1% for the conversion of NH_2 into HNO.

The high resolution infrared spectrum of the heavy atom antisymmetric stretch of the ketenyl radical (HCCO) was observed by means of infrared kinetic spectroscopy. Ketenyl was produced by 193 nm photolysis of ketene. The resulting transient absorption was probed with an infrared diode laser. Individual rovibrational transitions have been identified and molecular parameters have

been determined from a least-squares fit of the data. The band origin is located near 2023 cm^{-1}.

Acquisition of ketenyl infrared spectra allowed for determination of reaction rate constants by directly observing ketenyl decay. Kinetic studies of the ketenyl radical's reaction with nitric oxide, oxygen, acetylene and ethylene were conducted. A second order rate constant of $4.4(10)x10^{-11}$ $cm^3molecule^{-1}s^{-1}$ was obtained for the reaction with NO and a second order constant of $6.5x10^{-13}$ $cm^3molecule^{-1}s^{-1}$ was obtained for the reaction with O_2. Acetylene appeared not to react with the ketenyl radical. An upper limit of $3.8x10^{-13}$ $cm^3molecule^{-1}s^{-1}$ for the rate constant was determined by measuring the ketenyl decay in the presence of acetylene. The addition of ethylene appeared to slow the ketenyl decay. This behavior was attributed to the reaction of ethylene with a chemical species (probably H atoms) responsible for depletion of ketenyl.

ACKNOWLEDGEMENTS

I would like to express my appreciation to my advisor, Dr. Robert Curl who provided financial support, direction and much assistance in this research. His efforts made this work possible. I also want to thank Dr. Graham Glass for his help with reaction kinetics and Dr. Kermit Murray for his help obtaining the ketenyl kinetic data.

I especially want to thank my wife, Sarah Unfried, who postponed plans and made sacrifices to make this work possible, for her enduring support.

TABLE OF CONTENTS

LIST OF FIGURES

LIST OF TABLES

CHAPTER 1

INTRODUCTION

1.1 Kinetic Spectroscopy

In chemical reactions, reactants often don't form products directly, but form unstable, short-lived intermediates which react to form the products. Understanding the role and identity of these transient intermediates is important to understanding chemical reactions. The presence and importance of these intermediates has often been determined from the kinetic behavior of stable reactants and products. Direct observation is made difficult by the low steady state concentrations typically present during a reaction and the insignificant concentrations frequently remaining at the reaction's completion.

A useful technique for studying these unstable molecules is kinetic spectroscopy. With this technique large quantities of the unstable molecules are rapidly produced photolytically and are then spectroscopically probed. The sensitivity of this method is improved when intense photolysis sources are used (more unstable molecules are produced) along with intense probing sources (more signal to detect). In the experiments discussed here an ultraviolet excimer laser was used as the photolysis source and an infrared diode laser

with sensitive detectors spectroscopically probed the photolysis products.

Reactions can be studied by tuning the infrared probe laser to an absorption feature of a reactant or product and monitoring absorption as a function of time after initiating the reaction with the excimer laser. The time behavior of multiple products and reactants can be obtained by repeating the experiment, tuning the laser to an absorption of each of the products and reactants. From the transient absorption traces reaction rate constants and product yields can be determined.

Kinetic spectroscopy can also be used to obtain spectra of unstable molecules. To do so the frequency of the probe laser is stepped and the absorption is measured at a fixed time after the photolysis flash, repeating the photolysis at each frequency step. Thus, spectral features of unstable (and stable) products are detected by absorption of the probe laser beam. Since the concentration of the unstable species changes with time the spectrum obtained depends on the delay between the photolysis flash and absorption measurement. The resulting rovibrational spectrum can be used to monitor the species time behavior and can be analyzed to determine molecular parameters which provide information about the structure and bonding of the species observed.

In the work described here the infrared spectrum of the heavy atom antisymmetric stretch of the ketenyl radical was obtained and kinetic reaction behavior of ketenyl was studied. Also, the role, or

lack thereof, of the unstable species HNO in the thermal deNOx process was investigated by monitoring transient absorption of the species involved in the process and in a calibration reaction.

1.2 Diode Laser Spectrometer

The infrared diode laser is an ideal probing source because of the large number of molecules, stable and unstable, which absorb in the region of the infrared accessible with infrared diode lasers (3-30μm, this work was performed using the 3-6μm region). The diode laser has a narrow line width of ~10^{-4} cm^{-1} providing for Doppler limited resolution of molecular spectra.

The diode laser is a semiconductor in which lasing action results from transitions across the energy gap between the nearly empty conduction and nearly full valence bands. The laser is excited by applying a forward bias injection current which injects carriers across the p-n junction. Recombination of these carriers causes emission of a photon and is the gain mechanism for the diode laser.

The ends of the resonator cavity consist of the cleaved surfaces of the semiconductor crystal. Laser tuning is accomplished by changing the bandgap energy and the index of refraction, through changing the temperature. Temperature is controlled by directly heating the diode or by applying a current which results in I^2R heating. The infrared diode lasers used in this work typical had an output power of approximately 500 μW.

The apparatus, which is depicted in Fig. 1.1, has been described in detail elsewhere [1,2,3]. In these experiments the diode laser output was split into several beams, some of which were used to calibrate the laser frequency by observation of a reference spectrum and the transmission of two etalons. About one-half of the diode laser power was directed into the photolysis cell. This was a one meter IR multiple-pass (White) cell, with an IR path length of about 52m. The transmitted diode laser power was detected using a liquid nitrogen cooled InSb detector. The detector output was fed into a preamplifier, further amplified and collected by a transient digitizer interfaced to a computer. The computer was responsible for data acquisition as well as control of the applied diode laser current. Originally a DEC LSI-11 was used. It was replaced by a Compaq Deskpro386/25e (with math coprocessor, transient digitizer board-Markenrich Waag II, and A/D, D/A board-National Instruments AT-MIO-16). The excimer laser beam was directed into the multiple-pass cell through a CaF_2 window positioned directly below the D-mirrors of the White cell and was intercepted on the other end of the cell by a beam-block placed directly above the White cell notched mirror. This geometry resulted in an overlap region where the IR and UV beams intersected, in the middle third of the cell.

Figure 1.1

Schematic layout of the apparatus used in these experiments.

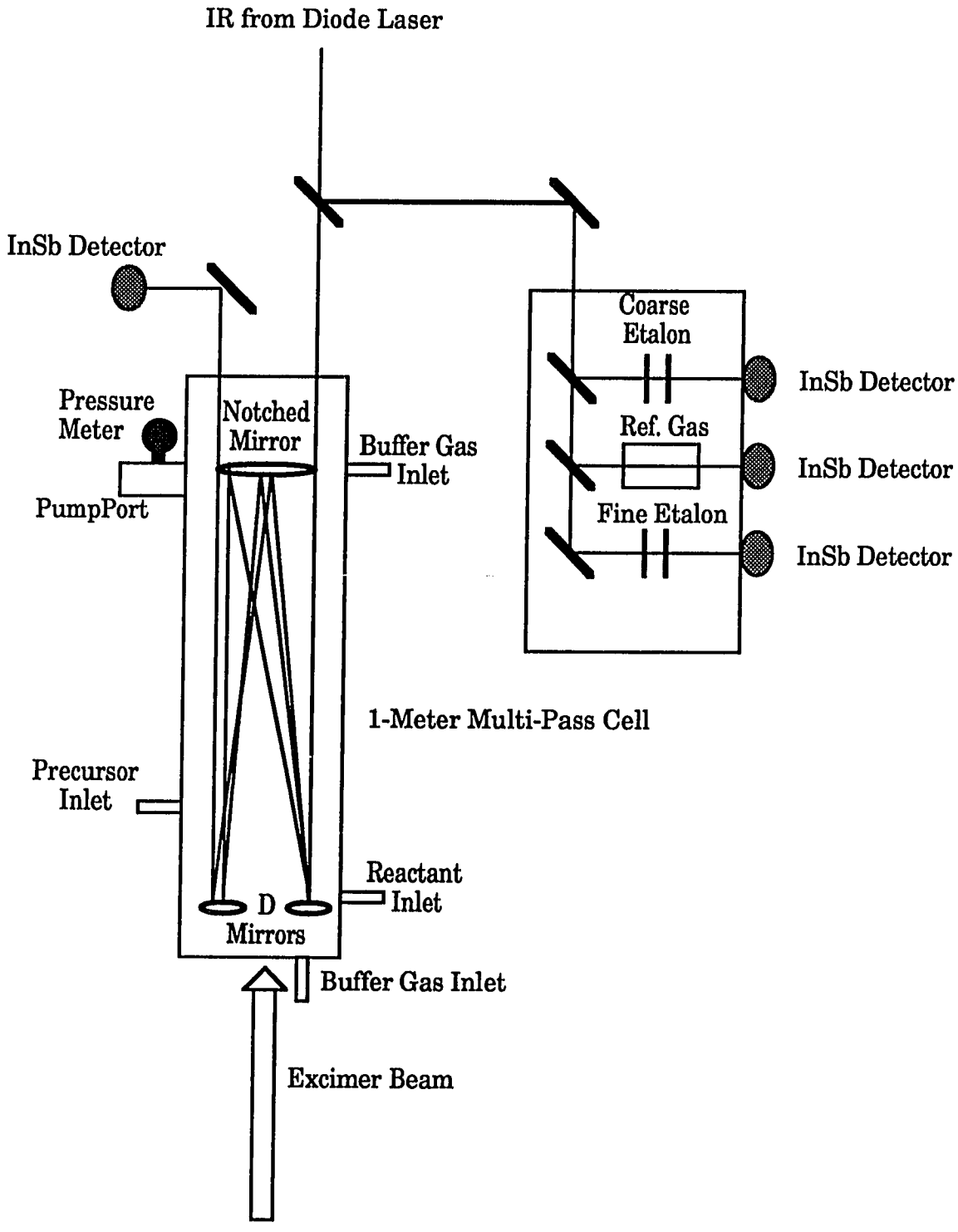
IR from Diode Laser
InSb Detector
Coarse
Etalon
InSb Detector
Pressure
Meter
Notched
Mirror
Buffer Gas
Inlet
Ref. Gas
InSb Detector
PumpPort
Fine Etalon
InSb Detector
1-Meter Multi-Pass Cell
Precursor
Inlet
Reactant
Inlet
D
Mirrors
Buffer Gas Inlet
Excimer Beam

CHAPTER 2

INVESTIGATION OF THE THERMAL DENOX PROCESS MECHANISM

2.1 Introduction

In the atmosphere, nitrogen oxides contribute to the creation of smog and acid rain. One method for reducing the emission of these pollutants by stationary sources such as electric power plants is the thermal $deNO_x$ process developed by Exxon [4]. In this process ammonia is added to the hot stack gases of the NOx emission source. It has been experimentally observed that the deNOx process works over the narrow temperature range between 875 and 1000 ^oC. If the temperature is too low, no significant NOx reduction is achieved and unreacted NH_3 is emitted as well as NOx. If the temperature is too high, the added NH_3 is converted to NO resulting in additional NOx emissions. A kinetic model explaining the temperature window and other observations has been developed by Miller and coworkers.[5]

Although the complete Miller reaction scheme involves many more reactions, the mechanism is dominated by the following reactions:

$$NH_3 + OH \rightarrow NH_2 + H_2O \quad (2.1)$$
$$NH_2 + NO \rightarrow H_2O + N_2 \quad (2.2a)$$
$$\rightarrow HN_2 + OH \quad (2.2b)$$
$$HN_2 + NO \rightarrow HNO + N_2 \quad (2.3)$$
$$HNO + M \rightarrow H + NO + M \quad (2.4)$$
$$H + O_2 \rightarrow OH + O \quad (2.5)$$
$$O + H_2O \rightarrow OH + OH \quad (2.6)$$
$$OH + HNO \rightarrow H_2O + NO \quad (2.7)$$
$$NH_2 + OH \rightarrow NH + H_2O \quad (2.8)$$
$$NH + O_2 \rightarrow HNO + O \quad (2.9)$$

The radical chain sequence (2.1)-(2.6) is self sustaining in the operating temperature regime if channel (2.2b) is at least 30% of reaction (2.2). At lower temperatures the activation energies of steps (2.4), (2.5), and (2.6) prevent the chain from propagating. At high temperatures steps (2.8) and (2.9) lead to the production of more NO. Chain branching (represented by (2.5) and (2.6)) is needed because the amount of NO removed is much greater than the amount of OH initially present.

HN_2 was introduced into the mechanism for two purposes. The first was to explain why H atoms were not observed [6,7,8,9] as a product of reaction (2.2) when the product OH was observed. [7,8,10] Secondly, at the time the mechanism was being developed, the branching ratio $k_{2.2b}/(k_{2.2a}+k_{2.2b})$ between channels (2.2a) and (2.2b) was thought [7,8] to be greater than 50%. With such a large branching ratio, the overall reaction scheme would become self-sustaining at too low a temperature if HN_2 produced by (2.2b) dissociated immediately into H atoms instead of reacting with NO to produce HNO via (2.3). However, more recent measurements of the

branching ratio [10,11,12,13] for reaction (2.2) are much lower, creating the opposite difficulty; namely, that the system is insufficiently self-sustaining, and, therefore, HN_2 stability has become less desirable.

It is very doubtful that HN_2 is sufficiently stable to play any role. Elaborate *ab initio* calculations [14,15] indicate that ground state HN_2 is unstable with respect to dissociation into H and N_2 with a lifetime of about 50 psec. As discussed above, a long-lived HN_2 may no longer be essential for explanation of the deNOx mechanism. However, if HN_2 is very short-lived or non-existent, why are H atoms not observed in the NH_2 + NO system when OH is almost [16] always observed? How else can OH be produced? If OH is being produced by some reaction other than that between NH_2 and NO, the Miller mechanism cannot work because it is the other product of (2.2b), i.e. HN_2 producing H atoms or HNO, that is driving the radical chain. Thus the possibility must be considered that some problem with the *ab initio* calculations caused the stability of HN_2 to be underestimated and that at room temperature reactions (2.2b) followed by (2.3) actually occur. Since those observations which failed to observe H atoms were never carried to temperatures as elevated as those where deNOx actually works, H rather than HN_2 could be produced at higher temperatures thus providing the chain branching H atoms needed to sustain the deNOx process. Therefore, it seems essential to decide whether (2.2b) plus (2.3) can explain the observations of OH but no H at room temperature. This possibility

was investigated by looking for the production of HNO using diode laser infrared kinetic spectroscopy.

2.2 Methodology

NH_2 was produced by excimer laser flash photolysis of NH_3 in the presence of NO and a rotational component of the NH stretch of HNO was monitored. To verify that the sensitivity is sufficient for this purpose, HNO was produced and calibrated by using the reaction scheme:

$$CF_2Cl_2 + h\nu\ (193\ \text{nm}) \rightarrow Cl + \ldots \tag{2.10}$$
$$Cl + H_2CO \rightarrow HCO + HCl \tag{2.11}$$
$$HCO + NO \rightarrow HNO + CO \tag{2.12}$$

The CO transient absorption from reaction (2.12) was compared with the H_2O transient absorption from reaction (2.2a) and the magnitude of the HNO signal expected from the deNOx process was calculated by using the signal observed from the HCO + NO reaction to calibrate our sensitivity to HNO.

The HNO signal expected from the reaction sequence (2.2b) plus (2.3) (the deNOx process) was calculated from the experimentally observed absorbances of CO and HNO produced by the HCO with NO reaction, the literature infrared cross sections for H_2O and CO, and the H_2O signal observed from the reaction of NH_2 with NO. The ratio of the HNO absorbance expected from the deNOx system to that produced from reaction (2.12) can be expressed as

$$\frac{(A_{HNO})_{2.2b+2.3}}{(A_{HNO})_{HCO}} = \frac{(2.2b)}{(2.2a)} \times \frac{\sigma_{CO}}{\sigma_{H_2O}} \times \frac{A_{H_2O}}{A_{CO}} \qquad (2.13)$$

Thus the absorbance of an H_2O line from the NH_2+NO reaction, the absorbance a CO line from the HCO+NO reaction, and the absorbance of HNO from HCO+NO must be measured to predict the HNO absorbance from (2.2b)+(2.3). The ratio (2.2b)/(2.2a) has been measured at room temperature many times with varying results. Here 0.15, a number consistent with the more recent measurements was used.

2.3 Experimental

In these experiments, the reagents were continuously flowed through the multiple pass infrared absorption cell described in Chapter 1 where one of the reagents was photolyzed by 193 nm (ArF) excimer laser pulses. Transient infrared absorptions by specific rovibrational transitions of species produced by chemical reactions initiated by the photolysis were observed using infrared laser diode probe sources. Frequency calibration was accomplished by sending part of the infrared beam through a 500 MHz etalon and a reference cell using various (CH_4, OCS, NO) reference gases.

As mentioned above, in order to provide intensity calibration, two sets of experiments were carried out: one on the model deNOx system and the other to provide a calibration HNO signal. The first system consisted of a mixture of 120 mTorr of NH_3 and 100 mTorr of

NO in a buffer of 20 Torr of He added to ensure thermal equilibrium and moderate the temperature rise following photolysis and reaction. The HNO calibration system consisted of a mixture of dichlorodifluoromethane (230 mTorr), formaldehyde (240 mTorr), and nitric oxide (100 mTorr) mixed in a helium buffer (20 Torr). At the flow rates used, the gas mixture in the cell was replenished approximately once every 15 to 20 seconds. Formaldehyde was produced by heating paraformaldehyde (95%) in flask using a heating mantel. (The tubing and valve connected to the flask were also heated to prevent repolymerization of the formaldehyde) All other gases were commercially obtained and had the following specified purities: He (99.995%), NO(99.0%), NH_3(99.99%), CCl_2F_2(99.9%). It should be noted that direct photolysis (193 nm) of methylformate to produce HCO was also successfully attempted. This HCO source was abandoned because methylformate has broad band absorptions which interfered with observation of CO which was necessary for the calibration.

Because the UV beam intersects the IR beam only in the middle of the cell, the product concentrations are not uniform throughout the region probed by the infrared beam. It is therefore important that the relative alignment of the UV and IR laser beams is similar for the two measurements on the same chemical system. Two different diode lasers were needed for each chemical system. Changing diodes required translation of the source collimating lens. Thus, the position and direction of these two infrared sources were

slightly different. However, this difference was minimal as evidenced by the very small adjustments need to maximize detector signal after switching diodes. The time required for a complete set of measurements was typically less than three hours. All gas flows could be made stable throughout an experiment including that of formaldehyde which polymerizes slowly. Note that a small variation in the formaldehyde partial pressure should not affect the size of the standard HNO signal because the limiting reagent in reaction (2.11) is the Cl produced by photolysis of CF_2Cl_2.

The magnitudes of the transient absorption signals and the total IR signals (obtained by chopping the total beam and acquiring the transient) were measured at the peak absorption frequencies. The transient absorption signals of all species being measured, H_2O, CO, and HNO, rose rapidly and reached a constant plateau level which was maintained for at least one millisecond. Measurement of these transient intensities were taken at a time approximately 500μs after the excimer flash. This time is far longer than the vibrational and rotational relaxation times of all species present in the system except for the CO vibrational relaxation time. The populations of vibrationally excited states of CO were relatively small: although transitions arising from $v=2 \leftarrow 1$ of CO were observed, their intensities were much smaller than similar rotational components of $v=1 \leftarrow 0$.

2.4 Observations

HNO was observed from the reaction of HCO with NO and is shown in Figs. 2.1, 2.3 and 2.4. Notice in Fig. 2.1 the decrease in the HNO absorbance immediately after the flash caused by photolysis of HNO produced in previous flashes. HNO reacts away very slowly and much is still present from the previous flashes when the excimer fires at the repetition rate of 20 Hz.

Clearly no HNO was produced at short times in the deNOx system as can be seen in Fig. 2.1. However, some HNO was produced on a longer time scale. In the NH_3 + NO system, HNO is produced by the relatively slow three body reaction of H, the other photolysis product of NH_3, with NO. Infrared absorption by this steady state concentration of HNO uncorrelated to the photolysis flash can be observed by diode laser frequency modulation detection as shown in Figure 2.2. To obtain frequency modulated absorption spectra, the diode was frequency modulated by about 50 MHz at 35 kHz and the White cell IR detector signal was sent to a 35 kHz lock-in amplifier followed by a analog to digital converter connected to the LSI 11 computer.

The concentration of HNO produced in this manner was larger when higher NO pressures were used and was detectable in transient absorption as a negative signal resulting from photolysis of HNO as shown in Figure 2.3. This low steady state concentration of HNO is probably faintly seen in Fig. 2.1 as the downward tendency after the

Figure 2.1

Transient absorption signals of HNO. The bold trace is the signal at 2632.8088 cm-1 observed from the reaction of NH_2 with NO. Pressures were as follows: He 19.6 Torr, NO 100 mTorr and NH_3 120 mTorr. The other trace is the standard HNO signal at the same frequency produced by the reaction of HCO with NO. Pressures were as follows: He 20.1 Torr, NO 100 mTorr, H_2CO 240 mTorr, and CCl_2F_2 230 mTorr. The excimer was fired at 20 Hz with about 150 mJ/pulse and the signals were averaged 2000 times.

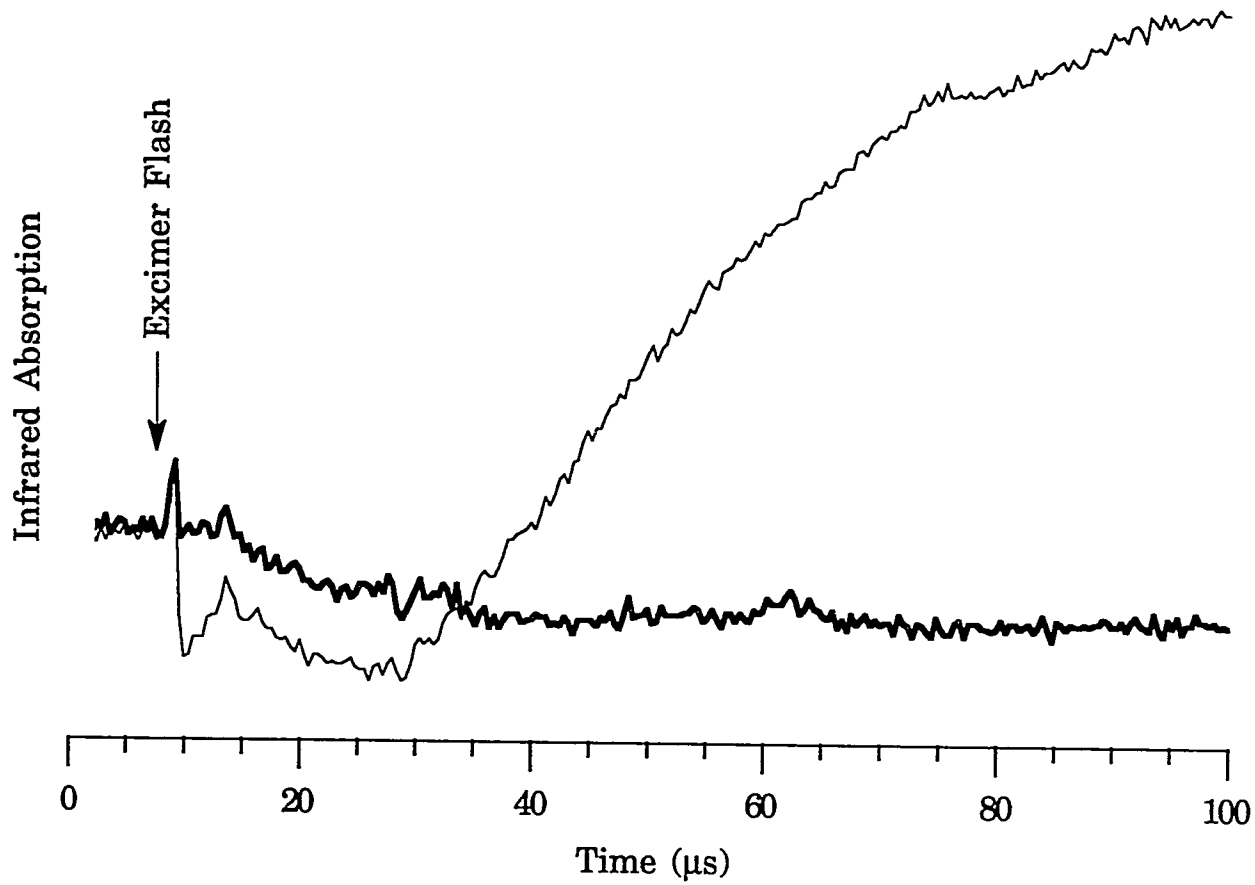
Infrared Absorption
Excimer Flash
0
20
40
60
80
100
Time (μs)

Figure 2.2

Frequency modulated absorption scans. Diode laser frequency was dithered at 35 kHz and scanned over the region shown from about 2632.6 to 2633.2 cm^{-1}. The amplified output of an InSb detector was fed into a lock-in detector to obtain the spectra shown. This was done for both the HCO system (top trace) and the deNOx system (bottom trace). For both the excimer laser was fired at 45 Hz. Data acquisition was uncorrelated with excimer laser timing. The absorptions complicating the HNO spectrum in the HCO system are due to formaldehyde. The dotted line is the spectrum obtained without photolysis. HNO line positions are marked with arrows. Note that between scans the lock-in amplifier phase changed by 180°.

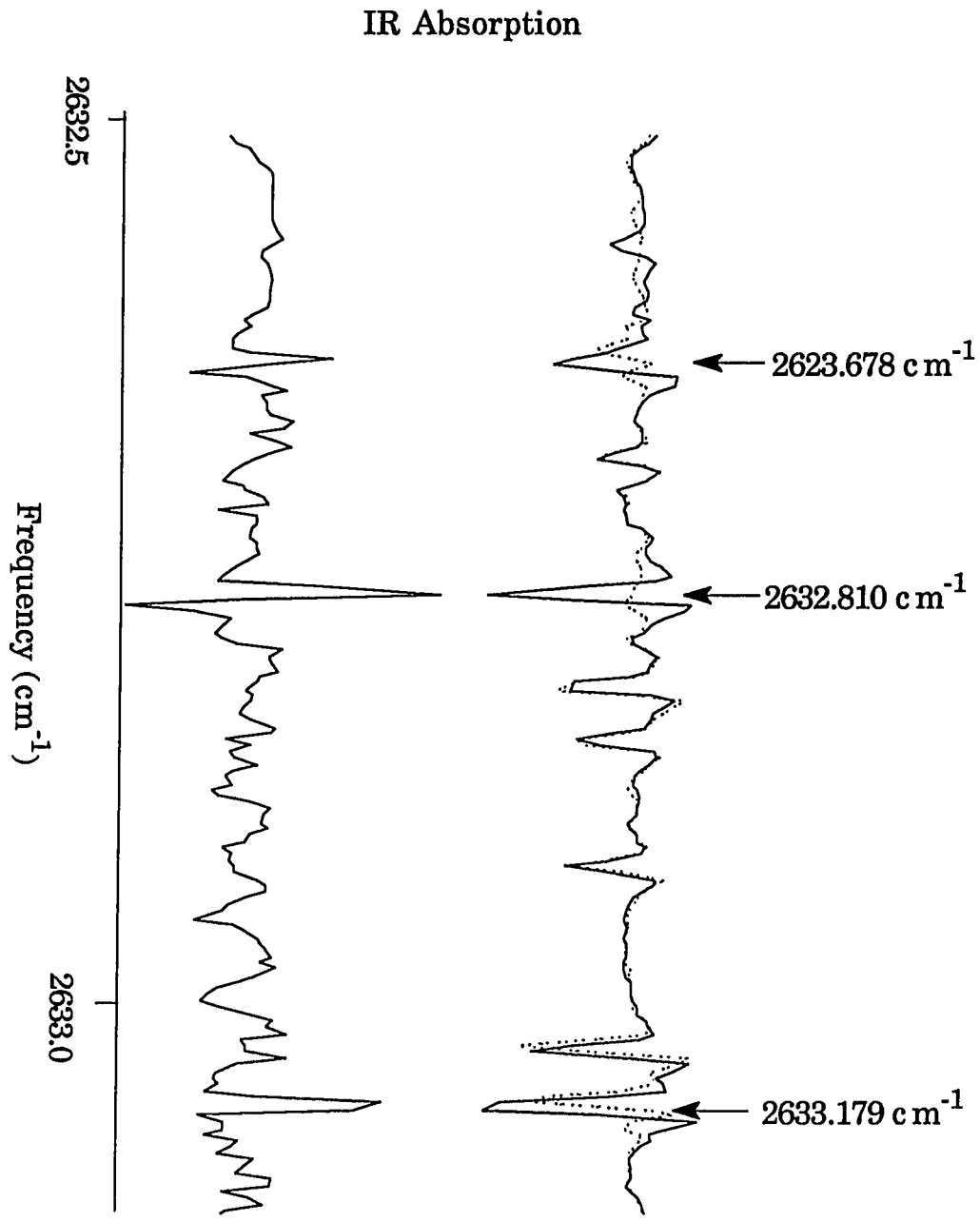
IR Absorption
2623.678 c m-1
2632.810 c m-1
2633.179 c m-1
2632.5
2633.0
Frequency (cm-1)

Figure 2.3

Transient absorption at the peak frequency 2632.8088 cm^{-1} of the HNO transition in the NH_2 + NO system with a higher NO concentration favoring the production of HNO by three body processes. Pressures were as follows: He 22.5 Torr, NO 2.7 Torr and NH_3 200 mTorr. For comparison the HNO signal from the HCO + NO reaction observed at the same frequency is included (upper trace). Pressures were as follows: He 23.8 Torr, NO 2.9 Torr, H_2CO 720 mTorr, and CCl_2F_2 1040 mT. For both traces the excimer laser was fired at 20 Hz with about 150 mJ/pulse and the signals were averaged 200 times.

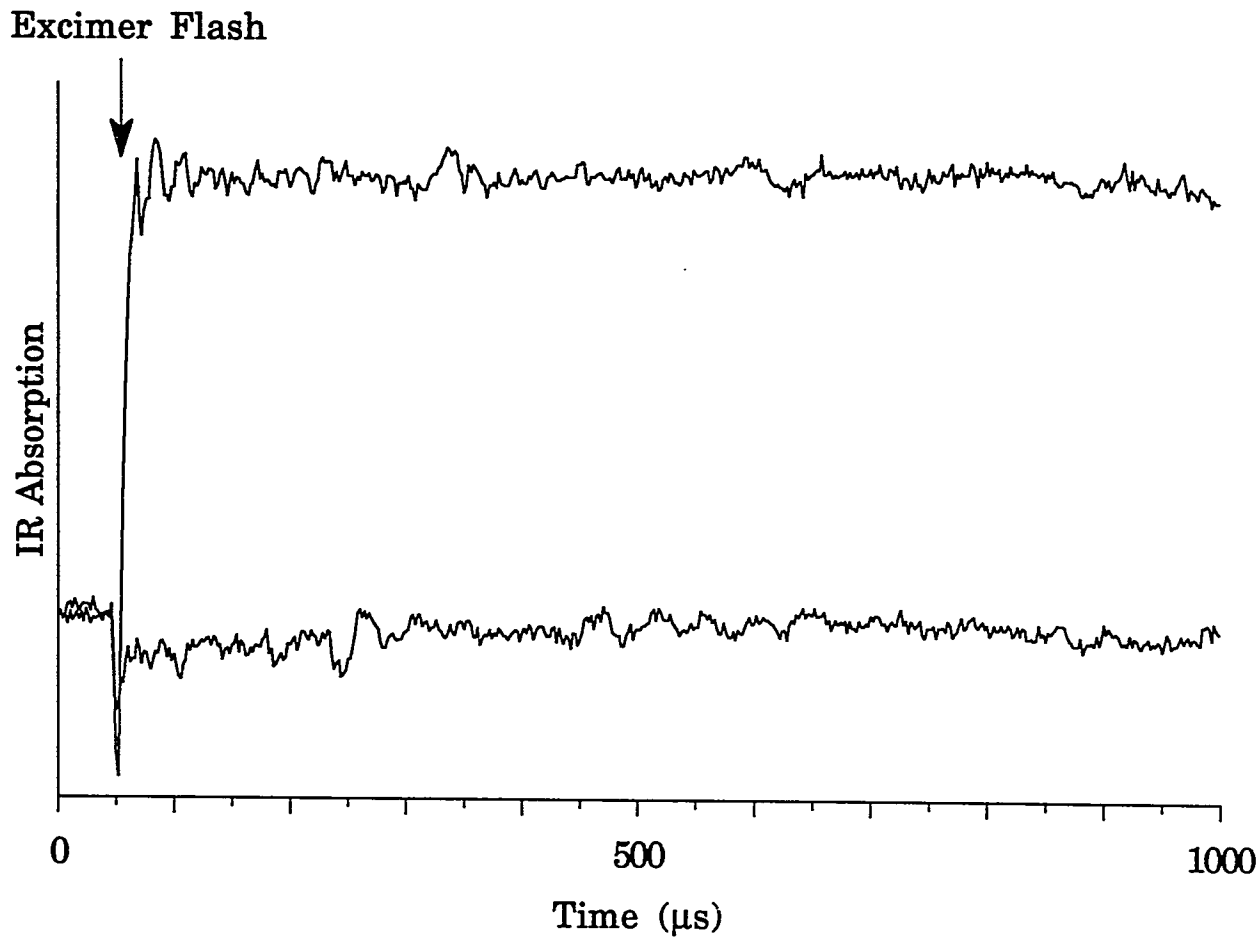
Excimer Flash
IR Absorption
0
500
1000
Time (μs)

flash at the HNO line position in the NH_3 + NO system. It should be noted that the HNO concentration produced from the reaction of H + NO was always considerably less than those typically produced by the reaction of NO with HCO.

To estimate the HNO signal expected from the sequence of reactions (2.2b) and (2.3), transient absorptions by H_2O in the NH_2+NO system and by CO in the HCO+NO system were measured. Because CO and H_2O are stable species, they are removed from the cell only by pumping. If their steady state concentration becomes too high, measurements of their absorption intensities become difficult because of total IR absorption (no light reaching the detector) or small transient diode frequency pulling over the absorption feature induced by excimer laser interference. Therefore, their transient absorptions were measured at very slow (1 Hz) pulse repetition rates. Fig. 2.4 shows all the transient signals involved in Eq. (2.13). Water is produced vibrationally hot by the NH_2 + NO reaction, and the transient water signal from the vibrational ground state in Fig. 2.4 shows an induction period. Any HNO signal from HN_2 + NO reaction would be expected to appear on the same or a slightly faster time scale since HN_2 would be produced at the same rate as $H_2O^{\dagger}$ and should react very rapidly with the NO.

Substituting the transient absorption data together with CO [17] and H_2O [18] literature absorption cross sections into Eq. (2.13), the HNO absorbance expected from channel (2.2b followed by 2.3) of the NH_2 + NO reaction can be calculated. Table 2.1 illustrates this

TABLE 2.1: CALCULATION OF THE HNO SIGNAL EXPECTED FROM REACTION 2.2B FOR FIG. 2.4

$(A_{HNO})_{HCO} \times 10^3$	6.1
A_{CO}	0.13
A_{H_2O}	0.031
σ_{CO} (cm^2)	4.06×10^{-17}
σ_{H_2O}(cm^2)	1.16×10^{-18}
Expected[a] $b(A_{HNO})_{2.2b} \times 10^3$	7.9
Expected $\frac{(A_{HNO})_{2.2b}}{(A_{HNO})_{HCO}}$	1.3

a) Assuming as noted that (2.2b)/(2.2a) branching ratio = 0.15

Figure 2.4

Transient absorption signals from the deNOx process and the calibration reaction. The scale for the HNO signal is percent absorption. The %Absorption for the H_2O and CO signals are larger and can obtained by dividing by the factors shown. For CO and HNO produced from the reaction of HCO with NO, pressures were as follows: He 20.1 Torr, NO 100 mTorr, H_2CO 240 mTorr, and CCl_2F_2 230 mTorr. HNO was monitored at 2633.8088 cm^{-1} and CO at 2090.6091 cm^{-1}. Pressures for the deNOx system were: He 19.6 Torr, NO 100 mTorr and NH_2 120 mTorr. HNO was observed at 2633.8088 cm^{-1} and H_2O was observed at 1837.1811 cm^{-1}. The excimer (~150 mJ/pulse) was fired at 20 Hz and the signals were averaged 2000 times each for the HNO traces; the repetition rate was 1 Hz and the signals were averaged 200 times each for the H_2O and CO traces.

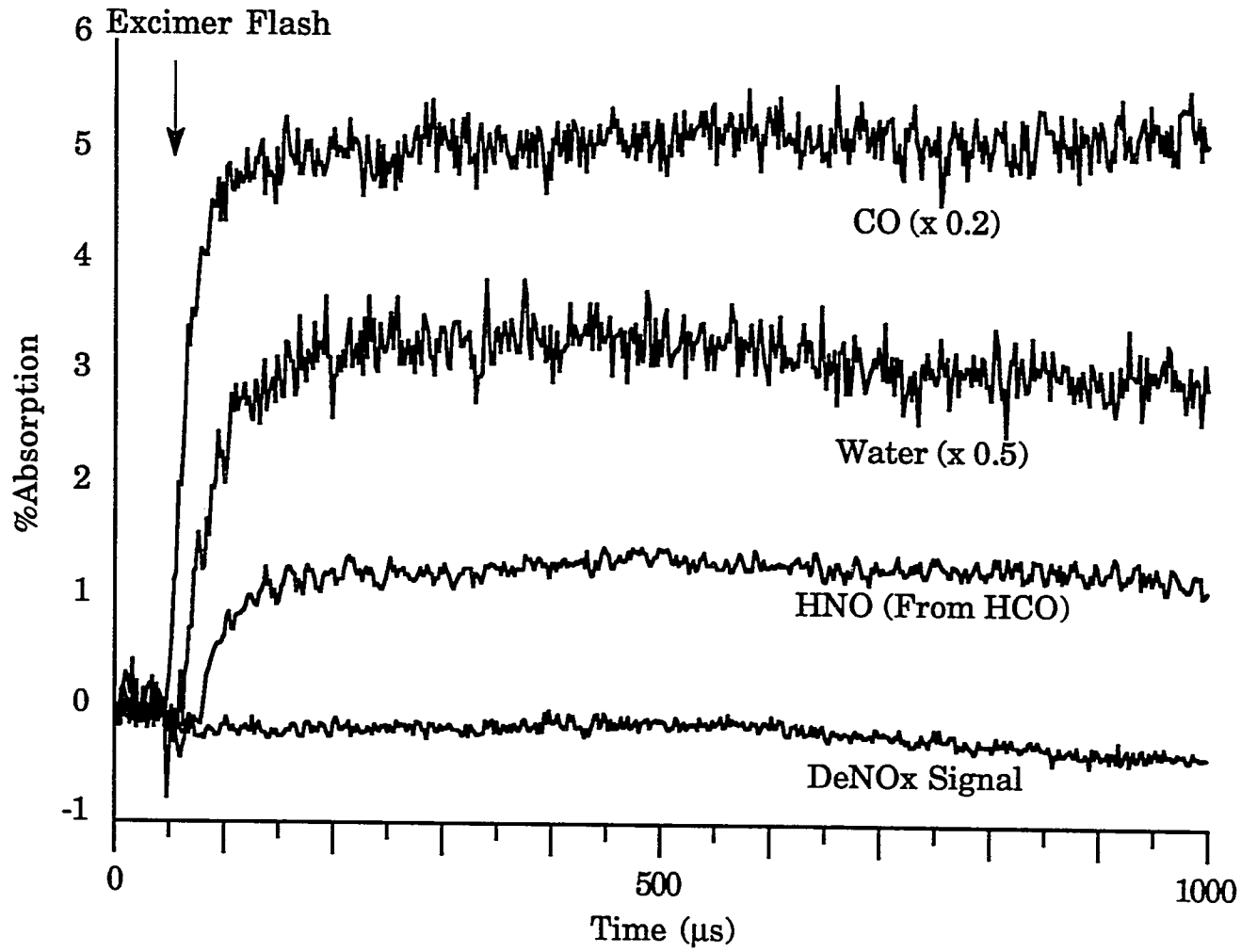
Excimer Flash
6
5
4
3
2
1
0
-1
%Absorption
CO (x 0.2)
Water (x 0.5)
HNO (From HCO)
DeNOx Signal
0
500
1000
Time (μs)

calculation for data corresponding to that shown in Figs. 2.1 and 2.4. The result of the calculation is that a signal approximately the same size as the HNO signal from HCO + NO, or about 40 times the observed noise, is predicted for the line labelled deNOx in Fig. 2.1 assuming the branching (2.2b)/(2.2a) is 0.15. Thus the upper limit of the HNO yield is reliably <1%.

2.5 Discussion

HNO was not observed in these experiments under conditions where HNO concentrations comparable to those expected for OH are easily observable. This absence of HNO establishes that the reaction sequence (2.2b) plus (2.3) is not significant at room temperature. Probably (2.3) would occur if HN_2 was present, and, therefore, it seems more likely to us that channel (2b) does not exist either because HN_2 is not produced or does not survive. Although the present observations are at room temperature rather than the elevated temperature of the Thermal deNOx process, it seems likely that HN_2 would be even less stable at elevated temperature.

Miller and Bowman [19] have recently discussed the effect of no HNO production on the Thermal deNOx mechanism in detail so that discussion here will be brief. Reaction (2.2a) is a radical sink. This means that some radical chain branching is required. Now the chain cannot be branched by reactions (2.5), and (2.6) through reaction

(2.4) because there is no HNO produced in the system, or by using the counterpart for unstable HN_2

$$NH_2 + NO \rightarrow N_2 + H + OH \tag{2.2c}$$

because there is no H produced in this system. Again the absence of H and thus (2.2c) has been demonstrated only at temperatures well below the deNOx operating temperature, but it seems unlikely that an entirely new channel producing OH is developing as the most recent branching ratio measurements [13] show weak dependence of OH yield on temperature. Thus a new scheme producing chain branching is required.

At present the source(s) of the OH observed in this system is unknown. It is possible that the observation of OH is an artifact of the laboratory methods used to produce NH_2. Thus Phillips has suggested [20] that NH is produced simultaneously with NH_2 via either

$$NH_2 + h\nu \rightarrow NH + H \tag{2.14}$$

for flash photolytic preparations of NH_2 or by

$$NH_2 + F \rightarrow HF + NH \tag{2.15}$$

for reactive flow experiments and reacts as follows:

$$NH + NO \rightarrow N_2 + OH \tag{2.16}$$

This would explain the wide range of OH yields from 13% to 65% measured [6,-8,10-13] for reaction (2.2) at room temperature, as the NH yield was not controlled in the various measurements. Further work is needed to explore this possibility.

CHAPTER 3

INFRARED FLASH KINETIC SPECTROSCOPY OF THE KETENYL RADICAL

3.1 Motivation

The ketenyl radical is important in hydrocarbon combustion since it is produced by the reaction of atomic oxygen with acetylene:

$$C_2H_2 + O \rightarrow HCCO + H \quad (3.1a)$$
$$\rightarrow CH_2 + CO \quad (3.1b)$$

In flames, hydrocarbon fuels are often at least partially pyrolyzed to acetylene prior to oxidation so that oxidation of acetylene has a general importance in hydrocarbon combustion.

The branching ratio of reaction (3.1) has been measured with estimates varying $0.1 \leq k_{3.1b}/k_{3.1} \leq 0.97$ [21]. However, recent measurements of the branching ratio appear to be in general agreement that (3.1a) forming ketenyl is approximately 70% of the total reaction between C_2H_2 and O and that the branching ratio is not very sensitive to temperature [22]. Thus substantial production of ketenyl radical via reaction (3.1a) is expected in hydrocarbon combustion.

In spite of ketenyl's importance in hydrocarbon combustion little is known of reactions destroying it. An understanding of these reactions is necessary if combustion is to be understood. A better understanding of the role of ketenyl in combustion may be obtained from the characterization of the reactions of ketenyl with the species present in the flame environment.

Because of the importance of ketenyl in combustion the observation of its infrared spectrum by diode laser kinetic spectroscopy was undertaken. The resulting high resolution infrared spectrum of ketenyl and use of the time behavior of ketenyl transient infrared absorptions to measure ketenyl reaction rate constants important in combustion are presented here.

3.2 Previous Work

The kinetic information concerning ketenyl reactions obtained prior to 1983 has been reviewed by Warnatz [23]. This information was mostly obtained through indirect observations. Since that time the only studies of reactions in which HCCO is a reactant have been carried out by Peeters, Schaekers, and Vinckier [21,24] who measured rates for the reactions HCCO + H and HCCO + O.

The microwave spectrum of ketenyl has been observed by Endo and Hirota [25], but there is little spectroscopic information in other wavelength regions. A previous report [26] of laser induced fluorescence has proved to be in error [27,28]. Jacox and Olson [29]

in a paper on C_2H reported a band at 2019.5 cm^{-1} which they believed to be ketenyl formed by reaction of O_2 in an argon matrix made by condensing Ar* and acetylene. Their surmise guided this work and proved to be correct. The high resolution infrared spectrum of the heavy atom antisymmetric stretch of the ketenyl radical (HCCO) with a band center near 2023 cm^{-1} is reported in this chapter. The kinetic behavior of ketenyl with species present in the combustion environment was also investigated and is described in Chapter 4.

3.3 Experimental

The experimental apparatus was described in Chapter 1. Ketene in a He buffer was flowed through the multipass IR (White) cell and photolyzed with an excimer laser (193 nm, ArF). For ketene production, He carrier gas was saturated with diketene by bubbling the He through diketene (98% Aldrich). The gas mixture then flowed through a 30 cm long vycor tube heated to 600°C (using four semicylindrical heating elements, Thermcraft model RL101, insulated with 2 square feet of $^1/_2$ inch blanket insulation and attached in series to a variable transformer), pyrolyzing the diketene to ketene. From here the ketene gas mixture flowed into the White cell. The helium was commercially obtained and had a specified purity of 99.995%. The total gas pressure was typically 25 torr and was controlled with a throttling valve between the cell and the vacuum

pump. Flow rates were such that gases were replenished about once every 25 seconds. Ketene pressure is estimated to have been typically 1 to 2 Torr (assuming complete pyrolysis of diketene and a diketene vapor pressure of about 10 Torr). Production of ketene was verified by comparison of normal absorption scans around 2149 cm^{-1} (Fig. 3.1) with previously observed ketene high resolution spectra [30].

The ketenyl spectrum was obtained by acquiring the infrared detector signal with a transient digitizer and taking the difference between before and after the excimer flash, stepping the diode laser probe frequency between flashes. Typical operation when using the Compaq computer for data acquisition was as follows: The transient digitizer acquired 436 points between 2.25 and 24 μs before the excimer flash. These points were averaged and subtracted from the average of 421 points taken between 2 and 23 μs after the flash. This process was repeated 10 times and the average of the 10 repetitions was stored at each frequency step. The excimer laser was operated at between 20 and 80 Hz. Scans were typically 1.5 cm^{-1} long and consisted of approximately 3000 frequency steps. Part of the infrared diode laser beam was split off and passed through a reference cell containing OCS or etalons which were used for frequency calibration.

The transient digitizer was triggered with the output from a photodiode (Hamamatsu model S1722-02) positioned above the UV beam block in the White cell which monitored reflected excimer

Figure 3.1

Normal absorption frequency scan over ketene lines near 2149 cm^{-1}. The upper trace is ketene produced from pyrolysis of diketene at 600°C and the lower ketene from acetone pyrolysis at 800°C. Ketene transitions are labeled for reference.

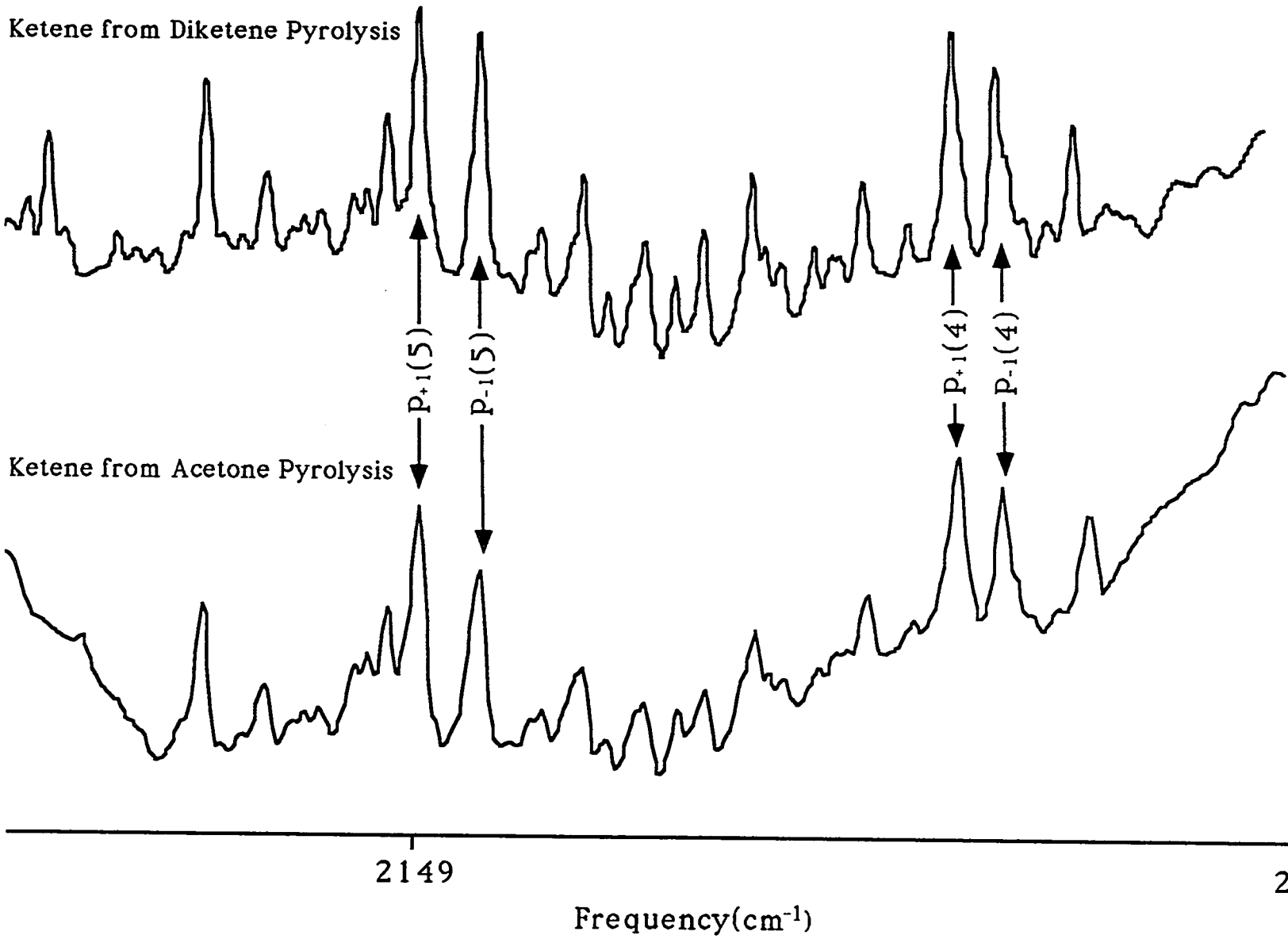
Ketene from Diketene Pyrolysis
Ketene from Acetone Pyrolysis
P+1(5)
P-1(5)
P+1(4)
P-1(4)
2149
2150
Frequency(cm-1)

output. This photodiode served to monitor excimer beam absorption in the White cell as well. A typical photodiode signal is displayed in the lower trace of Fig. 3.2. The signal has a rapid rise and a rapid fall followed by a slower tail. The rapid fall has been attributed to reflectance and the slow tail to fluorescence. Because of a crosstalk problem (trigger input on channel B affected data on channel A) this signal was converted into a shorter pulse seen in the upper trace of Fig. 3.2 (as short as the excimer interference spike) for triggering. The circuit for this conversion is displayed in Fig. 3.3.

3.4 Ketenyl Production

The initial intent was to produce HCCO by first photolyzing CCl_2F_2 to produce Cl atoms and have the Cl atoms abstract an H atom from ketene.

$$CF_2Cl_2 + h\nu \rightarrow ? + Cl \qquad (3.2)$$
$$Cl + H_2CCO \rightarrow HCl + HCCO \qquad (3.3)$$

Surprisingly, the ketenyl signals observed were much stronger if the CCl_2F_2 flow was turned off. Thus it appears that at 193 nm, a major photochemical channel directly producing ketenyl exists

$$H_2CCO + h\nu \rightarrow H + HCCO \qquad (3.4a)$$

in addition to the usual photochemical channel producing CH_2 and CO [31,32,33,34].

Figure 3.2

The lower trace shows a typical photodiode trace acquired with the transient digitizer. The photodiode is placed above the excimer laser beam block in the White Cell where it receives reflected excimer output. This signal is used to monitor UV absorption in the White Cell and when electronically shortened as shown in the upper trace to trigger the transient digitizer.

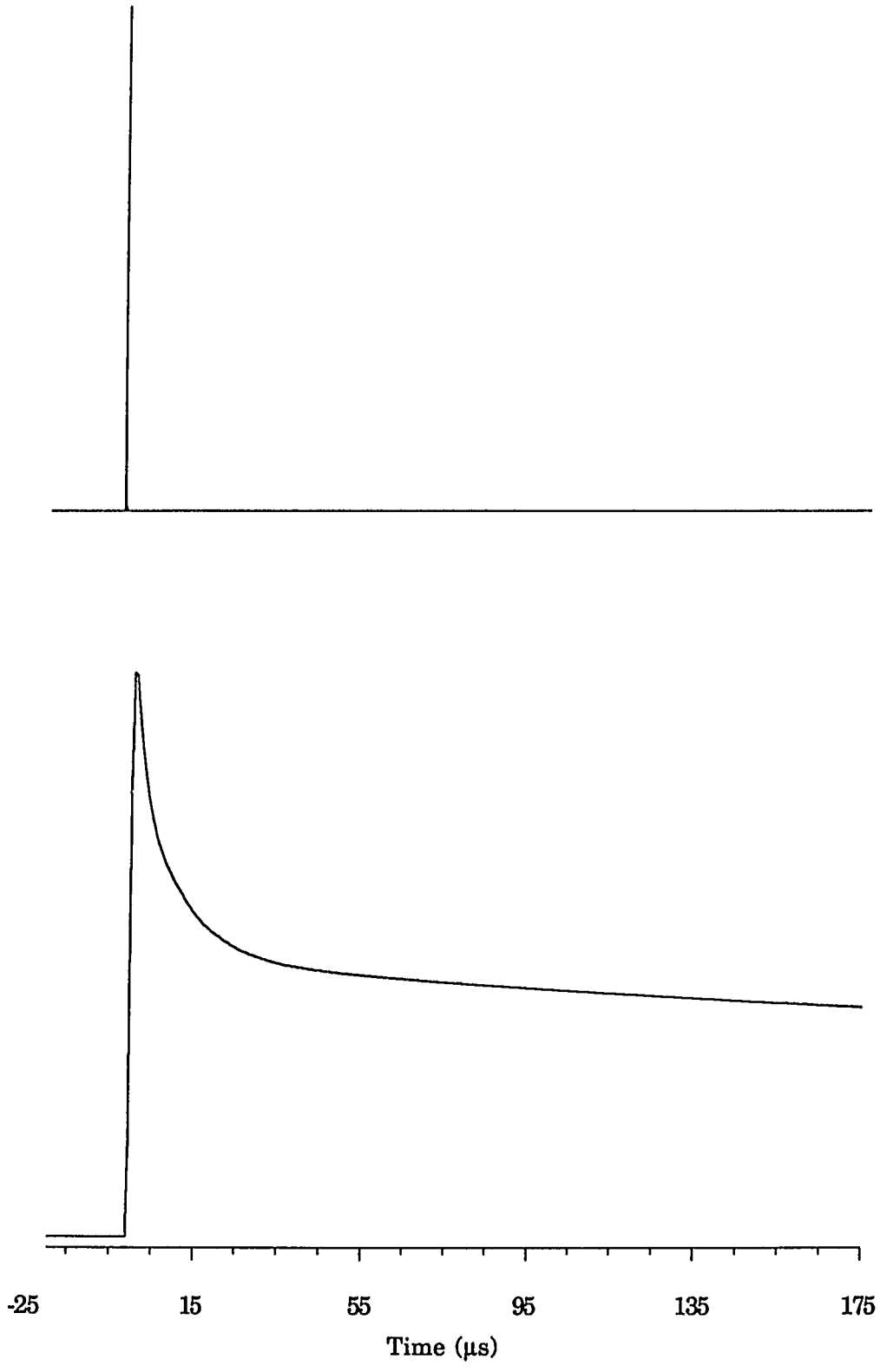
-25
15
55
95
135
175
Time (μs)

Figure 3.3

The circuit used to convert the photodiode signal into a pulse for triggering the transient digitizer. This is used to prevent interference from crosstalk.

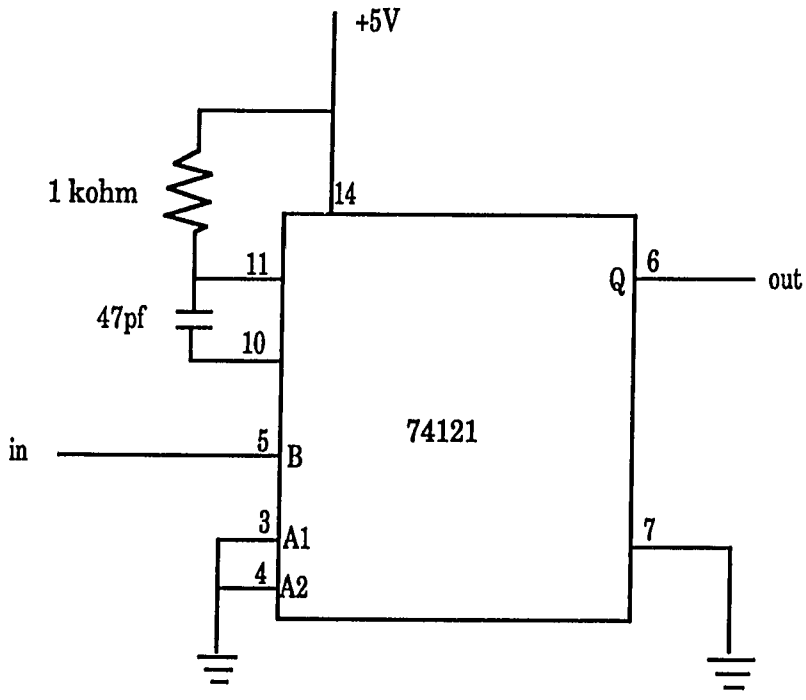
+5V
1 kohm
14
11
Q
6
out
47pf
10
74121
in
5
B
3
A1
7
4
A2

$$H_2CCO + h\nu \rightarrow CH_2 + CO \qquad (3.4b)$$

Channel (3.4b) appears to be present also as evidenced by the absorptions of vibrationally excited carbon monoxide which can be seen in Fig. 3.4. Fig. 3.5 shows the temporal profile of the CO $2 \leftarrow 3$ P(13) line at 2038.6253 cm^{-1} produced by photolysis of ketene at 193 nm.

The ketenyl spectra which were obtained in this work provided the first direct evidence for channel (3.4a). In the presence of several Torr of a suitable vibrational relaxant such as SF_6, the rise time of the ketenyl transient was almost as short as the 1 μsec rise time of the detector system demonstrating that ketenyl was produced directly by the photolysis of ketene. Ketene was also successfully produced by 800°C pyrolysis of acetone as is shown in Fig. 3.1 (A dry ice/acetone trap was used to remove unpyrolyzed acetone which otherwise would have absorbed much of the excimer beam.) Using acetone as the ketene precursor produced no gain or loss of absorption features ruling out the possibility that the transient absorptions were caused by photolysis of residual diketene.

3.5 Observed Spectrum

A typical frequency scan showing ketenyl transitions, with transition assigned, is displayed in Fig. 3.6. Attenuation of the infrared laser probe is caused by exciting rotational components of

Figure 3.4

Typical frequency scan containing strong carbon monoxide lines. Also notice the splitting in the K=0 lines which are labeled. This is spin-rotation splitting and is resolved only in the wings of this band for K=0.

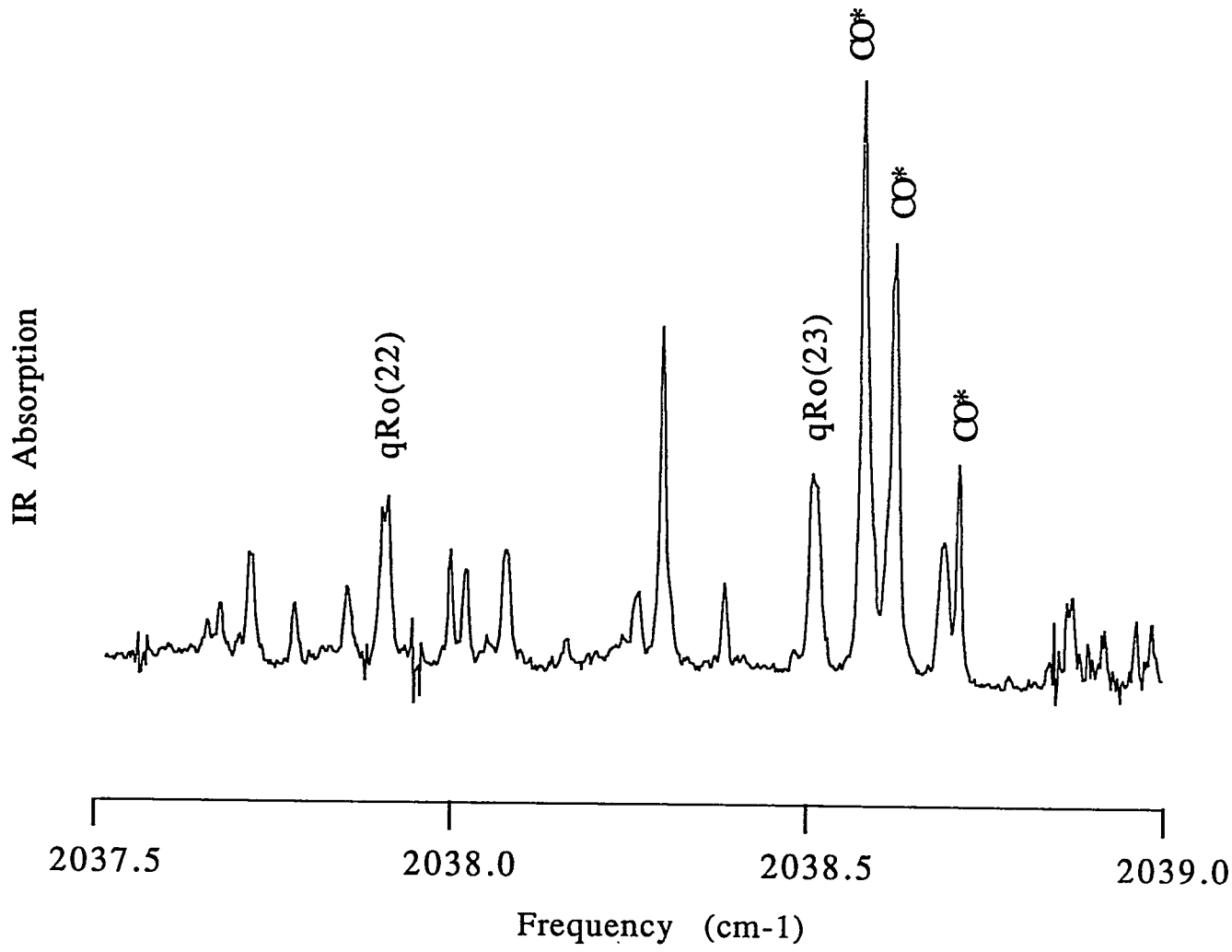
IR Absorption
qRo(22)
qRo(23)
CO*
CO*
CO*
2037.5
2038.0
2038.5
2039.0
Frequency (cm-1)

Figure 3.5

The temporal profile of the CO 2 ← 3 P(13) line at 2038.6253 cm^{-1} produced by the 193 nm photolysis of ketene. Notice the exponential return to baseline shown here. This was not seen in ketenyl, but was typical of the CO lines observed, with decay rates depending upon the excitation. More excited transitions tended to decay faster.

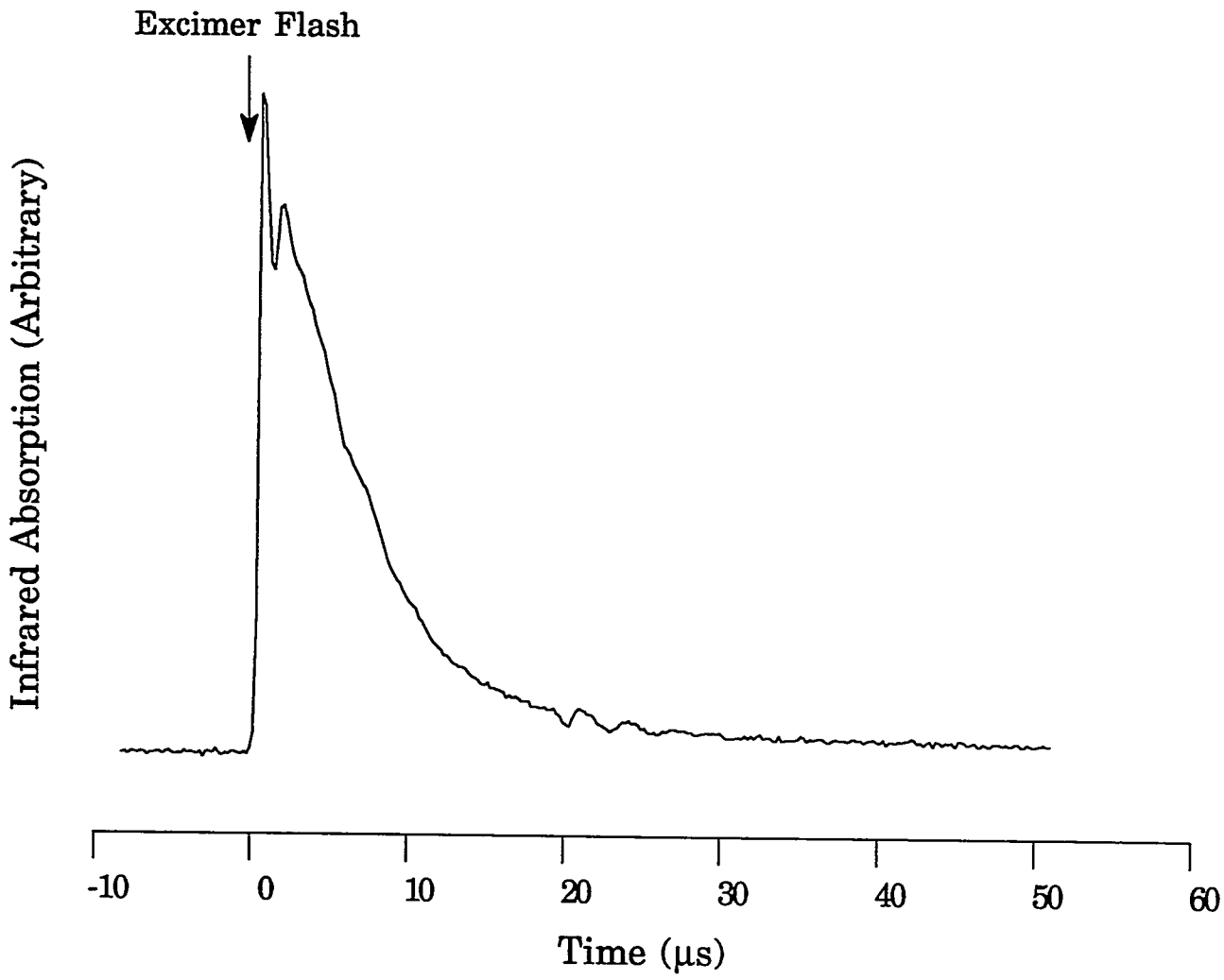
Excimer Flash
Infrared Absorption (Arbitrary)
-10
0
10
20
30
40
50
60
Time (μs)

Figure 3.6

Typical frequency scan over ketenyl lines. Assigned lines have been labeled with the transition's lower and upper state. Labels are defined as follows: $N_{K_a,K_c}Fx$ where x=1 for electron spin of +0.5 and x=2 for spin of -0.5. K_c and Fx are omitted where the separate lines are not resolved.

$6_0 \leftarrow 5_0$
$5_3 \leftarrow 4_3$ F2
$8_3 \leftarrow 7_3$ F1
$11_{1,11} \leftarrow 10_{1,10}$ F1
$11_{1,10} \leftarrow 10_{1,9}$ F1
$10_{1,10} \leftarrow 9_{1,9}$ F2
$10_{1,9} \leftarrow 9_{1,8}$ F2
$8_2 \leftarrow 7_2$ F2
$7_0 \leftarrow 6_0$
$6_3 \leftarrow 5_3$ F2
$9_2 \leftarrow 8_2$ F1
$9_3 \leftarrow 8_3$ F1
$12_{1,12} \leftarrow 11_{1,11}$ F1
$12_{1,11} \leftarrow 11_{1,10}$ F1
$11_{1,11} \leftarrow 10_{1,10}$ F2
$11_{1,10} \leftarrow 10_{1,9}$ F2
$9_2 \leftarrow 8_2$ F2
$8_0 \leftarrow 7_0$
$7_3 \leftarrow 6_3$ F2
$12_{1,12} \leftarrow 11_{1,11}$ F2
$13_{1,13} \leftarrow 12_{1,12}$ F1
$13_{1,12} \leftarrow 12_{1,11}$ F1
$12_{1,11} \leftarrow 11_{1,10}$ F2
$10_2 \leftarrow 9_2$ F2
$9_0 \leftarrow 8_0$
2027
2028
Frequency (cm^{-1})

the ketenyl heavy atom antisymmetric stretch vibration. The structure consists of P, Q and R branches corresponding to a change in the N quantum number of -1, 0 and +1 respectively with $\Delta K_a=0$. There are P, Q and R branches for each K_a ($K_a=0$ has only P and R branches). The N quantum number corresponds to the magnitude of the total rotational angular momentum and the K_a quantum number corresponds to the projection of the angular momentum on the a axis (the axis with the minimum moment of inertia). Since ketenyl is a *near* prolate asymmetric top molecule $\pm K$ are not degenerate as in a symmetric top, but for $|K|\neq 0$ there are actually two different levels for each N. These can be named by their correlation with the symmetric top limits: K_a corresponds to K in a prolate top molecule (where a is the unique axis) and K_c is K in the oblate top limit (c being the unique axis). This degeneracy lifting introduces a splitting of the absorption features which is resolved in these spectra only for K=1. An additional splitting arising from the to spin-rotation interaction is observed. Ketenyl is a radical with an unpaired electron. The magnetic moment of the electron spin interacts with the magnetic field created by molecular rotation and is responsible for an additional splitting of each line into two components observed in the wings of the K=0 band and in the K=1, K=2 and K=3 bands.

The ketenyl spectrum observed is dominated, as might be expected since the vibration is along the C-C and C-O bonds, by parallel a-type transitions ($\Delta K_a=0$). In principle, perpendicular b-

type transitions ($\Delta K_a=\pm 1$) are present, but they are not sufficiently intense to be visible with our sensitivity.

3.6 Assignment of Rotational Transitions

Identification of K=O lines was relatively easy due to their strong intensity and regular spacing. Assignment of individual lines was based upon combination differences calculated from molecular constants obtained by microwave spectroscopy [25]. Combination differences (the spacings between absorption features which share the same upper state level) depend only the molecule's ground state constants which, for ketenyl, were accurately determined by microwave spectroscopy.

Such a combination difference is illustrated in Fig. 3.7. Since the $^qR_0(1)$ and $^qP_0(3)$ transitions have the same upper state, the difference between these frequencies is the energy separation of the the 3_{03} and 1_{01} levels of the lower state. From this infrared data, a difference of 3.613 cm^{-1} between the $^qR_0(1)$ and $^qP_0(3)$ lines is obtained. A separation of 3.611 cm^{-1} is calculated from the microwave constants [25]. The difference of 0.002 cm^{-1} is within experimental error.

Assignment of K=1, 2, and 3 transitions proved somewhat more difficult. K=1 transitions are deceptively easy to recognize by their characteristic four line pattern arising from electron spin and asymmetry splitting shown in Fig. 3.6. The four line groups

Figure 3.7

Illustration of combination difference assignment check and its dependence on ground state constants.

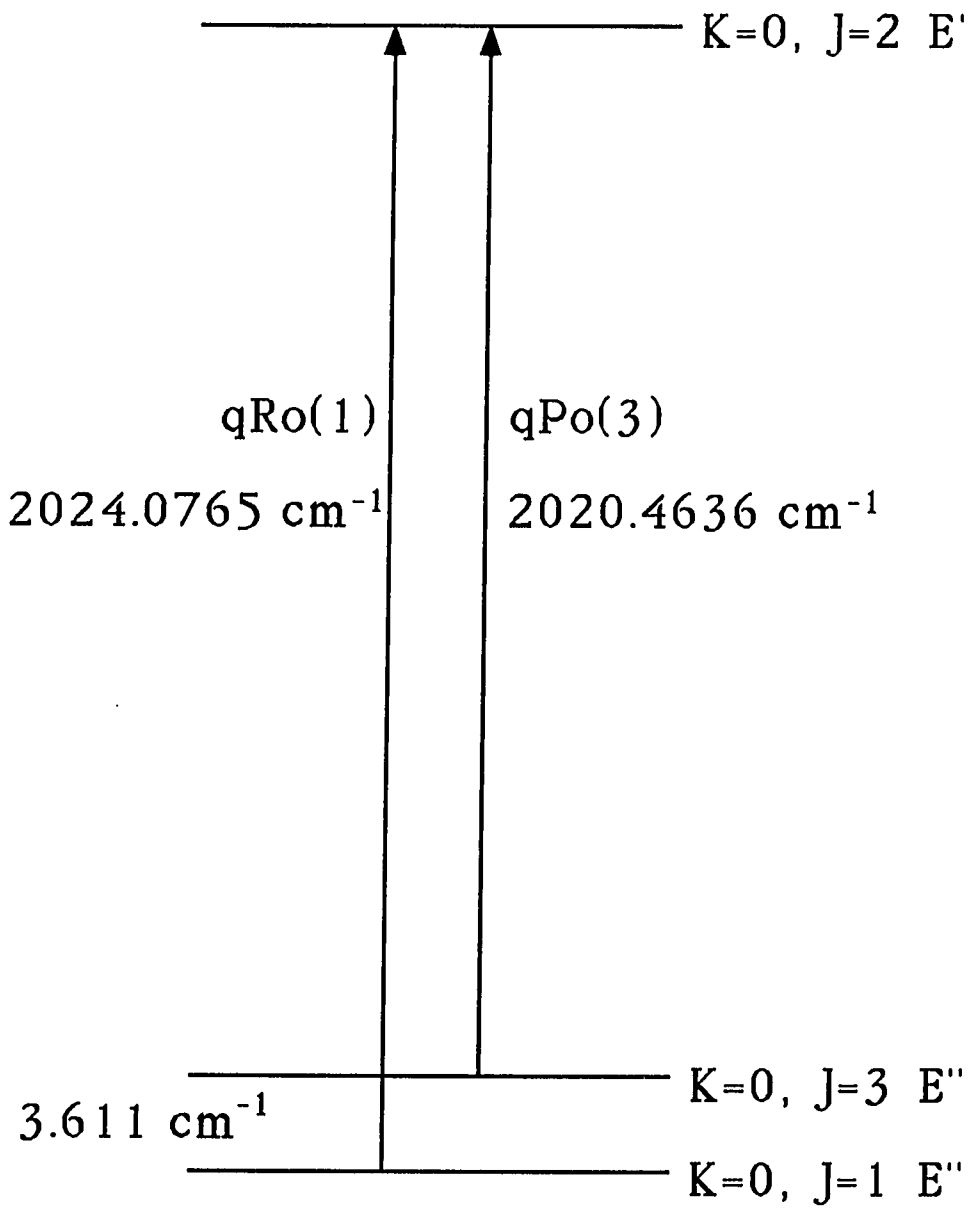

qRo(1) - qPo(3) =3.613 cm^{-1}

(overlapping in Fig. 3.6 to make three- and two-line groups) are due to K=1 transitions, but all four are not the same N transition, as was originally assumed, since the spin-rotation splitting is large.

To assign K=1, 2, and 3 transitions, series of lines spaced by approximately 0.7 cm^{-1} with changes in the spacing which progress smoothly (could be reasonably fit to a second or third order curve) were found in the experimental data. Combination differences determined from ground state constants were added to and subtracted from (R and P branch respectively) these series to predict other series. This trial and error process was repeated many times until a pair of P and R series related to each other by ground state energy differences was found for each K.

3.7 Fitting the Observed Spectra

The program used to fit the observed spectra was a modified version of the program written by Dane and Curl [1,3]. A listing of the modified version is in appendix II. The Hamiltonian used in this work included 19 parameters for a given vibrational state corresponding to 3 rotational constants (α,β,γ), 5 quartic ($\Delta K,\Delta NK,\Delta N,d1,d2$), 1 sextic ($\Phi KN$) centrifugal distortion constants, 4 spinrotation interaction constants (α_S, $\beta_S,\gamma_S,\varepsilon_{ab}$), 5 quartic ($\Delta K^S,\Delta NK^S,\Delta N^S,\Delta KN^S,\Delta N^S$) and 1 sextic ($\Phi K^S$) spinrotation centrifugal distortion constants. This rotational Hamiltonian is displayed below:

$$
\begin{aligned}
H = {} & \alpha N_a^2 + \beta N^2 + \gamma(N_+^2+N_-^2) \\
& - \Delta_K N_a^4 - \Delta_{NK} N^2 N_a^2 - \Delta_N N^4 + d_1 N^2(N_+^2+N_-^2) + d_2(N_+^4+N_-^4) + \\
& \Phi_{KN} N^2 N_a^4 + \\
& \alpha_s N_a S_a + \beta_s(N\cdot S) + \gamma_s(N_b S_b - N_c S_c) + \\
& \varepsilon_{ab}(N_a S_b + N_b S_a) + \\
& \Delta_K^s N_a^3 S_a + \frac{1}{2}\Delta_{NK}^s\left(N^2 N_a S_a + N_a S_a N^2\right) + \Delta_{KN}^s N_a^2 (N\cdot S) + \\
& \Delta_N^s N^2 (N\cdot S) + d_1^s(N_+^2+N_-^2)(N\cdot S) + \\
& \Phi_K^s N_a^5 S_a
\end{aligned}
$$

In order to obtain the energy levels associated with this Hamiltonian, the Hamiltonian matrix must be set up in a suitable basis. Such a basis is $|N|K|\gamma J\rangle$ where K ($\equiv K_a$) is the prolate symmetric top K and γ (=0 or 1) is used in:

$$|N|K|\gamma\rangle = \frac{1}{\sqrt{2}}\left(|N|K|\rangle + (-1)^{\gamma}|N\text{-}K\rangle\right)$$

γ can be correlated with the K_c value used to compute the level labeling. J is the quantum number representing the total angular momentum including electron spin and can take values $J=N+\frac{1}{2}$ and $J=N-\frac{1}{2}$. This Hamiltonian is diagonal in K except for the small terms in N_+ (N_-) and S_+ (S_-) and ε_{ab}. It is far from diagonal in N because the term α_s is large and connects N with N±1. To calculate the Hamiltonian matrix, matrices representing N^2, N_a^2, N_+^2, N_-^2, N_+^4, N_-^4, $N\cdot S$ and $N_a S_a$ are set up and the appropriate terms computed by matrix multiplication.

The program uses constants provided by the user to predict the frequencies of transitions. To determine new constants these predicted frequencies are subtracted from the user provided line positions and assignments and the residuals reduced by least squares fitting.

To verify proper operation of the program microwave transitions observed by Hirota [25] were fit and the result compared to the output of a program by Sears [35]. Agreement of the constants obtained by fitting the microwave spectra and those presented by Hirota was fair. Agreement was not as good as could have been expected from fitting on the same lines. However, the discrepancies were always less than or comparable to 2.5 times the standard deviation given by Hirota and the residuals (absorption frequency observed value minus calculated) obtained in the fitting were comparable to those of Hirota. The ground state constants used for fitting the infrared spectra in this work were those obtained from this fitting.

The initial plan was to obtain a universal fit on the upper state. In attempts to obtain a universal fit errors larger than the experimental error were obtained, so each of the K stacks was fit independently. For each of the K stacks five effective upper state constants (eight for K=1) were determined. These constants consisted of ν_K, β, Δ_N, α_S and β_S (also γ, d_1 and γ_S for K=1). Since one K stack was fit at a time, the excited state parameters which allow for K dependence were fixed to their ground state values for the fit

on the infrared data and the remaining five (eight for K=1) constants fitted. All observed lines were given equal weight in these fits.

Table 4.1 gives the constants determined in this manner. Figures 3.8 and 3.9 show the change in selected effective constants plotted versus K^2. Normally these plots would be linear or at least smooth curves. Figure 3.10 shows β and α_s for the upper and lower states plotted versus K^2. These plots show that it is the upper and not the lower state which is perturbed. K=1 seems especially perturbed.

This perturbation may be due to a Fermi resonance with a combination level of lower fundamentals. Considering vibration frequencies from *ab initio* calculations by Wagner[36] there are several plausible combination bands which may be interacting with the heavy atom antisymmetric stretch fundamental. These include $\omega_4+\omega_3$ at 1938 cm^{-1}, $3\omega_4$ at 2076 cm^{-1}, $\omega_5+3\omega_6$ at 2222 cm^{-1} and $4\omega_6$ at 2180 cm^{-1}. Because of the large uncertainties in the *ab initio* vibrational frequencies, it is not possible to select one of these possibilities as most likely.

The frequencies of the observed transitions as well as the differences between the observed and calculated values are listed in Appendix I. The observed band origin at 2022.64 cm^{-1} agrees well with matrix isolation value proposed by Jacox and Olson [9] of 2019.5 cm^{-1}.

Table 3.1: Parameters Resulting from Least-Squares Fit

Constant	Ground State	K=0	K=1	K=2	K=3
ν		0.202264E+04	0.201989E+04	0.202160E+04	0.202244E+04
α	0.407511E+02	f	f	f	f
β	0.361304E+00	0.358860E+00	0.358927E+00	0.359159E+00	0.359037E+00
γ	0.108663E-02	f	0.104773E-02	f	f
ΔK	0.605644E+00	f	f	f	f
ΔNK	0.795487E-05	f	f	f	f
ΔJ	0.128933E-06	0.124939E-06	0.184489E-06	0.503253E-06	0.490785E-07
d_1	-0.405157E-08	f	-0.218145E-07	f	f
d_2	0.677556E-09	f	f	f	f
ΦKN	-0.391513E-06	f	f	f	f
α_s	-0.589883E+01	-0.420407E+01	-0.730484E+01	-0.641673E+01	-0.671190E+01
β_s	-0.472787E-03	-0.464915E-03	0.371204E-02	0.100563E-01	-0.137104E-01
γ_s	-0.949548E-03	f	-0.728165E-03	f	f
ε_{ab}	0.529926E-01	f	f	f	f
ΔK_s	0.688982E+00	f	f	f	f
ΔNK_s	0.619978E-04	f	f	f	f
ΔN_s	-0.330012E-06	f	f	f	f
ΔKN_s	-0.208364E-03	f	f	f	f
δJ_s	-0.170884E-06	f	f	f	f
ΦK_s	-0.389645E-01	f	f	f	f

f indicates constant fixed to ground state value. All constants are given in cm^{-1}.

Figure 3.8

Parameters determined in least-squares fit plotted versus K^2. These plots should be linear (or at least smoothly varying) for an unperturbed system.

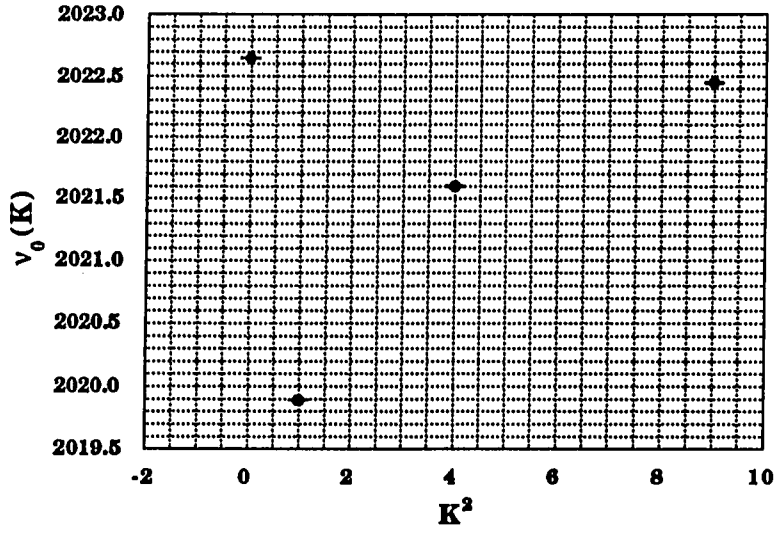
2023.0
2022.5
2022.0
2021.5
2021.0
2020.5
2020.0
2019.5
ν_0 (K)
-2
0
2
4
6
8
10
K^2

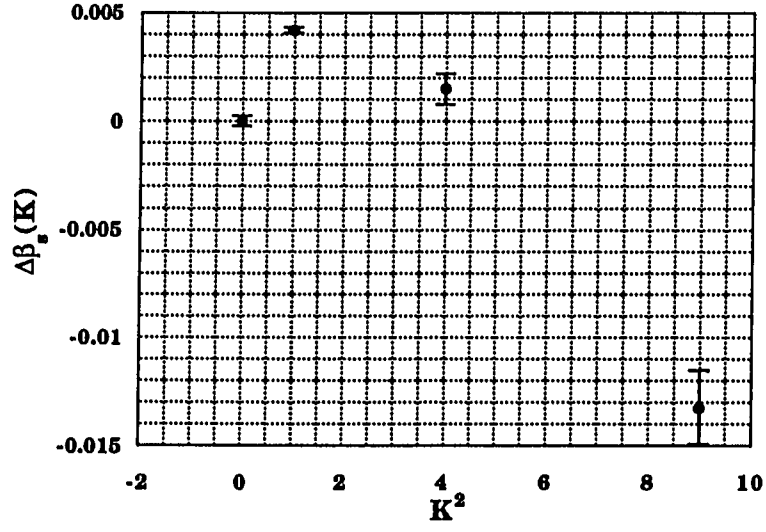
0.005
0
-0.005
-0.01
-0.015
$\Delta\beta_s$ (K)
-2
0
2
4
6
8
10
K^2

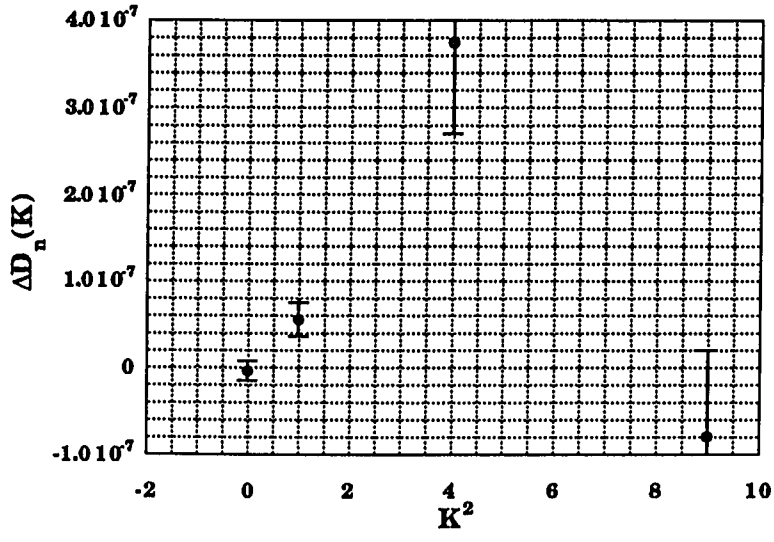
$4.0\,10^{-7}$
$3.0\,10^{-7}$
$2.0\,10^{-7}$
$1.0\,10^{-7}$
0
$-1.0\,10^{-7}$
ΔD_n (K)
-2
0
2
4
6
8
10
K^2

Figure 3.9

Parameters determined in least-squares fit plotted versus K^2. These plots should be linear (or at least smoothly varying) for an unperturbed system.

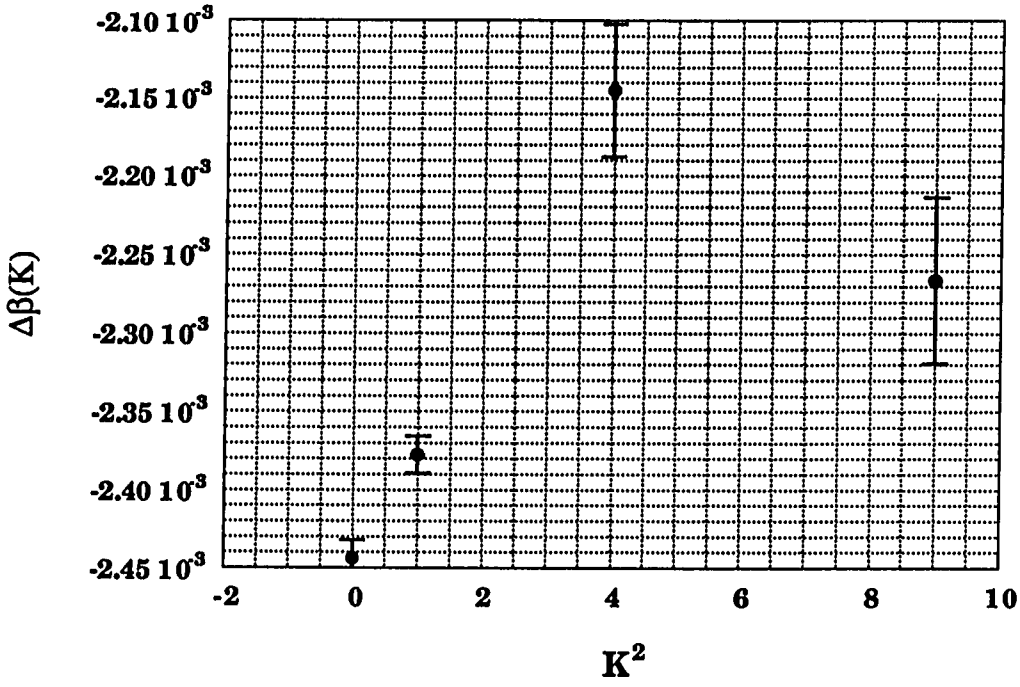
-2.10 10-3
-2.15 10-3
-2.20 10-3
-2.25 10-3
-2.30 10-3
-2.35 10-3
-2.40 10-3
-2.45 10-3
Δβ(K)
-2
0
2
4
6
8
10
K2

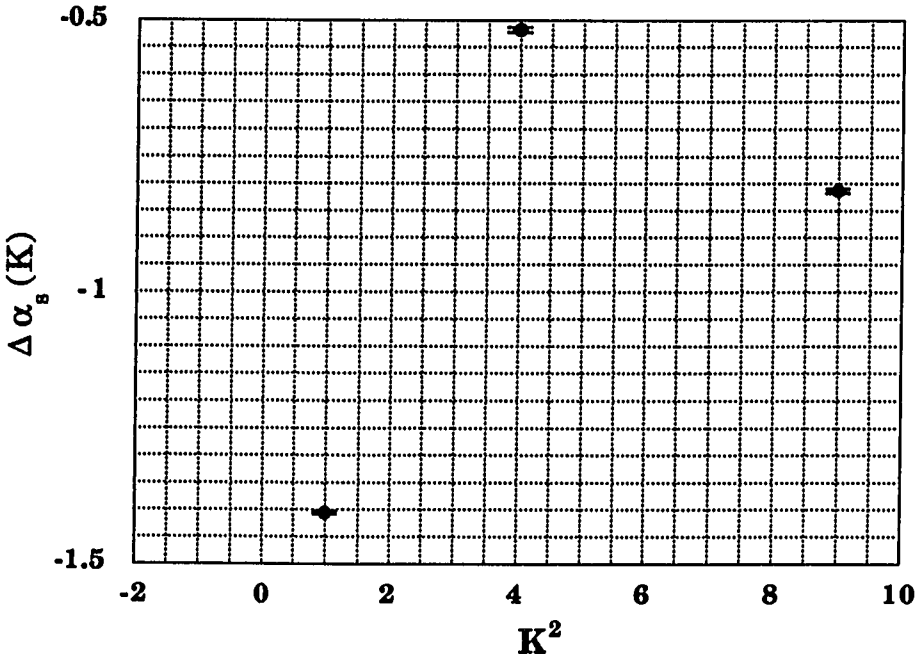
-0.5
-1
-1.5
Δ αs (K)
-2
0
2
4
6
8
10
K2

Figure 3.10

Effective constants for ground and excited states plotted versus K^2. These plots illustrate the nonlinearity observed in Fig. 3.9 is due mainly to upper state behavior. The effective β values were determined from $\beta(K) = \beta + \Delta_{NK}K^2 + \Phi_{KN}K^4$ for each K level. The effective α_s values were determined from $\alpha_s(K) = \alpha_s + \Delta_K{}^s K^2 + \Phi_K{}^s K^4$ for each K level.

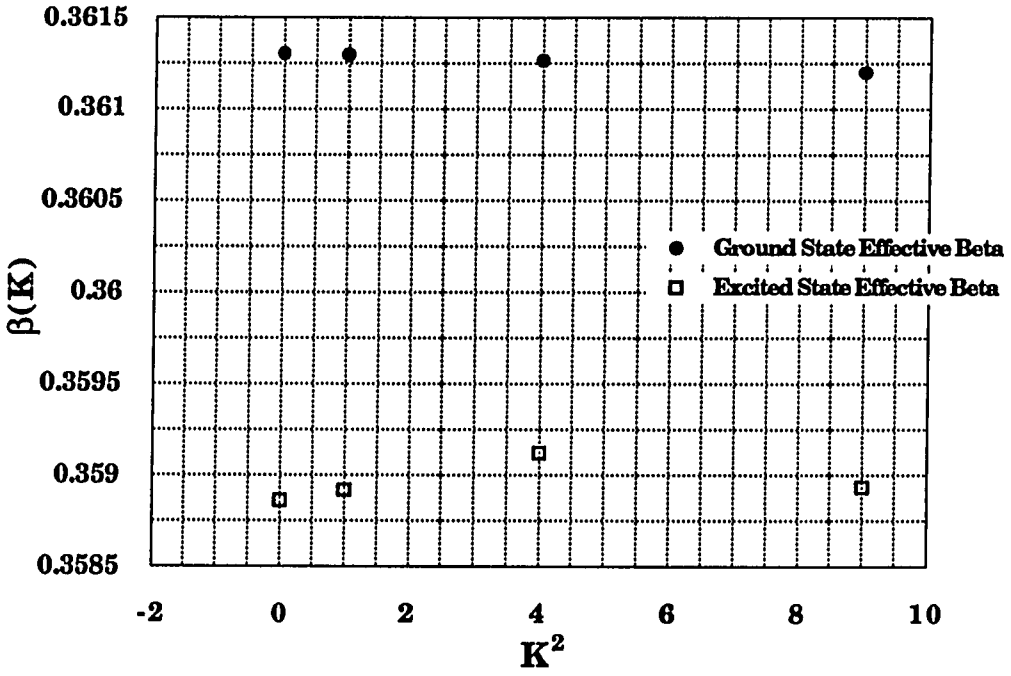
0.3615
0.361
0.3605
0.36
0.3595
0.359
0.3585
β(K)
-2
0
2
4
6
8
10
K²
Ground State Effective Beta
Excited State Effective Beta

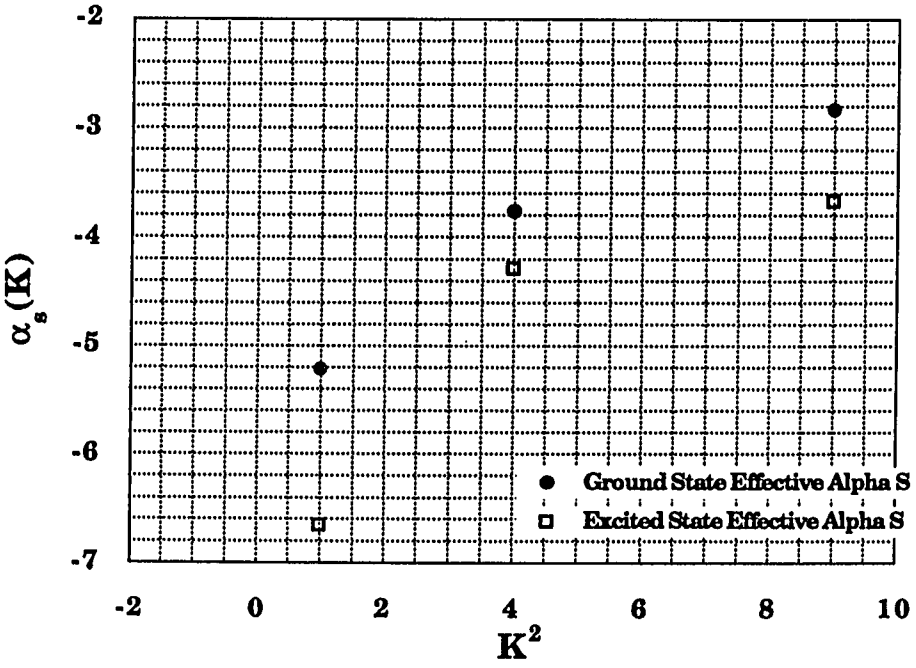
-2
-3
-4
-5
-6
-7
α_s (K)
-2
0
2
4
6
8
10
K²
Ground State Effective Alpha S
Excited State Effective Alpha S

3.8 Conclusion

The high resolution spectrum of the ketenyl radical heavy atom antisymmetric stretch has been observed. This was the first time the high resolution infrared spectra of a ketenyl band has been obtained. Assignment of the spectrum as ketenyl was confirmed by comparisons with microwave and matrix isolation spectra. Molecular parameters have been obtained with a least-squares fit on the experimental data.

There are other HCCO bands which may be observed including the C-H stretch which may have observable perpendicular transitions which would allow for the determination of additional molecular parameters. Also, the high resolution infrared DCCO spectrum is still to be observed. Some attempts were made to observe this species during this work. To search for DCCO, D_2CCO was produced from pyrolysis of deuterated acetone and photolyzed at 193 nm. The diode laser was used to probe the region from 1950 cm^{-1} to 2050 cm^{-1} without detecting DCCO transitions.

CHAPTER 4

KETENYL CHEMICAL KINETICS

4.1 Ketenyl Decay

For kinetic studies the ketenyl radical was produced as discussed in Chapter 3 by pyrolyzing diketene and photolyzing the resulting ketene.

Fig. 4.1 depicts the time behavior of a typical transient infrared absorption of a ketenyl line in this system at several photolysis laser pulse energies. As can be seen, the absorption decays rapidly with time as is expected for a reactive free radical. The time decay exhibits second order behavior with the initial rate of decay much larger at higher excimer energies where a higher concentration of radicals was produced. At long times all the traces approach the same limiting behavior as is predicted by second order kinetics. This is compelling evidence that ketenyl was not reacting rapidly with precursor ketene, but rather with a species produced by the photolysis. The second order decay may occur because ketenyl reacts with itself, with H atoms, or with other photolysis products (for example CH_2). At the higher pulse energies the amount of ketene photolyzed is equivalent to a partial pressure of about 10 mTorr (~3×10^{14} molecules/cm^3) based upon absorbing about 50% of

Fig 4.1

Typical time behavior of a ketenyl transition without added reagents. The line center for this transition is at 2038.302 cm^{-1}. He pressure is 25 Torr. The ketene pressure is estimated to be 4 Torr by assuming that the helium flow is saturated with diketene and the pyrolysis of diketene to ketene has 100% efficiency. These traces are the average of 500 excimer shots.

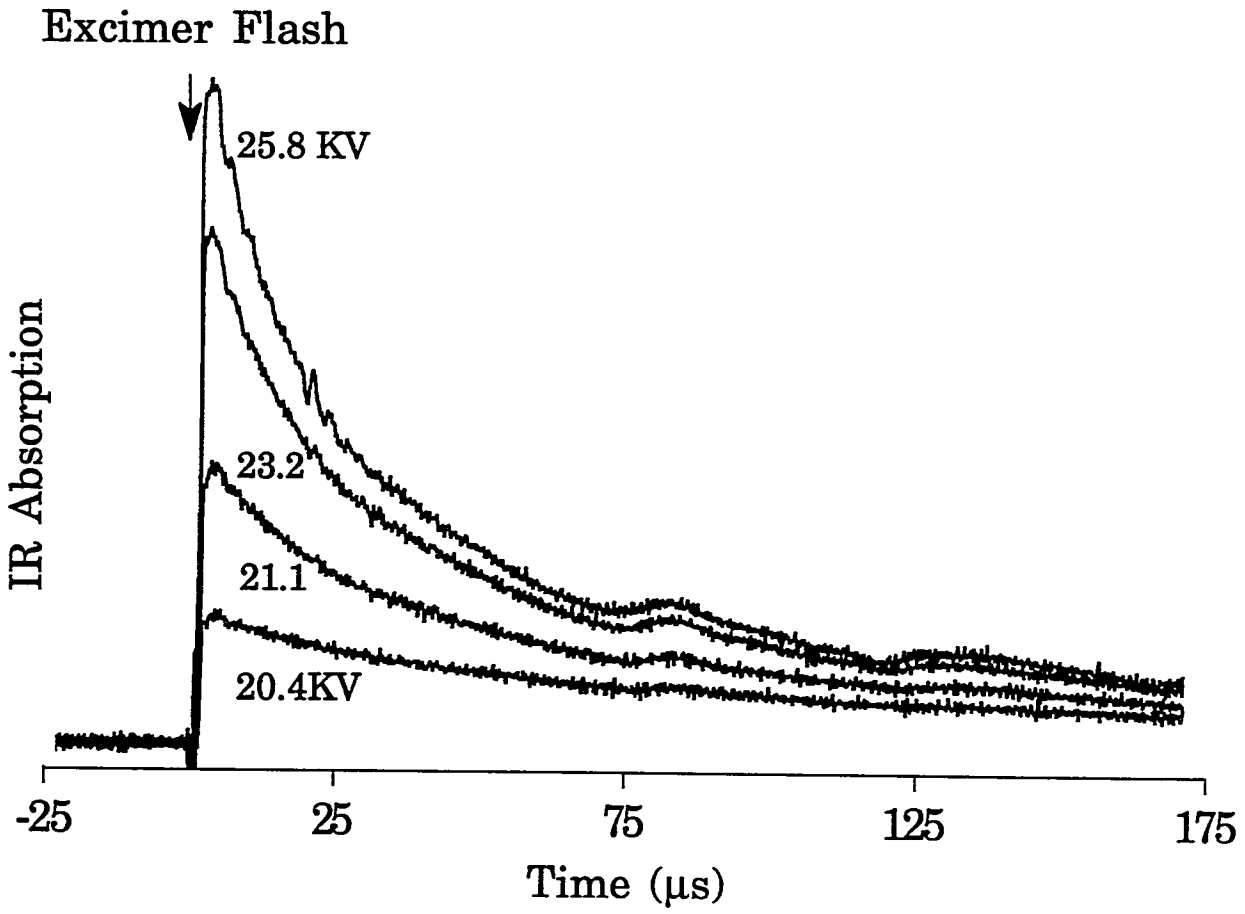
Excimer Flash
25.8 KV
23.2
21.1
20.4KV
IR Absorption
-25
25
75
125
175
Time (μs)

an excimer pulse containing 10^{17} photons in a volume of about 100 cm^3. Vinckier, Schaekers and Peeters [24] have measured a rate constant for the reaction between H and HCCO of 1.5×10^{10} $cm^3 molecule^{-1} s^{-1}$ which predicts a time to half reaction of 20 μsec at initial concentrations for H and HCCO of 3×10^{14} molecules cm^{-3}. This is in rough agreement with the highest initial signal trace of Fig. 4.1. Thus the observed decay could be explained entirely by the reaction of ketenyl with H.

4.2 Measurement of Reaction Rate Constants

To better understand the reactions of the ketenyl radical, its time behavior was monitored in the presence of various species and reaction rate constants were determined. To measure rate constants, the diode laser was tuned to the maximum of a ketenyl rovibrational line and the absorption signal as a function of time was acquired with various reactants at various pressures. The ketenyl reactions studied were assumed to be bimolecular and second order reaction rate constants were determined where possible. To determine each rate constant an excess of stable species reactant (NO, 98%; O_2, 99.6%; C_2H_2, with a charcoal filter ~99%[37]; or C_2H_4, 99.0%) was introduced into the White cell with the ketene. The ketene was photolyzed and the ketenyl temporal profile was recorded by monitoring a rovibrational transition. This was repeated 500 to 3000 times and the temporal profiles were averaged. By comparison of the signal

levels before the photolysis flash with that long after the flash, a zero signal level was estimated. Then the natural logarithm of the observed signal above this zero level was least squares fitted with a linear function of time weighting each point by the value of the corresponding signal. The points used in this fitting were those between 90% and 10% of the maximum signal. The resulting first order signal decay constants were then plotted versus the corresponding reactant pressures to create a Stern-Volmer plot. The choice of reactant pressures used was limited on the high side by the infrared detector's response time and on the low side by the second order ketenyl decay rate which occurred in the absence of additional reactant and contributed to the decay. Fig. 4.2 illustrates the problem of ketenyl second order contribution to the decay. With higher ketenyl pressures, there was a significant second order contribution resulting in a decay which was clearly not exponential. The pseudo first order rate constant then depended upon the portion of the decay used for the exponential fit. To lessen this problem, especially for the slower ketenyl reactions, the ketenyl pressure was reduced by decreasing the excimer power. This decreased the second order contribution to the decay, but by sacrificed some signal.

Figure 4.2

Illustration of the difficulty caused by the second order decay of ketenyl on measurement of reaction rate constants. The upper plot, the average of 2000 time traces at 2032.247 cm^{-1} ($^{q}R_{0}(13)$), shows the time behavior of ketenyl in the presence of 117 mTorr of nitric oxide. The lower plot is the natural log of the infrared absorption intensity, as in upper plot, plotted versus time. For an exponential decay this would be a straight line. Several lines suggesting different fits are included. The non-exponential behavior was caused by a second order decay in addition to, and independent of, the decay due to the NO reaction. This difficulty was avoided somewhat by reducing the ketenyl pressure.

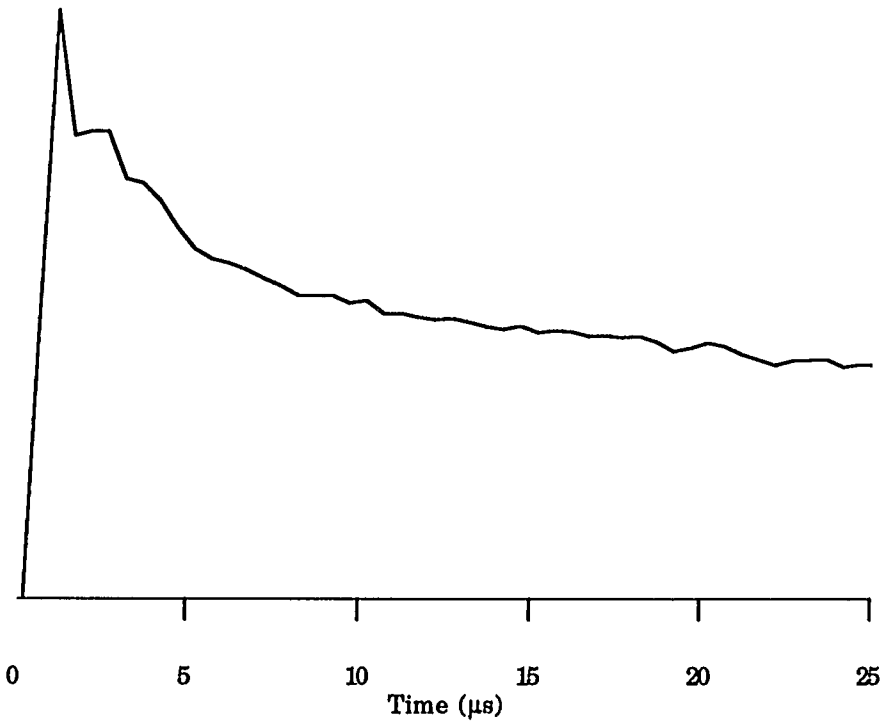
0
5
10
15
20
25
Time (μs)

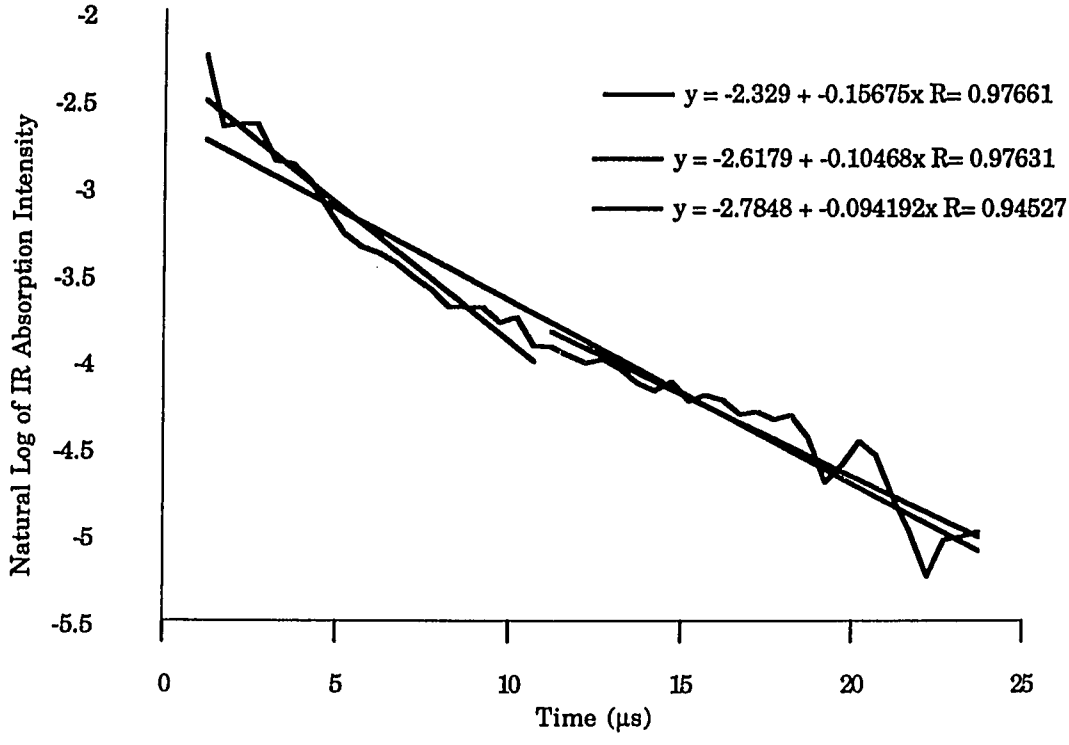
-2
-2.5
-3
-3.5
-4
-4.5
-5
-5.5
Natural Log of IR Absorption Intensity
y = -2.329 + -0.15675x R= 0.97661
y = -2.6179 + -0.10468x R= 0.97631
y = -2.7848 + -0.094192x R= 0.94527
0
5
10
15
20
25
Time (μs)

4.3 Reaction with Nitric Oxide

In this experiment, the diode laser was tuned to the maximum of a ketenyl rovibrational line, and the absorption signal as a function of time was acquired at various NO pressures. Typical time traces are shown in Fig. 4.3. These and other traces were used in constructing the Stern-Volmer plot displayed in Fig. 4.4. The rate constant thus obtained is $4.4(10)\times10^{-11}$ $cm^3 molecule^{-1} s^{-1}$. The uncertainty is estimated on the basis of previous experience with measuring rate constants using the same technique.

4.4 Reaction with Oxygen

The reaction of ketenyl with oxygen has the potential to be an important route for ketenyl depletion in combustion under lean conditions. Three possible reaction channels for ketenyl's reaction with O_2 are as follows:

$$HCCO + O_2 \rightarrow CO_2 + CO + H \quad (4.1a)$$
$$\rightarrow 2CO + OH \quad (4.1b)$$
$$\rightarrow CO_2 + HCO \quad (4.1c)$$

These reactions are exothermic by 467 kJ/mole, 252 kJ/mole and 528 kJ/mole respectively. The HCO produced in channel 4.1c will have a tendency to undergo rapid unimolecular decay to H + CO if a significant fraction of the energy of the products is HCO vibration.

Figure 4.3

Transient absorption signals of HCCO for various pressures of nitric oxide. The line that was monitored is the $^{q}R_{0}(13)$ transition at 2032.247 cm^{-1}. Each trace is the average of 2000 excimer shots. The top trace is ketenyl with no added NO. Lower traces have NO pressures of 41, 117, 160 and 204 mTorr respectively.

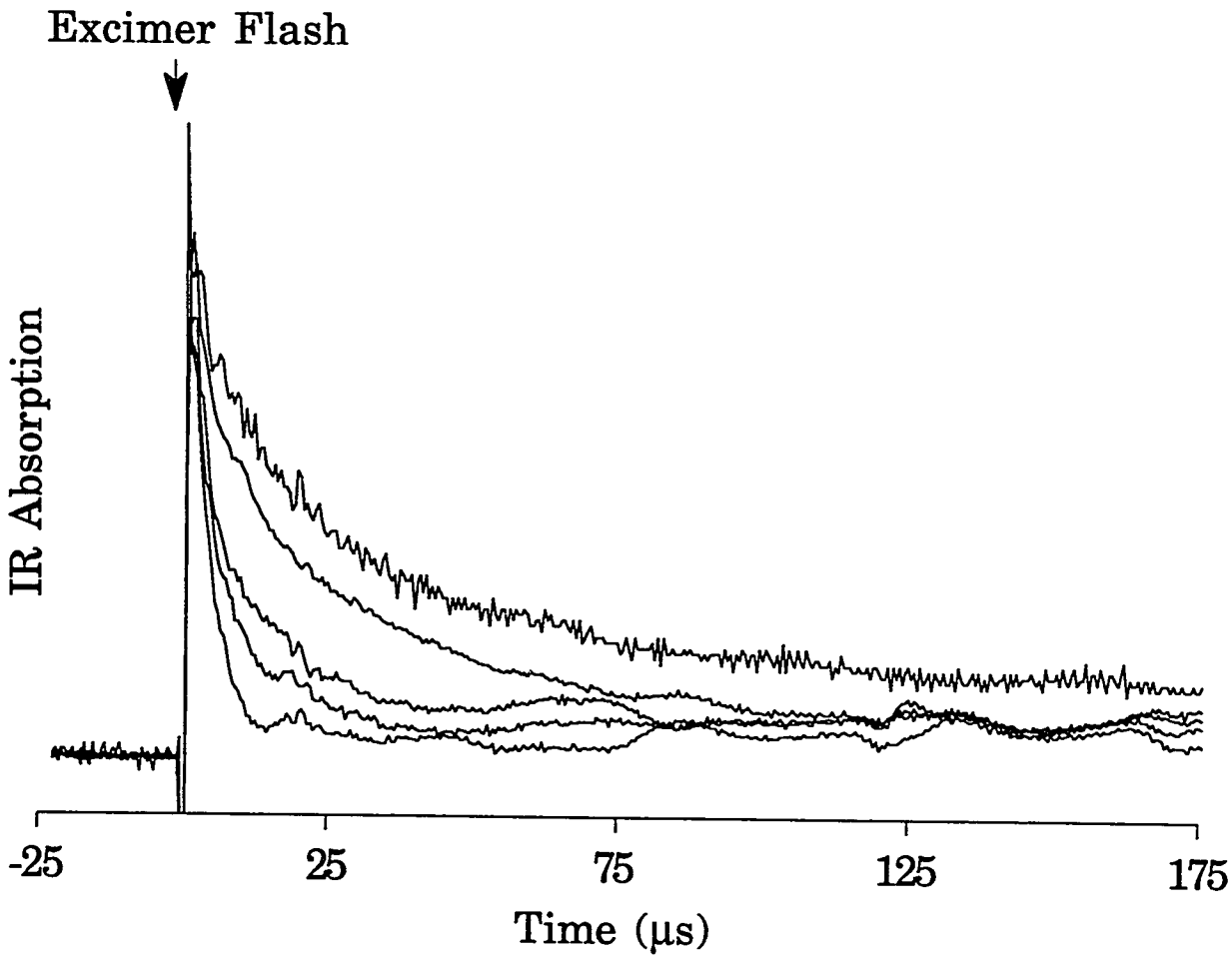
Excimer Flash
IR Absorption
-25
25
75
125
175
Time (μs)

Figure 4.4

Stern-Volmer plot with ketenyl nitric oxide pseudo first order rate constants plotted versus nitric oxide pressure. The resulting bimolecular rate constant for the reaction between ketenyl and NO is 4.4×10^{-11} $cm^3 molecules^{-1} sec^{-1}$.

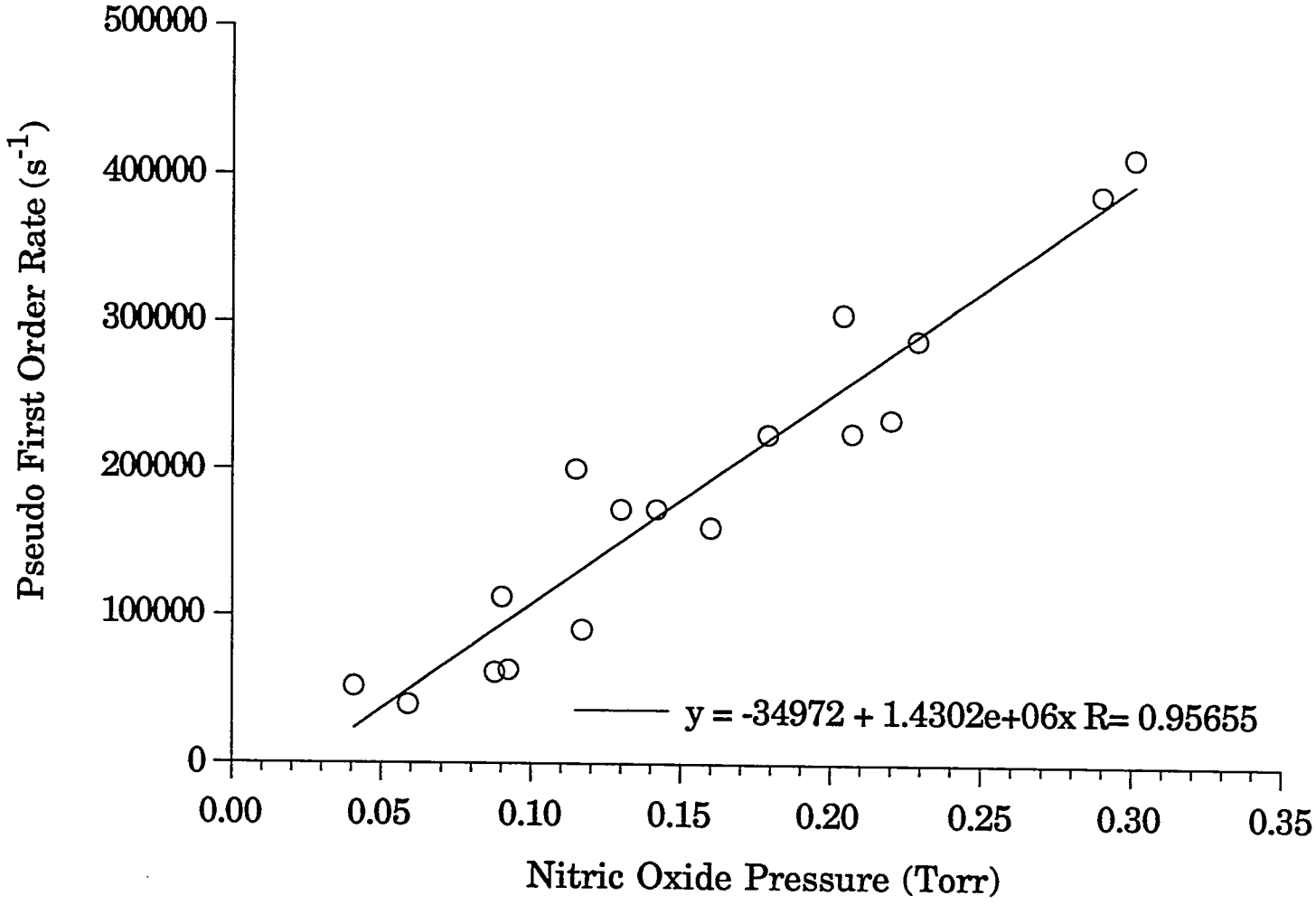
500000
400000
300000
200000
100000
0
Pseudo First Order Rate (s^{-1})
0.00
0.05
0.10
0.15
0.20
0.25
0.30
0.35
Nitric Oxide Pressure (Torr)
y = -34972 + 1.4302e+06x R= 0.95655

This will make 4.1c essentially the same as 4.1a. Another possible reaction channel is:

$$HCCO + O_2 \rightarrow C_2O + HO_2 \qquad (4.1.d)$$

This channel is endothermic by 112 kJ/mole and is therefore closed.

A rate constant of 6.5×10^{-13} $cm^3 molecule^{-1} s^{-1}$ was determined for the reaction ketenyl with oxygen reaction. Ketenyl was produced in the presence of oxygen and ketenyl time traces where were obtained at various oxygen pressures. These time traces were used to create a Stern-Volmer plot and determine the bimolecular reaction rate constant. Since the rate constant was determined from the direct observations of a reactant, it does not depend through which channels the reaction proceeds. The Stern-Volmer plot for calculating this value is displayed in Fig. 4.6. and typical decay traces used to create the Stern-Volmer plot are displayed in Fig. 4.5.

CO_2 was investigated as a possible product for this reaction. A mixture of ketene and oxygen (static fill) was photolyzed and CO_2 production was spectroscopically observed with a normal absorption scan over CO_2 absorption features. In order for the CO_2 to be produced, oxygen, ketene and excimer photolysis were all necessary. Unfortunately the diode laser used for probing was not stable enough to allow for acquisition of a temporal profile, so the time of CO_2 production, and whether it is directly produced, is unknown.

Indeed, there is no evidence to suggest that the CO_2 observed was actually from the reaction of ketenyl with oxygen. The CO_2 may

Figure 4.5

Transient absorption signals of HCCO for various pressures of oxygen. The line monitored is the $^{q}P_{0}(22)$ line at 2014.426 cm^{-1}. Each trace is the average of 5000 excimer shots. The top trace is ketenyl with 3.0 Torr O_2. The middle trace was with an O_2 pressure of 5.6 Torr and the lower trace had an O_2 pressure of 6.9 Torr. Total pressure was approximately 30 Torr. Signal to noise was sacrificed, by decreasing the ketenyl pressure, in these time scans to decrease the rate of the second order reaction which contributes to the decay.

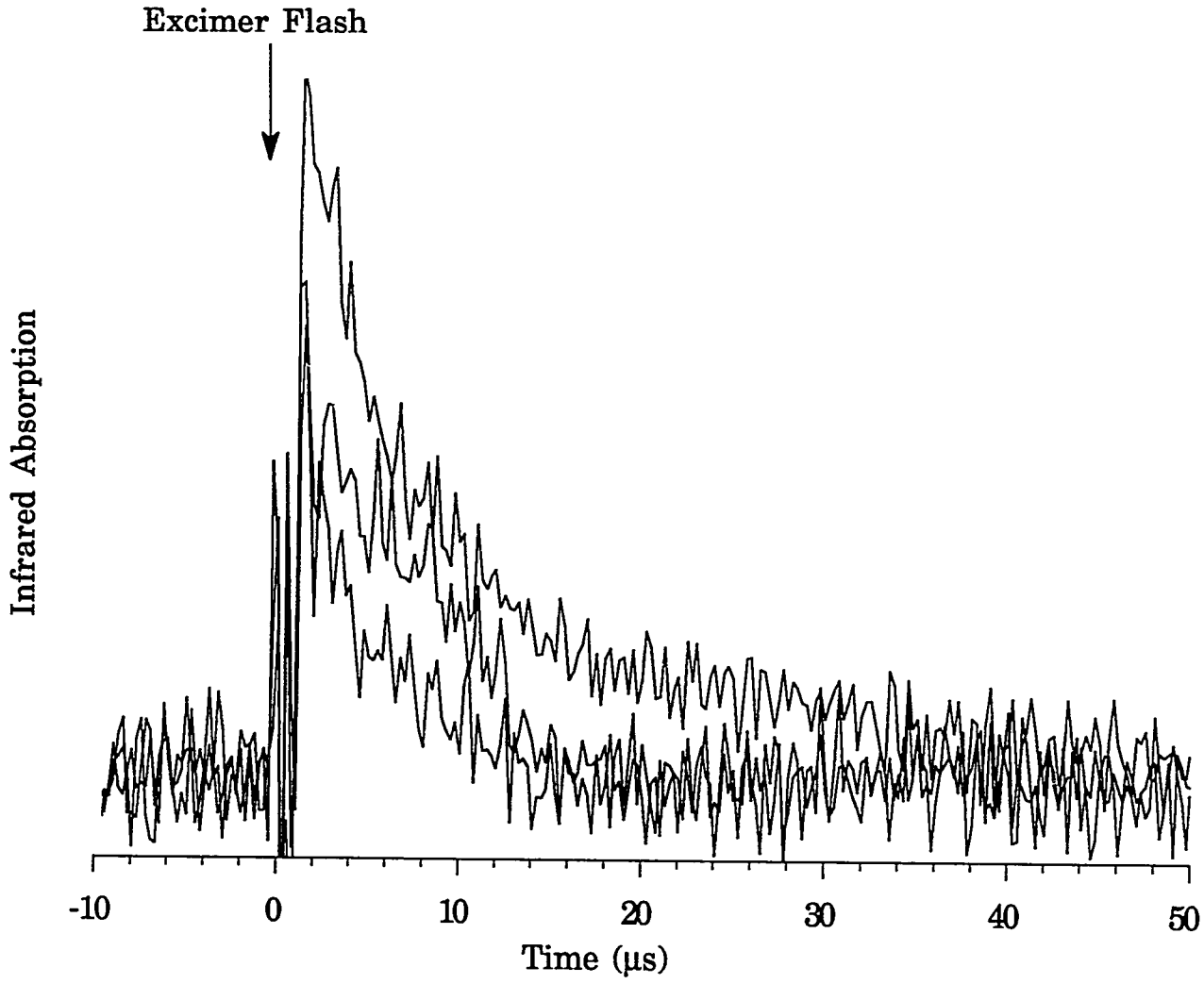
Excimer Flash
Infrared Absorption
-10
0
10
20
30
40
50
Time (μs)

Figure 4.6

Stern-Volmer plot for ketenyl oxygen reaction. Pseudo first order decay rate constants are plotted versus oxygen pressure. The resulting bimolecular rate constant for the reaction between ketenyl and O_2 is 6.5×10^{-13} $cm^3 molecule^{-1} s^{-1}$.

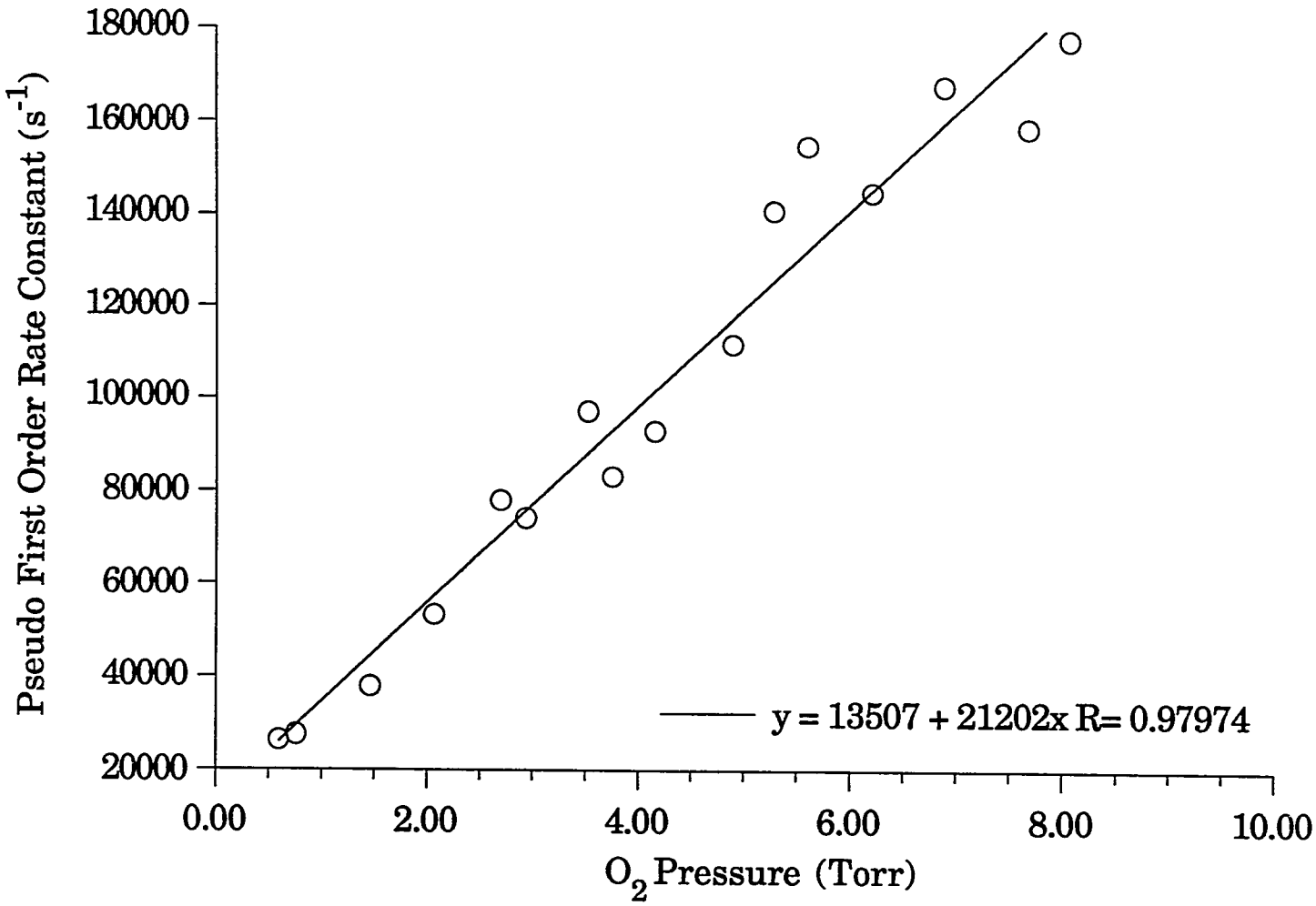
Pseudo First Order Rate Constant (s^{-1})
180000
160000
140000
120000
100000
80000
60000
40000
20000
0.00
2.00
4.00
6.00
8.00
10.00
O_2 Pressure (Torr)
y = 13507 + 21202x R= 0.97974

have been produced by the reaction of CH_2 or another photolysis product with oxygen.

The $^1CH_2$ reaction with oxygen has several possible channels which produce CO_2:

$$^1CH_2 + O_2 \rightarrow 2H + CO_2 \quad (4.2a)$$
$$\rightarrow H_2 + CO_2 \quad (4.2b)$$
$$\rightarrow H_2O + CO \quad (4.2c)$$
$$\rightarrow H + OH + CO \quad (4.2d)$$
$$\rightarrow OH + HCO \quad (4.2e)$$

It may be possible to determine the source of the CO_2 with a diode laser sufficiently stable to obtain time traces comparing the CO_2 signal in the presence and absence of a methylene quencher.

4.5 Reaction with Acetylene

On the time scale of these experiments acetylene appears not to react with ketenyl. Additional ketenyl loss by reaction with acetylene is imperceptible compared with the ketenyl decay by other reactions. Thus, addition of acetylene did not appear to increase the rate of disappearance of ketenyl; however, it did decrease the amount of ketenyl produced by absorbing part of the excimer beam. An upper limit for the reaction rate of ketenyl with acetylene was determined using the pseudo first order rate constant of 45400 s^{-1} obtained by fitting an exponential to a ketenyl decay trace (Fig. 4.7) obtained in the presence of 3.65 Torr of acetylene. The upper bound for the second order rate constant of the acetylene-ketenyl reaction

Figure 4.7

Ketenyl transient absorption signal with 3.65 Torr acetylene. The $^{q}P_{0}(22)$ line at 2014.426 cm^{-1} was monitored here. The trace is the average over 2000 excimer shots. Signal to noise was sacrificed in this time scan to decrease the rate of the second order reaction which contributes to the decay.

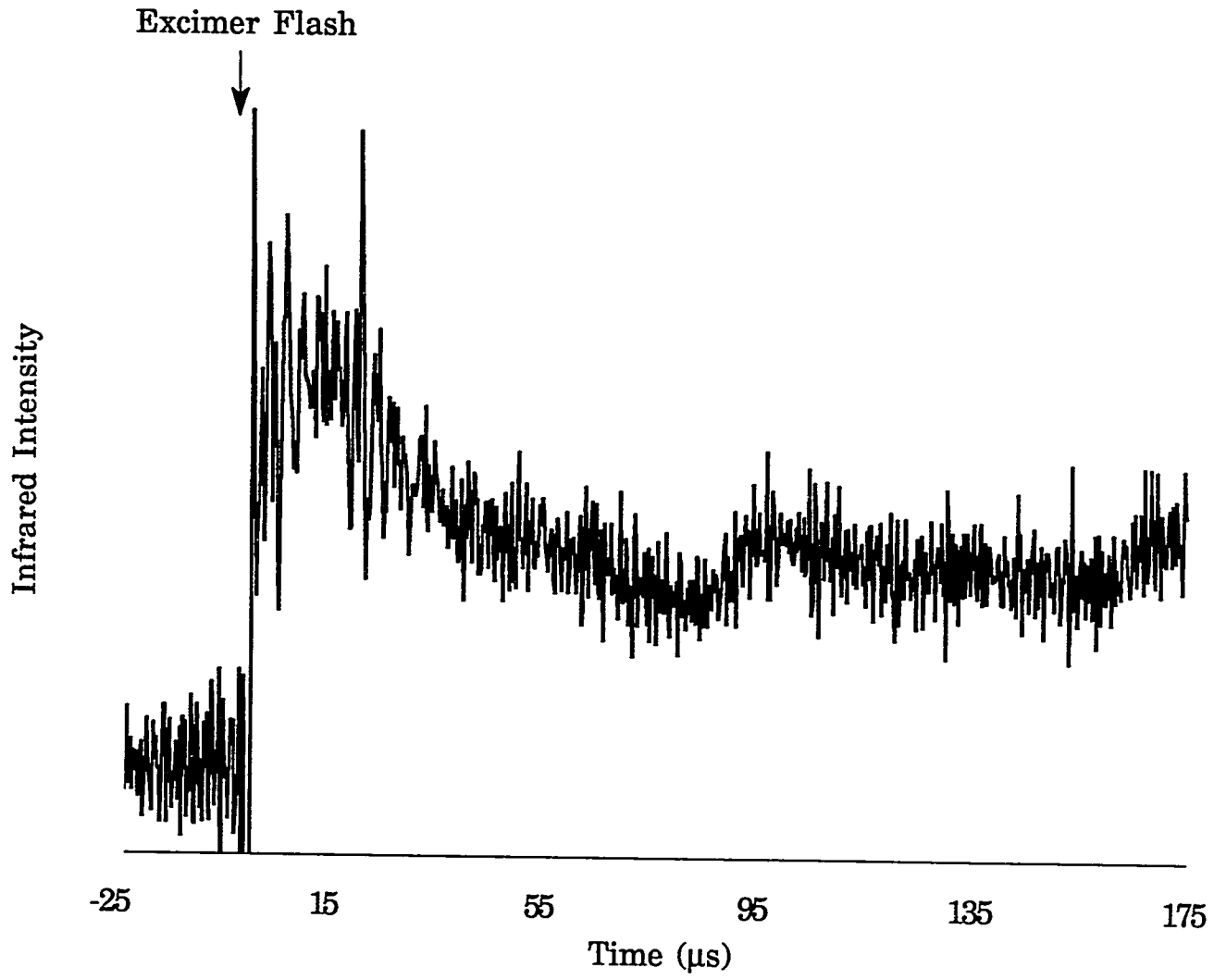
Excimer Flash
Infrared Intensity
-25
15
55
95
135
175
Time (μs)

was determined to be 3.8×10^{-13} $cm^3 molecule^{-1} s^{-1}$. Remember the pseudo first order rate was determined using a clearly non-exponential decay trace making the coefficients for the fit different using other portions of the trace for the fit. The upper bound above is based on the largest decay rate obtained from several fits on this time trace. This decay rate agrees with other traces obtained with low ketenyl pressures.

4.6 Reaction with Ethylene

Ethylene addition appeared to slow the ketenyl decay. Fig. 4.8 shows ketenyl decay with and without added ethylene. When ethylene was added, the ketenyl concentration directly after the excimer flash was less than when no ethylene was present. This was probably due to dilution of the ketene when the ethylene was added to the reactant stream. After the rapid rise the ketenyl concentration rapidly decreased, as when no ethylene was present, but leveled off earlier and at a higher concentration. This may be due to ethylene's reaction with and removal of a reactant in the ketenyl depletion reaction. One possible such reactant is atomic hydrogen produced with ketenyl by excimer photolysis (reaction 3.4a). The cause of the ketenyl decay needs to be better understood before the behavior caused by the ethylene can be properly explained.

Figure 4.8

Ketenyl transient absorption with and without added ethylene. The bold trace is ketenyl with ethylene. For this time trace the $^{q}P_{0}(22)$ line at 2014.426 cm^{-1} was monitored. Each trace is the average of transients obtained over 5000 excimer pulses. Ethylene pressure was 6.5 Torr and the total pressure was 28.8 Torr.

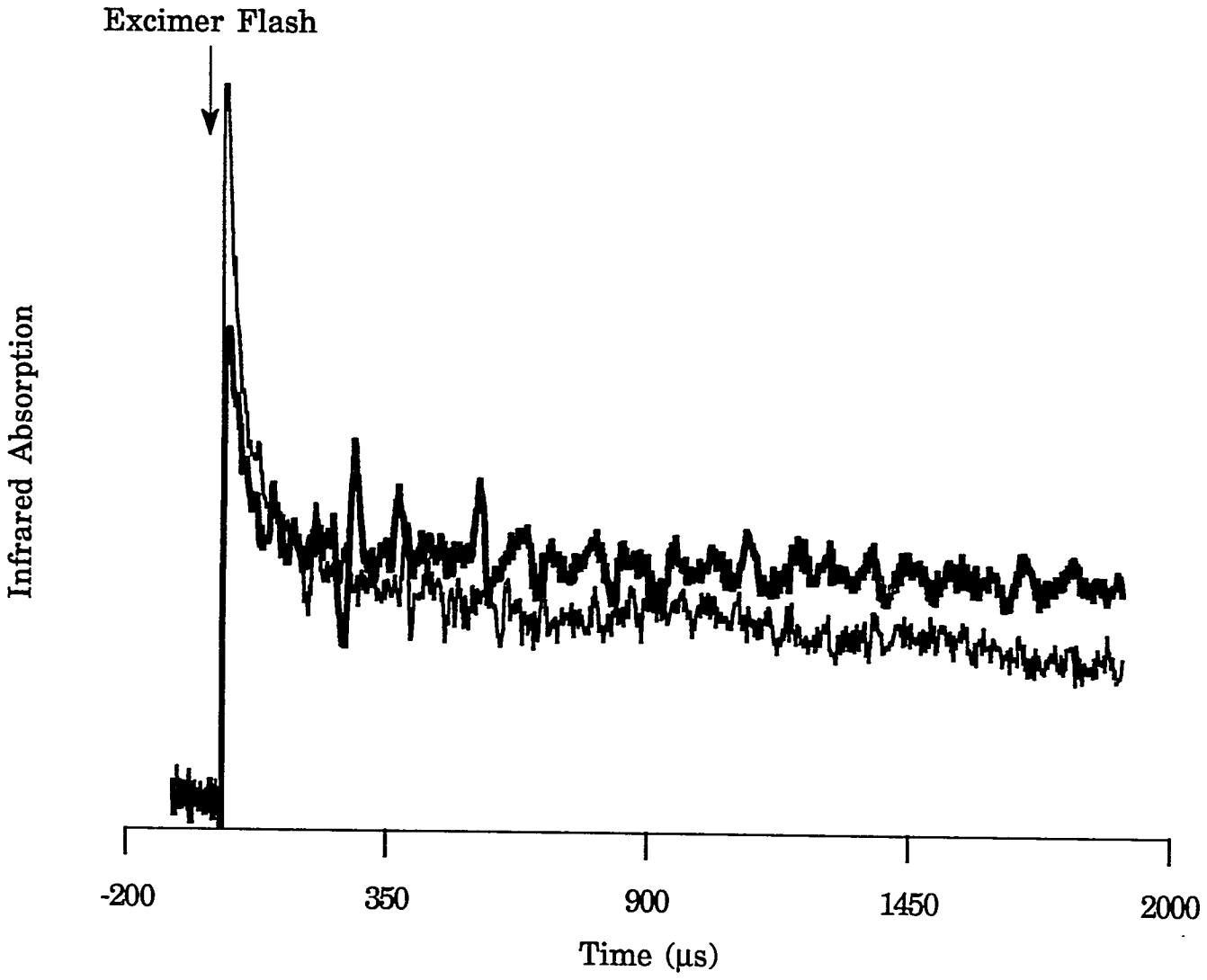
Excimer Flash
Infrared Absorption
-200
350
900
1450
2000
Time (μs)

4.7 Discussion

Observation of ketenyl infrared absorption has facilitated the study of ketenyl reactions by allowing direct probing of the radical concentration. In this work rates for ketenyl's reaction with nitric oxide, oxygen, and acetylene were measured by direct observation of ketenyl for the first time. There is still much to be learned about ketenyl reactions as well the kinetics of its production.

Lyman alpha monitoring of hydrogen atoms could be used determine the branching ratio in reaction 3.4. Hydrogen atoms are produced in the ketenyl channel 3.4a. CH_2, a product in channel 3.4b, can be converted to atomic hydrogen if molecular hydrogen is added by: $CH_2 + H_2 \rightarrow CH_3 + H$ Thus, the branching ratio could be determined from the relative concentrations of atomic hydrogen with and without added H_2.

More work needs to be done determining the products from ketenyl reactions. Some potential products can be observed with additional laser diodes (HCO, CO_2, etc.) and others with the color center laser spectrometer (OH). Also the reactions of ketenyl with the other photolysis products are of interest and remain relatively unexplored.

CHAPTER 5

CONCLUSION

The infrared kinetic spectroscopy technique has proved useful in the study of short-lived species and reactions involving short-lived species. Rapid, high concentration production of short-lived species using an excimer laser combined with the sensitivity provided by an infrared diode laser probe permitted the observation several short lived species and permitted the study of their reactions.

Using diode laser infrared kinetic spectroscopy, a search was made for the HNO molecule in the deNOx reaction system, NH_2+NO, at room temperature. No HNO attributable to the deNOx process was observed. This measurement eliminated a proposed reaction step used in the modelling of the process.

Also, much was learned about the ketenyl radical. In this work a new route to the ketenyl radical was discovered. The high resolution infrared spectrum of the heavy atom antisymmetric stretch of the ketenyl radical (HCCO) was observed. Reaction rate constants for ketenyl with several species present in the combustion environment, where ketenyl plays an important role, were determined. Ketenyl production by 193nm photolysis deserves further study as the CH_2/HCCO branching ratio remains unknown. It is possible that this can be measured using Lyman alpha absorption.

Reactions of ketenyl with the other photolysis products could be explored. For the reactions for which rate constants were measured, work to determine the reaction products could be done. Some potential products can be observed with additional laser diodes (HCO, CO_2, etc.) and others with the color center laser spectrometer (OH). With respect to ketenyl spectroscopy, the ketenyl radical's C-H stretch band may be accessible with the color center laser spectrometer. This band should exhibit strong perpendicular transitions which will permit the determination of additional molecular parameters describing the K structure in both the ground and excited state. DCCO should have transitions observable using the diode laser spectrometer, and the high resolution infrared DCCO spectra could also be studied.

REFERENCES

[1] C. B. Dane, D. R. Lander, R. F. Curl, F. K. Tittel, Y. Guo, M. I. F. Ochsner and C. B. Moore, *J. Chem. Phys.* **88**, 2121 (1988).

[2] D. R. Lander, K. G. Unfried, J. W. Stephens, G. P. Glass and R. F. Curl, *J. Phys. Chem.* **93**, 4109 (1989).

[3] C. B. Dane, Ph.D. Dissertation, Rice University, Houston, TX (1987).

[4] R. K. Lyon, US Patent 3,900,554. R. K. Lyon, *Environ. Sci. Technol.* **21**, 231 (1987).

[5] J. A. Miller, M. C. Branch and R. J. Kee, *Combust. Flame* **43**, 81 (1981). M. C. Branch, R. J. Kee and J. A. Miller, *Comb. Sci. and Tech.* **29**, 147 (1982).

[6] M. Gehring, K. Hoyermann, H. Schacke and J. Wolfrum, Symp *(Int.) Combust. [Proc.]* **14th**, 99 (1973).

[7] J. A. Silver and C. E. Kolb, *J. Phys. Chem.* **86**, 3240 (1982).

[8] P. Andersen, A. Jacobs, C. Kleinermanns and J. Wolfrum, *Symp. (Int.) Combust. [Proc.]* **19th**, 11 (1982).

[9] A. R. Whyte and L. F. Phillips, *J. Phys. Chem.* **88**, 5670 (1984).

[10] J. L. Hall, D. Zeitz, J. W. Stephens, J. V. V. Kasper, G. P. Glass, R. F. Curl and F. K. Tittel, *J. Phys. Chem.* **90**, 2501 (1986).

[11] D. A. Dolson, *J. Phys. Chem.* **90**, 6714 (1986).

[12] J. A. Silver and C. E. Kolb, *J. Phys. Chem.* **91**, 3714 (1987).

[13] B. Atakan, A. Jacobs, M. Wahl, R. Weller and J. Wolfrum, *Chem. Phys. Lett.* **155**, 609 (1989).

[14] L. A. Curtiss, D. L. Drapcho and J. A. Pople, *Chem. Phys. Lett.* **103**, 437 (1984).

[15] S. P.Walch, R. J. Duchovic and C. M. Rohlfing, *J. Chem. Phys.* **90**, 3230 (1989).

[16] OH was searched for and not observed by L. J. Stief, W. D. Brobst, D. F. Nava, R. P. Borkowski and J. V. Michael, *J. Chem. Soc., Farad Trans.* **2 78**, 1391 (1982).

[17] L. S. Rothman, AFGL Atmospheric Absorption Line Parameters Compilation (1982).

[18] R. A. Toth, private communication.

[19] J. A. Miller and C. T. Bowman, *Prog. Energy. Combust. Sci.* **15**, 287 (1989).

[20] L. F. Phillips, *Chem. Phys. Letters* **135**, 269 (1987)
[21] J. Peeters, M. Schaekers, and C. Vinckier, *J. Phys. Chem.* **90**, 6552 (1986).
[22] J. V. Michael and A. F. Wagner, *J. Phys. Chem.* **94**, 2453 (1990).
[23] J. Warnatz, *Combustion Chemistry*, W. C. Gardiner, Ed. p. 197 (Springer - Verlag, New York, 1984).
[24] C. Vinckier, M. Schaekers, and J. Peeters, *J. Phys. Chem.* **89**, 508 (1985) .
[25] Y. Endo, and E. Hirota, *J. Chem. Phys.* **86**, 4319 (1987).
[26] G. Inoue and M. Suzuki, *J. Chem. Phys.* **84** 3709 (1986).
[27] G. Inoue and M. Suzuki, *J. Chem. Phys.* **92**, 815 (1990).
[28] M. A. Hanratty and H. H. Nelson, *J. Chem. Phys.* **92**, 814 (1990).
[29] M. Jacox, and B. Olson, *J. Chem. Phys.* **86**, 3134 (1987).
[30] J. L. Duncan, A. M. Ferguson, J. Harper, K. H. Tonge and F. Hegelund, *J. Mol. Spec.* **122**, 72 (1987).
[31] H. Bitto, I. Chen, and C. B. Moore, *J. Chem. Phys.* **85**, 5101 (1986).
[32] D. Nesbitt, H. Petek, M. Foltz, S. Filseth, D. Bamford, and C. B. Moore, *J. Chem. Phys.* **83**, 223 (1985).
[33] W. Braun, A. Bass, and M. Pilling, *J. Chem. Phys.* **52**, 5131 (1970).
[34] R. Norrish, H. Crone, and O. Saltmarsh, *J. Chem. Soc.* 1533 (1933).
[35] T. J. Sears, *Comput. Phys. Commun.* **34**, 123 (1984).
[36] L. B. Harding and A. F. Wagner, *J. Phys. Chem.* **90**, 2974 (1986).
[37] Previous analysis reported less than 1% acetone after filtering. J. W. Stephens, J. L. Hall, H. Solka, W-B. Yan, R. F. Curl and G. P. Glass, *J. Phys. Chem.* **91**, 5740 (1987).

APPENDIX I

The following is a list of the measured frequencies of HCCO heavy atom antisymmetric stretch recorded at Rice University with a diode laser spectrometer between 1995 and 2045 cm^{-1}. Each transition is labeled with P, X, N and K for the upper and lower energy levels. The total angular momentum quantum number, J, is given by N + X. N and K are the rotational quantum numbers in the prolate limit ($K=K_a$) and P is the parity of K_c (0 for even and 1 for odd).

P'	X'	N'	K'	P"	X"	N"	K"	ν(cm^{-1})	Obs.-Calc.
1	0.5	33	0	0	0.5	34	0	1995.3514	-0.0113
0	0.5	32	0	1	0.5	33	0	1996.2338	-0.0103
1	0.5	31	0	0	0.5	32	0	1997.1104	-0.0103
1	0.5	25	0	0	0.5	26	0	2002.2610	-0.0199
0	0.5	24	0	1	0.5	25	0	2003.1241	-0.0002
0	0.5	22	0	1	0.5	23	0	2004.7984	0.0016
1	0.5	21	0	0	0.5	22	0	2005.6267	0.0009
0	0.5	20	0	1	0.5	21	0	2006.4469	-0.0032
1	0.5	19	0	0	0.5	20	0	2007.2692	-0.0006
1	0.5	17	0	0	0.5	18	0	2008.8901	-0.0040
0	0.5	16	0	1	0.5	17	0	2009.7000	0.0008
1	0.5	15	0	0	0.5	16	0	2010.4983	-0.0011
0	0.5	14	0	1	0.5	15	0	2011.2882	-0.0066
1	0.5	13	0	0	0.5	14	0	2012.0984	0.0130
1	0.5	11	0	0	0.5	12	0	2013.6516	-0.0005
0	0.5	10	0	1	0.5	11	0	2014.4257	-0.0025
1	0.5	9	0	0	0.5	10	0	2015.2020	0.0025
0	0.5	8	0	1	0.5	9	0	2015.9643	-0.0016
1	0.5	7	0	0	0.5	8	0	2016.7283	0.0009
0	0.5	6	0	1	0.5	7	0	2017.4811	-0.0030
1	0.5	5	0	0	0.5	6	0	2018.2335	-0.0025
0	0.5	4	0	1	0.5	5	0	2018.9830	0.0001
1	0.5	3	0	0	0.5	4	0	2019.7250	-0.0000
0	0.5	2	0	1	0.5	3	0	2020.4636	0.0013

P'	X'	N'	K'	P"	X"	N"	K"	ν(cm^{-1})	Obs.-Calc.
1	0.5	1	0	0	0.5	2	0	2021.1940	-0.0006
0	0.5	2	0	1	0.5	1	0	2024.0765	0.0018
1	0.5	3	0	0	0.5	2	0	2024.7793	-0.0034
0	0.5	4	0	1	0.5	3	0	2025.4838	-0.0019
1	0.5	5	0	0	0.5	4	0	2026.1808	-0.0030
0	0.5	6	0	1	0.5	5	0	2026.8755	-0.0015
1	0.5	7	0	0	0.5	6	0	2027.5668	0.0015
0	0.5	8	0	1	0.5	7	0	2028.2498	0.0011
1	0.5	9	0	0	0.5	8	0	2028.9282	0.0010
0	0.5	10	0	1	0.5	9	0	2029.6002	-0.0006
1	0.5	11	0	0	0.5	10	0	2030.2724	0.0029
0	0.5	12	0	1	0.5	11	0	2030.9336	0.0004
1	0.5	13	0	0	0.5	12	0	2031.5931	0.0011
0	0.5	14	0	1	0.5	13	0	2032.2480	0.0021
1	0.5	15	0	0	0.5	14	0	2032.8980	0.0031
0	0.5	16	0	1	0.5	15	0	2033.5431	0.0042
1	0.5	17	0	0	0.5	16	0	2034.1796	0.0016
0	0.5	18	0	1	0.5	17	0	2034.8136	0.0014
1	0.5	19	0	0	0.5	18	0	2035.4424	0.0010
0	0.5	20	0	1	0.5	19	0	2036.0651	-0.0007
1	0.5	21	0	0	0.5	20	0	2036.6755	-0.0096
0	0.5	22	0	1	0.5	21	0	2037.3038	0.0042
1	0.5	23	0	0	0.5	22	0	2037.9128	0.0038
0	0.5	24	0	1	0.5	23	0	2038.5171	0.0035

P'	X'	N'	K'	P"	X"	N"	K"	ν(cm^{-1})	Obs.-Calc.
1	0.5	25	0	0	0.5	24	0	2039.1162	0.0030
1	0.5	29	0	0	0.5	28	0	2041.4684	0.0062
0	0.5	30	0	1	0.5	29	0	2042.0432	0.0061
1	0.5	31	0	0	0.5	30	0	2042.6102	0.0032
0	0.5	32	0	1	0.5	31	0	2043.1848	0.0128
1	0.5	33	0	0	0.5	32	0	2043.7430	0.0110
1	-0.5	33	0	0	-0.5	34	0	1995.3514	-0.0120
0	-0.5	32	0	1	-0.5	33	0	1996.2338	-0.0107
1	-0.5	31	0	0	-0.5	32	0	1997.1104	-0.0106
1	-0.5	25	0	0	-0.5	26	0	2002.2610	-0.0196
0	-0.5	24	0	1	-0.5	25	0	2003.1241	0.0001
0	-0.5	22	0	1	-0.5	23	0	2004.7984	0.0021
1	-0.5	21	0	0	-0.5	22	0	2005.6267	0.0013
0	-0.5	20	0	1	-0.5	21	0	2006.4469	-0.0027
1	-0.5	19	0	0	-0.5	20	0	2007.2692	0.0001
1	-0.5	17	0	0	-0.5	18	0	2008.8901	-0.0035
0	-0.5	16	0	1	-0.5	17	0	2009.7000	0.0014
1	-0.5	15	0	0	-0.5	16	0	2010.4983	-0.0006
0	-0.5	14	0	1	-0.5	15	0	2011.2882	-0.0061
1	-0.5	13	0	0	-0.5	14	0	2012.0984	0.0135
1	-0.5	11	0	0	-0.5	12	0	2013.6516	0.0000
0	-0.5	10	0	1	-0.5	11	0	2014.4257	-0.0020
1	-0.5	9	0	0	-0.5	10	0	2015.2020	0.0030
0	-0.5	8	0	1	-0.5	9	0	2015.9643	-0.0011

P'	X'	N'	K'	P"	X"	N"	K"	ν(cm^{-1})	Obs.-Calc.
1	-0.5	7	0	0	-0.5	8	0	2016.7283	0.0014
0	-0.5	6	0	1	-0.5	7	0	2017.4811	-0.0025
1	-0.5	5	0	0	-0.5	6	0	2018.2335	-0.0020
0	-0.5	4	0	1	-0.5	5	0	2018.9830	0.0006
1	-0.5	3	0	0	-0.5	4	0	2019.7250	0.0004
0	-0.5	2	0	1	-0.5	3	0	2020.4636	0.0018
1	-0.5	1	0	0	-0.5	2	0	2021.1940	-0.0001
0	-0.5	2	0	1	-0.5	1	0	2024.0765	0.0013
1	-0.5	3	0	0	-0.5	2	0	2024.7793	-0.0038
0	-0.5	4	0	1	-0.5	3	0	2025.4838	-0.0023
1	-0.5	5	0	0	-0.5	4	0	2026.1808	-0.0034
0	-0.5	6	0	1	-0.5	5	0	2026.8755	-0.0019
1	-0.5	7	0	0	-0.5	6	0	2027.5668	0.0010
0	-0.5	8	0	1	-0.5	7	0	2028.2498	0.0006
1	-0.5	9	0	0	-0.5	8	0	2028.9282	0.0006
0	-0.5	10	0	1	-0.5	9	0	2029.6002	-0.0010
1	-0.5	11	0	0	-0.5	10	0	2030.2724	0.0025
0	-0.5	12	0	1	-0.5	11	0	2030.9336	0.0000
1	-0.5	13	0	0	-0.5	12	0	2031.5931	0.0007
0	-0.5	14	0	1	-0.5	13	0	2032.2480	0.0017
1	-0.5	15	0	0	-0.5	14	0	2032.8980	0.0028
0	-0.5	16	0	1	-0.5	15	0	2033.5431	0.0038
1	-0.5	17	0	0	-0.5	16	0	2034.1796	0.0012
0	-0.5	18	0	1	-0.5	17	0	2034.8136	0.0011

P'	X'	N'	K'	P"	X"	N"	K"	ν(cm^{-1})	Obs.-Calc.
1	-0.5	19	0	0	-0.5	18	0	2035.4424	0.0006
0	-0.5	20	0	1	-0.5	19	0	2036.0651	-0.0009
1	-0.5	21	0	0	-0.5	20	0	2036.6755	-0.0099
0	-0.5	22	0	1	-0.5	21	0	2037.3038	0.0040
1	-0.5	23	0	0	-0.5	22	0	2037.9128	0.0035
0	-0.5	24	0	1	-0.5	23	0	2038.5171	0.0033
1	-0.5	25	0	0	-0.5	24	0	2039.1162	0.0028
1	-0.5	29	0	0	-0.5	28	0	2041.4684	0.0062
0	-0.5	30	0	1	-0.5	29	0	2042.0432	0.0062
1	-0.5	31	0	0	-0.5	30	0	2042.6102	0.0033
0	-0.5	32	0	1	-0.5	31	0	2043.1848	0.0130
1	-0.5	33	0	0	-0.5	32	0	2043.7430	0.0113
1	0.5	3	1	0	0.5	4	1	2016.1420	0.0029
1	0.5	5	1	0	0.5	6	1	2014.7662	-0.0012
1	0.5	6	1	0	0.5	7	1	2014.0320	-0.0027
1	0.5	7	1	0	0.5	8	1	2013.3694	0.0031
1	0.5	9	1	0	0.5	10	1	2011.9446	0.0125
1	0.5	10	1	0	0.5	11	1	2011.1373	0.0027
1	0.5	11	1	0	0.5	12	1	2010.4647	-0.0007
1	0.5	12	1	0	0.5	13	1	2009.6323	-0.0038
1	0.5	13	1	0	0.5	14	1	2008.9620	-0.0061
1	0.5	14	1	0	0.5	15	1	2008.1075	-0.0005
1	0.5	15	1	0	0.5	16	1	2007.4401	-0.0021
1	0.5	16	1	0	0.5	17	1	2006.5525	0.0006

P'	X'	N'	K'	P"	X"	N"	K"	ν(cm^{-1})	Obs.-Calc.
1	0.5	17	1	0	0.5	18	1	2005.8862	-0.0034
1	0.5	18	1	0	0.5	19	1	2004.9670	-0.0023
1	0.5	21	1	0	0.5	22	1	2002.7079	-0.0019
1	0.5	22	1	0	0.5	23	1	2001.7285	0.0001
0	0.5	3	1	1	0.5	4	1	2016.1273	0.0028
0	0.5	5	1	1	0.5	6	1	2014.7388	-0.0001
0	0.5	6	1	1	0.5	7	1	2014.0726	0.0017
0	0.5	7	1	1	0.5	8	1	2013.3271	0.0049
0	0.5	9	1	1	0.5	10	1	2011.8773	0.0053
0	0.5	10	1	1	0.5	11	1	2011.2104	0.0077
0	0.5	11	1	1	0.5	12	1	2010.3867	-0.0025
0	0.5	12	1	1	0.5	13	1	2009.7206	0.0001
0	0.5	13	1	1	0.5	14	1	2008.8712	-0.0045
0	0.5	14	1	1	0.5	15	1	2008.2079	-0.0007
0	0.5	15	1	1	0.5	16	1	2007.3311	-0.0022
0	0.5	16	1	1	0.5	17	1	2006.6697	0.0005
0	0.5	17	1	1	0.5	18	1	2005.7593	-0.0045
0	0.5	18	1	1	0.5	19	1	2005.1007	-0.0031
0	0.5	21	1	1	0.5	22	1	2002.5472	-0.0007
0	0.5	22	1	1	0.5	23	1	2001.8997	-0.0004
1	-0.5	4	1	0	-0.5	5	1	2017.0493	0.0006
1	-0.5	5	1	0	-0.5	6	1	2016.2692	-0.0023
1	-0.5	6	1	0	-0.5	7	1	2015.4380	0.0035
1	-0.5	7	1	0	-0.5	8	1	2014.6670	-0.0010

P'	X'	N'	K'	P"	X"	N"	K"	ν(cm^{-1})	Obs.-Calc.
1	-0.5	8	1	0	-0.5	9	1	2013.8165	0.0047
1	-0.5	10	1	0	-0.5	11	1	2012.1967	0.0128
1	-0.5	11	1	0	-0.5	12	1	2011.4358	-0.0098
1	-0.5	12	1	0	-0.5	13	1	2010.5525	0.0024
1	-0.5	13	1	0	-0.5	14	1	2009.8231	-0.0022
1	-0.5	14	1	0	-0.5	15	1	2008.9050	-0.0035
1	-0.5	15	1	0	-0.5	16	1	2008.1973	0.0012
1	-0.5	16	1	0	-0.5	17	1	2007.2570	0.0002
1	-0.5	17	1	0	-0.5	18	1	2006.5525	-0.0035
1	-0.5	18	1	0	-0.5	19	1	2005.5916	-0.0011
1	-0.5	19	1	0	-0.5	20	1	2004.9037	0.0004
1	-0.5	21	1	0	-0.5	22	1	2003.2340	-0.0027
1	-0.5	22	1	0	-0.5	23	1	2002.2209	-0.0000
1	-0.5	23	1	0	-0.5	24	1	2001.5590	0.0041
0	-0.5	3	1	1	-0.5	4	1	2017.8535	0.0038
0	-0.5	4	1	1	-0.5	5	1	2017.0676	-0.0025
0	-0.5	5	1	1	-0.5	6	1	2016.2405	-0.0026
0	-0.5	6	1	1	-0.5	7	1	2015.4639	-0.0067
0	-0.5	7	1	1	-0.5	8	1	2014.6222	-0.0016
0	-0.5	8	1	1	-0.5	9	1	2013.8630	-0.0012
0	-0.5	10	1	1	-0.5	11	1	2012.2557	0.0025
0	-0.5	11	1	1	-0.5	12	1	2011.3680	0.0002
0	-0.5	12	1	1	-0.5	13	1	2010.6375	0.0011
0	-0.5	13	1	1	-0.5	14	1	2009.7286	-0.0019

P'	X'	N'	K'	P"	X"	N"	K"	ν(cm^{-1})	Obs.-Calc.
0	-0.5	14	1	1	-0.5	15	1	2009.0148	0.0029
0	-0.5	15	1	1	-0.5	16	1	2008.0883	0.0042
0	-0.5	16	1	1	-0.5	17	1	2007.3760	-0.0015
0	-0.5	17	1	1	-0.5	18	1	2006.4240	-0.0024
0	-0.5	18	1	1	-0.5	19	1	2005.7300	-0.0013
0	-0.5	19	1	1	-0.5	20	1	2004.7554	-0.0001
0	-0.5	21	1	1	-0.5	22	1	2003.0632	-0.0066
0	-0.5	22	1	1	-0.5	23	1	2002.3994	0.0016
1	0.5	5	1	0	0.5	4	1	2022.9855	-0.0083
1	0.5	6	1	0	0.5	5	1	2023.7040	-0.0026
1	0.5	7	1	0	0.5	6	1	2024.3966	0.0019
1	0.5	8	1	0	0.5	7	1	2025.1074	-0.0001
1	0.5	9	1	0	0.5	8	1	2025.7858	-0.0005
1	0.5	10	1	0	0.5	9	1	2026.4930	-0.0017
1	0.5	11	1	0	0.5	10	1	2027.1642	0.0024
1	0.5	12	1	0	0.5	11	1	2027.8677	0.0046
1	0.5	13	1	0	0.5	12	1	2028.5204	0.0028
1	0.5	14	1	0	0.5	13	1	2029.2087	-0.0016
1	0.5	15	1	0	0.5	14	1	2029.8554	0.00334
1	0.5	16	1	0	0.5	15	1	2030.5349	-0.0002
1	0.5	17	1	0	0.5	16	1	2031.1620	-0.0025
1	0.5	18	1	0	0.5	17	1	2031.8354	-0.0018
1	0.5	19	1	0	0.5	18	1	2032.4556	0.0006
1	0.5	20	1	0	0.5	19	1	2033.1165	0.0002

P'	X'	N'	K'	P"	X"	N"	K"	ν(cm^{-1})	Obs.-Calc.
1	0.5	22	1	0	0.5	21	1	2034.3770	0.0048
1	0.5	23	1	0	0.5	22	1	2034.9709	0.0011
1	0.5	24	1	0	0.5	23	1	2035.6111	0.0061
0	0.5	5	1	1	0.5	4	1	2022.9955	-0.0081
0	0.5	6	1	1	0.5	5	1	2023.6930	-0.0018
0	0.5	7	1	1	0.5	6	1	2024.4105	0.0029
0	0.5	8	1	1	0.5	7	1	2025.0927	0.0005
0	0.5	9	1	1	0.5	8	1	2025.8003	-0.0029
0	0.5	10	1	1	0.5	9	1	2026.4762	-0.0002
0	0.5	11	1	1	0.5	10	1	2027.1832	0.0018
0	0.5	12	1	1	0.5	11	1	2027.8444	0.0021
0	0.5	13	1	1	0.5	12	1	2028.5406	0.0012
0	0.5	14	1	1	0.5	13	1	2029.1838	-0.0037
0	0.5	15	1	1	0.5	14	1	2029.8728	-0.0027
0	0.5	16	1	1	0.5	15	1	2030.5092	-0.0018
0	0.5	17	1	1	0.5	16	1	2031.1849	-0.0041
0	0.5	18	1	1	0.5	17	1	2031.8116	-0.0009
0	0.5	19	1	1	0.5	18	1	2032.4795	-0.0001
0	0.5	20	1	1	0.5	19	1	2033.0914	-0.0005
0	0.5	22	1	1	0.5	21	1	2034.3512	0.0019
0	0.5	23	1	1	0.5	22	1	2034.9984	0.0069
0	0.5	24	1	1	0.5	23	1	2035.5841	-0.0007
1	-0.5	4	1	0	-0.5	3	1	2023.1590	-0.0009
1	-0.5	5	1	0	-0.5	4	1	2023.8510	-0.0014

P'	X'	N'	K'	P"	X"	N"	K"	ν(cm^{-1})	Obs.-Calc.
1	-0.5	6	1	0	-0.5	5	1	2024.5546	-0.0007
1	-0.5	7	1	0	0.5	6	1	2025.2205	-0.0023
1	-0.5	8	1	0	-0.5	7	1	2025.9095	-0.0012
1	-0.5	9	1	0	-0.5	8	1	2026.5596	-0.0001
1	-0.5	10	1	0	-0.5	9	1	2027.2404	0.0037
1	-0.5	11	1	0	-0.5	10	1	2027.8677	-0.0040
1	-0.5	12	1	0	-0.5	11	1	2028.5406	0.0005
1	-0.5	13	1	0	-0.5	12	1	2029.1624	-0.0011
1	-0.5	14	1	0	-0.5	13	1	2029.8264	0.0024
1	-0.5	15	1	0	-0.5	14	1	2030.4402	0.0029
1	-0.5	16	1	0	-0.5	15	1	2031.0898	-0.0000
1	-0.5	17	1	0	-0.5	16	1	2031.7000	0.0062
1	-0.5	18	1	0	-0.5	17	1	2032.3398	0.0020
1	-0.5	19	1	0	-0.5	18	1	2032.9368	0.0036
1	-0.5	20	1	0	-0.5	19	1	2033.5690	0.0014
1	-0.5	21	1	0	-0.5	20	1	2034.1565	0.0013
1	-0.5	22	1	0	-0.5	21	1	2034.7770	-0.0017
1	-0.5	23	1	0	-0.5	22	1	2035.3599	0.0005
1	-0.5	24	1	0	-0.5	23	1	2035.9701	-0.0004
1	-0.5	25	1	0	-0.5	24	1	2036.5414	-0.0041
0	-0.5	4	1	1	-0.5	3	1	2023.1510	0.0002
0	-0.5	5	1	1	-0.5	4	1	2023.8630	-0.0004
0	-0.5	6	1	1	-0.5	5	1	2024.5404	-0.0021
0	-0.5	7	1	1	-0.5	6	1	2025.2382	0.0010

P'	X'	N'	K'	P"	X"	N"	K"	ν(cm^{-1})	Obs.-Calc.
0	-0.5	8	1	1	-0.5	7	1	2025.8917	-0.0031
0	-0.5	9	1	1	-0.5	8	1	2026.5767	-0.0001
0	-0.5	10	1	1	-0.5	9	1	2027.2213	0.0028
0	-0.5	11	1	1	-0.5	10	1	2027.8928	0.0018
0	-0.5	12	1	1	-0.5	11	1	2028.5204	0.0004
0	-0.5	13	1	1	-0.5	12	1	2029.1838	-0.0005
0	-0.5	14	1	1	-0.5	13	1	2029.8049	0.0023
0	-0.5	15	1	1	-0.5	14	1	2030.4595	0.0004
0	-0.5	16	1	1	-0.5	15	1	2031.0680	0.0003
0	-0.5	17	1	1	-0.5	16	1	2031.7170	0.0010
0	-0.5	18	1	1	-0.5	17	1	2032.3177	0.0020
0	-0.5	19	1	1	-0.5	18	1	2032.9579	0.0030
0	-0.5	22	1	1	-0.5	21	1	2034.7583	-0.0012
0	-0.5	23	1	1	-0.5	22	1	2035.3765	-0.0006
0	-0.5	24	1	1	-0.5	23	1	2035.9561	0.0014
0	-0.5	25	1	1	-0.5	24	1	2036.5529	-0.0062
0	0.5	9	2	1	0.5	10	2	2013.6555	-0.0065
0	0.5	11	2	1	0.5	12	2	2012.1963	0.0093
0	0.5	12	2	1	0.5	13	2	2011.4358	-0.0040
0	0.5	13	2	1	0.5	14	2	2010.6875	0.0010
0	0.5	14	2	1	0.5	15	2	2009.9254	-0.0008
0	0.5	15	2	1	0.5	16	2	2009.1576	-0.0023
0	0.5	16	2	1	0.5	17	2	2008.3833	-0.0030
0	0.5	17	2	1	0.5	18	2	2007.6034	-0.0034

P'	X'	N'	K'	P"	X"	N"	K"	ν(cm^{-1})	Obs.-Calc.
0	0.5	18	2	1	0.5	19	2	2006.8202	0.0005
0	0.5	19	2	1	0.5	20	2	2006.0256	-0.0011
0	0.5	20	2	1	0.5	21	2	2005.2260	0.0003
1	0.5	9	2	0	0.5	10	2	2013.6555	-0.0065
1	0.5	11	2	0	0.5	12	2	2012.1963	0.0094
1	0.5	12	2	0	0.5	13	2	2011.4358	-0.0041
1	0.5	13	2	0	0.5	14	2	2010.6875	0.0012
1	0.5	14	2	0	0.5	15	2	2009.9254	-0.0010
1	0.5	15	2	0	0.5	16	2	2009.1576	-0.0020
1	0.5	16	2	0	0.5	17	2	2008.3833	-0.0034
1	0.5	17	2	0	0.5	18	2	2007.6034	-0.0030
1	0.5	18	2	0	0.5	19	2	2006.8202	0.0000
1	0.5	19	2	0	0.5	20	2	2006.0256	-0.0006
1	0.5	20	2	0	0.5	21	2	2005.2260	-0.0004
0	-0.5	3	2	1	-0.5	4	2	2019.4337	-0.0043
0	-0.5	5	2	1	-0.5	6	2	2017.8818	0.0011
0	-0.5	6	2	1	-0.5	7	2	2017.0967	0.0020
0	-0.5	7	2	1	-0.5	8	2	2016.2992	-0.0055
0	-0.5	8	2	1	-0.5	9	2	2015.5162	0.0053
0	-0.5	9	2	1	-0.5	10	2	2014.7097	-0.0040
0	-0.5	10	2	1	-0.5	11	2	2013.9208	0.0078
0	-0.5	12	2	1	-0.5	13	2	2012.2990	-0.0029
0	-0.5	13	2	1	-0.5	14	2	2011.4895	-0.0019
0	-0.5	14	2	1	-0.5	15	2	2010.6750	-0.0020

P'	X'	N'	K'	P"	X"	N"	K"	ν(cm^{-1})	Obs.-Calc.
1	-0.5	3	2	0	-0.5	4	2	2019.4337	-0.0043
1	-0.5	5	2	0	-0.5	6	2	2017.8818	0.0016
1	-0.5	6	2	0	-0.5	7	2	2017.0967	0.0020
1	-0.5	7	2	0	-0.5	8	2	2016.2992	-0.0055
1	-0.5	8	2	0	-0.5	9	2	2015.5162	0.0050
1	-0.5	9	2	0	-0.5	10	2	2014.7097	-0.0039
1	-0.5	10	2	0	-0.5	11	2	2013.9208	0.0077
1	-0.5	12	2	0	-0.5	13	2	2012.2990	-0.0030
1	-0.5	13	2	0	-0.5	14	2	2011.4895	-0.0017
1	-0.5	14	2	0	-0.5	15	2	2010.6750	-0.0022
0	0.5	9	2	1	0.5	8	2	2027.6554	-0.0006
0	0.5	11	2	1	0.5	10	2	2029.0258	0.0043
0	0.5	12	2	1	0.5	11	2	2029.7012	0.0024
0	0.5	13	2	1	0.5	12	2	2030.3760	0.0042
0	0.5	14	2	1	0.5	13	2	2031.0399	-0.0005
0	0.5	15	2	1	0.5	14	2	2031.7000	-0.0039
0	0.5	16	2	1	0.5	15	2	2032.3619	-0.0007
0	0.5	17	2	1	0.5	16	2	2033.0151	-0.0004
0	0.5	18	2	1	0.5	17	2	2033.6708	0.0076
0	0.5	19	2	1	0.5	18	2	2034.3040	-0.0004
0	0.5	20	2	1	0.5	19	2	2034.9430	0.0028
1	0.5	9	2	0	0.5	8	2	2027.6554	-0.0006
1	0.5	11	2	0	0.5	10	2	2029.0258	0.0042
1	0.5	12	2	0	0.5	11	2	2029.7012	0.0024

P'	X'	N'	K'	P"	X"	N"	K"	ν(cm^{-1})	Obs.-Calc.
1	0.5	13	2	0	0.5	12	2	2030.3760	0.0041
1	0.5	14	2	0	0.5	13	2	2031.0399	-0.0004
1	0.5	15	2	0	0.5	14	2	2031.7000	-0.0041
1	0.5	16	2	0	0.5	15	2	2032.3619	-0.0005
1	0.5	17	2	0	0.5	16	2	2033.0151	-0.0006
1	0.5	18	2	0	0.5	17	2	2033.6708	0.0079
1	0.5	19	2	0	0.5	18	2	2034.3040	-0.0007
1	0.5	20	2	0	0.5	19	2	2034.9430	0.0032
0	-0.5	3	2	1	-0.5	2	2	2023.9398	-0.0043
0	-0.5	5	2	1	-0.5	4	2	2025.3777	0.0000
0	-0.5	6	2	1	-0.5	5	2	2026.0813	-0.0002
0	-0.5	7	2	1	-0.5	6	2	2026.7772	0.0002
0	-0.5	8	2	1	-0.5	7	2	2027.4683	0.0036
0	-0.5	9	2	1	-0.5	8	2	2028.1487	0.0037
0	-0.5	10	2	1	-0.5	9	2	2028.8197	0.0013
0	-0.5	11	2	1	-0.5	10	2	2029.4819	-0.0032
0	-0.5	12	2	1	-0.5	11	2	2030.1515	0.0060
0	-0.5	13	2	1	-0.5	12	2	2030.7985	-0.0012
0	-0.5	14	2	1	-0.5	13	2	2031.4440	-0.0041
1	-0.5	3	2	0	-0.5	2	2	2023.9398	-0.0043
1	-0.5	5	2	0	-0.5	4	2	2025.3777	0.0000
1	-0.5	6	2	0	-0.5	5	2	2026.0813	-0.0001
1	-0.5	7	2	0	-0.5	6	2	2026.7772	0.0002
1	-0.5	8	2	0	-0.5	7	2	2027.4683	0.0036

P'	X'	N'	K'	P"	X"	N"	K"	ν(cm^{-1})	Obs.-Calc.
1	-0.5	9	2	0	-0.5	8	2	2028.1487	0.0036
1	-0.5	10	2	0	-0.5	9	2	2028.8197	0.0013
1	-0.5	11	2	0	-0.5	10	2	2029.4819	-0.0033
1	-0.5	12	2	0	-0.5	11	2	2030.1515	0.0060
1	-0.5	13	2	0	-0.5	12	2	2030.7985	-0.0013
1	-0.5	14	2	0	-0.5	13	2	2031.4440	-0.0039
1	0.5	6	3	0	0.5	7	3	2015.9271	-0.0009
1	0.5	7	3	0	0.5	8	3	2015.2148	0.0026
1	0.5	8	3	0	0.5	9	3	2014.4888	-0.0029
1	0.5	9	3	0	0.5	10	3	2013.7700	0.0039
1	0.5	11	3	0	0.5	12	3	2012.2990	0.0005
1	0.5	14	3	0	0.5	15	3	2010.0547	0.0009
1	0.5	15	3	0	0.5	16	3	2009.2968	0.0030
1	0.5	16	3	0	0.5	17	3	2008.5264	-0.0016
1	0.5	17	3	0	0.5	18	3	2007.7504	-0.0058
1	0.5	19	3	0	0.5	20	3	2006.1935	-0.0021
1	0.5	20	3	0	0.5	21	3	2005.4099	0.0031
1	0.5	21	3	0	0.5	22	3	2004.6143	0.0018
0	0.5	6	3	1	0.5	7	3	2015.9271	-0.0009
0	0.5	7	3	1	0.5	8	3	2015.2148	0.0026
0	0.5	8	3	1	0.5	9	3	2014.4888	-0.0029
0	0.5	9	3	1	0.5	10	3	2013.7700	0.0039
0	0.5	11	3	1	0.5	12	3	2012.2990	0.0005
0	0.5	14	3	1	0.5	15	3	2010.0547	0.0009

P'	X'	N'	K'	P"	X"	N"	K"	ν(cm^{-1})	Obs.-Calc.
0	0.5	15	3	1	0.5	16	3	2009.2968	0.0030
0	0.5	16	3	1	0.5	17	3	2008.5264	-0.0016
0	0.5	17	3	1	0.5	18	3	2007.7504	-0.0058
0	0.5	19	3	1	0.5	20	3	2006.1935	-0.0021
0	0.5	20	3	1	0.5	21	3	2005.4099	0.0031
0	0.5	21	3	1	0.5	22	3	2004.6143	0.0018
1	-0.5	6	3	0	-0.5	7	3	2018.7058	-0.0006
1	-0.5	7	3	0	-0.5	8	3	2017.9075	-0.0082
1	-0.5	10	3	0	-0.5	11	3	2015.5105	-0.0080
1	-0.5	11	3	0	-0.5	12	3	2014.7158	0.0034
0	-0.5	6	3	1	-0.5	7	3	2018.7058	-0.0006
0	-0.5	7	3	1	-0.5	8	3	2017.9075	-0.0082
0	-0.5	10	3	1	-0.5	11	3	2015.5105	-0.0080
0	-0.5	11	3	1	-0.5	12	3	2014.7158	0.0034
1	0.5	6	3	0	0.5	5	3	2025.7267	-0.0024
1	0.5	7	3	0	0.5	6	3	2026.4221	-0.0010
1	0.5	8	3	0	0.5	7	3	2027.1169	0.0017
1	0.5	9	3	0	0.5	8	3	2027.8070	0.0021
1	0.5	10	3	0	0.5	9	3	2028.4922	0.0003
1	0.5	11	3	0	0.5	10	3	2029.1730	-0.0027
1	0.5	14	3	0	0.5	13	3	2031.2064	0.0016
1	0.5	15	3	0	0.5	14	3	2031.8792	0.0062
1	0.5	16	3	0	0.5	15	3	2032.5377	0.0010
1	0.5	17	3	0	0.5	16	3	2033.1954	-0.0004

P'	X'	N'	K'	P"	X"	N"	K"	ν(cm^{-1})	Obs.-Calc.
1	0.5	19	3	0	0.5	18	3	2034.5013	0.0011
1	0.5	20	3	0	0.5	19	3	2035.1439	-0.0014
1	0.5	21	3	0	0.5	20	3	2035.7872	0.0016
0	0.5	6	3	1	0.5	5	3	2025.7267	-0.0024
0	0.5	7	3	1	0.5	6	3	2026.4221	-0.0010
0	0.5	8	3	1	0.5	7	3	2027.1169	0.0017
0	0.5	9	3	1	0.5	8	3	2027.8070	0.0021
0	0.5	10	3	1	0.5	9	3	2028.4922	0.0003
0	0.5	11	3	1	0.5	10	3	2029.1730	-0.0027
0	0.5	14	3	1	0.5	13	3	2031.2064	0.0016
0	0.5	15	3	1	0.5	14	3	2031.8792	0.0062
0	0.5	16	3	1	0.5	15	3	2032.5377	0.0010
0	0.5	17	3	1	0.5	16	3	2033.1954	-0.0004
0	0.5	19	3	1	0.5	18	3	2034.5013	0.0011
0	0.5	20	3	1	0.5	19	3	2035.1439	-0.0014
0	0.5	21	3	1	0.5	20	3	2035.7872	0.0016
1	-0.5	6	3	0	-0.5	5	3	2027.6554	0.0059
1	-0.5	7	3	0	-0.5	6	3	2028.3442	0.0030
1	-0.5	8	3	0	-0.5	7	3	2029.0258	0.0003
1	-0.5	9	3	0	-0.5	8	3	2029.7012	-0.0016
1	-0.5	10	3	0	-0.5	9	3	2030.3760	0.0023
1	-0.5	11	3	0	-0.5	10	3	2031.0399	0.0014
0	-0.5	6	3	1	-0.5	5	3	2027.6554	0.0059
0	-0.5	7	3	1	-0.5	6	3	2028.3442	0.0030

P'	X'	N'	K'	P"	X"	N"	K"	ν(cm^{-1})	Obs.-Calc.
0	-0.5	8	3	1	-0.5	7	3	2029.0258	0.0003
0	-0.5	9	3	1	-0.5	8	3	2029.7012	-0.0016
0	-0.5	10	3	1	-0.5	9	3	2030.3760	0.0023
0	-0.5	11	3	1	-0.5	10	3	2031.0399	0.0014

APPENDIX II

The following is a listing of the two programs used to fit the ketenyl spectra. The first program "AROT" reads two input files; for001.dat which contains the initial "guessed" values and errors of the molecular parameters and for002.dat which contains a listing of the frequencies and assignments of the transitions to be fit. AROT creates two files. One is fort.3 which contains a prediction based on the input constants and errors associated with the fit. The second is fort.4 which contains derivitives to be used in the second program "FITDAT". FITDAT reads fort.3, fort.4 and for007.dat which contains weighting, scaling and number of eigenvalues information. FITDAT creates three files. NEW.CON contains new molecular constants determined from the derivitives and errors. FIT.DAT contains information about the fit: eigenvectors, eigenvalues, errors etc. fort.8 contains a covariance matrix. The program AROT is a modified version of ASYR created and used by Bent Dane for fitting HCO. FITDAT also created by Brent Dane was used unchanged. For the ketenyl fitting these programs were run on a Silicon Graphics Irix workstation.

```
      PROGRAM AROT
C+
C A program to produce a derivative and observed-calculated matrices
from
C   a set of experimental observations for the purpose of least-
squaring.
C   It is set up for an asymmetric top doublet molecule and uses
Watson's
C   A-reduction formulation of the Hamiltonian.
C
C Required subroutines:
PRDICT,E,EWORK,SP2,SPA2,SPASA,SPDOTS,SPOD,SPSAB,
C
SPSOD,SR,SIXJ,THREEJ,GMPRD,GMSUM,GMSCAL,IDENT,DIAG,EIGEN,HFDER,GETDER,
C   XPOSE,XFORM
C
C       Date:   01-JUL-87
C       Author: bd, RFC
C       Mod:3/15/91 RFC
C
C Description of common block variables:
C
C       CONST   Molecular parameters of lower and upper states.
C                  1  A-(B+C)/2          13  LK
C                  2  (B+C)/2            14  presently unused
C                  3  (B-C)/4            15  eAA-0.5*(eBB+eCC)
C                  4  DK                 16  0.5*(eBB+eCC)
C                  5  DJK                17  (eBB-eCC)/2
C                  6  DJ                 18  eAB
C                  7  d1                 19  DKS
C                  8  d2                 20  DJKS
C                  9  HK                 21  DJS
C                 10  HKJ                22  DKJS
C                 11  HJK                23  dJS
C                 12  HJ                 24  HKS
C       ORIGIN  Transition band center.
C       IP      Parity of KC (2 if not resolved).
C       N       Rotational quantum number N.
C       K       Rotational quantum number KA.
C       X       0.5 or -0.5 where J=N+X.
C       IW      0 for lower state, 1 for upper.
C       OBS     Experimentally observed transition frequency.
C       ENGY    Calculated energy level.
C       IC      Flag indicating whether an energy has been calculated.
C       DERIV   Derivatives with respect to each parameter.
C                  1-24  lower state.
C                 25-48  upper state.
C                    49  band origin.
C       DIFF    Observed-calculated for each transition.
C       NM      Number of energies calculated in a given
diagonalization.
C       IPCA    Parity labels for calculated energies.
C       NCA     N quantum numbers.
C       KCA     KA quantum numbers.
C       XCA     JC=NC+XC.
C       IWCA    0 for lower state energies, 1 for upper state.
```

```
C       DG      Energies returned on diagonal of diagonalized
Hamiltonian.
C       EDER    Derivatives with repect to each parameter for calculated
C                 energies.
C-
        IMPLICIT DOUBLE PRECISION (A-H,O-Z)
        DIMENSION IDER(2),WF(1200),SQS(10),WGT(10),NTR(10),SC(49)
C
        COMMON/CON/CONST(2,25),ORIGIN
        COMMON/DATA/IP(2,1200),N(2,1200),K(2,1200),X(2,1200),IW(2,1200),
&     OBS(1200)
        COMMON/PRED/ENGY(2,1200),IC(2,1200)
        COMMON/DER/DERIV(2,1200,50),DIFF(1200)
        COMMON/MAT/NM,IPCA(100),NCA(100),KCA(100),XCA(100),IWCA(100),
&     DG(100),EDER(100,24)
C
C Read original constants from constant file (FOR001.DAT).
C
      open(1,file='for001.dat')
        DO 100 I=1,2
          DO 90 J=1,24
            READ(1,*) CONST(I,J)
  90      CONTINUE
 100    CONTINUE
        READ(1,*) ORIGIN
        READ(1,*) SC
        CLOSE(1)
C
C Options?
C
        open(2,file='for002.dat')
        READ(2,*) ILEV  !1 to create energy level file.
        READ(2,*) IDER  !1 to calculate derivatives (dimension 2).
C
C Read observed transitions and assignments (FOR002.DAT).
C
        I=1
 110    READ(2,*,END=130) IP(1,I),X(1,I),N(1,I),K(1,I),IDN,IDK,IDW,
&     OBS(I),WF(I),IFIT
        IF(IFIT.EQ.0) GOTO 110
        IF(IP(1,I).EQ.2) THEN
          IP(1,I)=1
          IP(2,I)=2
        ELSE
          IP(1,I)=IAND(IP(1,I)+K(1,I),1)
          IP(2,I)=1-IP(1,I)
        ENDIF
        X(2,I)=X(1,I)
        N(2,I)=N(1,I)+IDN
        K(2,I)=K(1,I)+IDK
        IW(1,I)=0
        IW(2,I)=IDW
        I=I+1
        GOTO 110
C
 130    NLIN=I-1
        CLOSE(2)
```

```
C
C Predict energies from initial constants for each transition.
C

      CALL PRDICT(0,NLIN,IDER)
      CALL PRDICT(1,NLIN,IDER)
C
C Zero sums and sort weights.
C
        SQ=0.D0
        SQW=0.D0
        WTMAX=0.D0
        DO 140 I=1,10
          WGT(I)=0.D0
          SQS(I)=0.D0
          NTR(I)=0
 140    CONTINUE
C
        NWT=0
        DO 160 I=1,NLIN
        IF(WF(I).GT.WTMAX) WTMAX=WF(I)
          DO 150 J=1,NWT
            IF(WF(I).EQ.WGT(J)) GOTO 155
 150      CONTINUE
          NWT=NWT+1
          WGT(NWT)=WF(I)
          J=NWT
 155      NTR(J)=NTR(J)+1
 160    CONTINUE
C
C Write constants to FOR003.DAT.
C
        WRITE(3,1600) 0,ORIGIN,SC(49)
1600    FORMAT(' ',I2,2X,E22.15,28X,E11.4)
        DO 210 I=1,24
 210      WRITE(3,1800) I,(CONST(J,I),J=2,1,-1),SC(I+24),SC(I)
1800    FORMAT(' ',I2,2(2X,E22.15),2X,2(2X,E11.4))
C
C Compute transition frequencies, obs-calc, and output to FOR003.DAT.
C
        DO 190 I=1,NLIN
          CALC=ENGY(2,I)-ENGY(1,I)
          DIFF(I)=OBS(I)-CALC
          SQ=DIFF(I)**2+SQ
          SQW=(WF(I)*DIFF(I))**2+SQW
          DO 170 J=1,NWT
 170        IF(WF(I).EQ.WGT(J)) SQS(J)=DIFF(I)**2+SQS(J)
          DO 180 J=1,48
            DERIV(1,I,J)=DERIV(2,I,J)-DERIV(1,I,J)
            IF(IW(1,I).NE.IW(2,I)) DERIV(1,I,49)=1.D0
 180      CONTINUE
          WRITE(3,1000) 1,WF(I),IP(2,I),X(2,I),N(2,I),K(2,I),IW(2,I),
&     IP(1,I),X(1,I),N(1,I),K(1,I),IW(1,I),OBS(I),CALC,DIFF(I)
1000      FORMAT(' ',I1,X,E6.1,3X,2(I1,1X,F4.1,1X,I2,1X,I1,1X,I1,3X),
&     2(F12.4,1X),F11.6)
 190    CONTINUE
C
```

```
C Calculate and write standard deviations.
C
        SQ=DSQRT(SQ/NLIN)
        SQW=DSQRT(SQW/NLIN)
        WRITE(3,1200) SQ,SQW,SQW/WTMAX
1200    FORMAT(/' Unweighted ',E8.2,6X,'Weighted ',E8.2,6X,
&     'Weighted/Max.wt. ',E8.2/)
        WRITE(3,*) 'Weight            St. dev.        # obs.'
        WRITE(3,*) '----------------------------------------'
        DO 200 I=1,NWT
          WRITE(3,1400)WGT(I),DSQRT(SQS(I)/NTR(I)),NTR(I)
1400      FORMAT(' ',E8.2,10X,E8.2,10X,I3)
 200    CONTINUE
C
C Write energy levels to FOR007.DAT.
C
        IF(ILEV.NE.0) THEN
          WRITE(7,*) NLIN
          DO 230 I=1,2
            DO 220 J=1,NLIN
              WRITE(7,2000) IP(I,J),X(I,J),N(I,J),K(I,J),IW(I,J),
&       ENGY(I,J)
2000          FORMAT(' ',I1,4X,F4.1,4X,I2,4X,I2,4X,I1,4X,F10.4)
 220        CONTINUE
            WRITE(7,*) ' '
 230      CONTINUE
        ENDIF
C
C Write derivatives and obs-calc to FOR004.DAT.
C
        IF((IDER(1).EQ.0).AND.(IDER(2).EQ.0)) GOTO 900
        WRITE(4,*) NLIN,0
        WRITE(4,*) ((DERIV(1,I,J),J=1,50),I=1,NLIN)
        WRITE(4,*) (DIFF(I),I=1,NLIN)
C
 900    CALL EXIT
        END
C
C-----------------------------------------------------------------------
C

        SUBROUTINE PRDICT(IWR,NLIN,IDER)
C+
C A subroutine to predict energy levels for a set of experimentally
observed
C   transitions.
C
C Arguments:
C
C       IWR     0 for lower state, 1 for upper.
C       NLIN    Number of transitions.
C       IDER    1 to calculate derivatives as well as energies.
C-
        IMPLICIT DOUBLE PRECISION (A-H,O-Z)
        DIMENSION EIVEC(82,82),IDER(2)
C
        COMMON/CON/CONST(2,25),ORIGIN
```

```
        COMMON/DATA/IP(2,1200),N(2,1200),K(2,1200),X(2,1200),IW(2,1200),
&     OBS(1200)
        COMMON/PRED/ENGY(2,1200),IC(2,1200)
        COMMON/DER/DERIV(2,1200,50),DIFF(1200)
        COMMON/MAT/NM,IPCA(100),NCA(100),KCA(100),XCA(100),IWCA(100),
&     DG(100),EDER(100,24)
C
C Reset calculation flag for each energy level.
C
      DO 100 I=1,2
        DO 100 J=1,NLIN
 100    IC(I,J)=0
C
C Look only at levels having IW=IWR.
C
        DO 600 L=1,NLIN*2
C
          ICALC=0
          IASS=0
          DO 500 IST=1,2
            DO 400 I=1,NLIN
              IF((IC(IST,I).EQ.1).OR.(IW(IST,I).NE.IWR)) GOTO 400
              IF(ICALC.EQ.0) THEN
                IPWRK=IAND(IP(IST,I),1)
            CALL E(IW(IST,I),N(IST,I),X(IST,I),IPWRK,EIVEC,IDER)
            ICALC=1
                IASS=1
              ENDIF
              DO 300 J=1,NM
                IF(NCA(J) .NE.N(IST,I))  GOTO 300
                IF(KCA(J) .NE.K(IST,I))  GOTO 300
                IF(XCA(J) .NE.X(IST,I))  GOTO 300
                IF(IWCA(J).NE.IW(IST,I)) GOTO 300
                IF(IPCA(J).NE.IAND(IP(IST,I),1)) GOTO 300
                IASS=0
                ENGY(IST,I)=DG(J)
                IC(IST,I)=1
                DO 200 M=1,24
                  DERIV(IST,I,IWCA(J)*24+M)=EDER(J,M)
 200            CONTINUE
                GOTO 400
 300          CONTINUE
              IF(IASS.EQ.1) THEN
                IC(IST,I)=1
                WRITE(3,*)'Incorrect assignment line #',I
                IASS=0
              ENDIF
 400        CONTINUE
 500      CONTINUE
          IF(ICALC.EQ.0) GOTO 700
          ICALC=0
 600    CONTINUE
 700    RETURN
        END
C
C-----------------------------------------------------------------------
C
```

```
      SUBROUTINE E(IWR,NR,XR,IPR,EIVEC,IDER)
C+
C This subroutine calculates the rotational, centrifugal distortion,
C   and spin-rotational energy of a planar triatomic such as HCO.
C   The working matrices have been dimensioned for N<=40.
C
C Arguments:
C
C       IWR     0 for lower state, 1 for upper.
C       NR      N rotational number.
C       XR      0.5 or -0.5 where J=NR+XR.
C       IPR     Parity of KC.
C       EIVEC   Matrix of eigenvectors stored columnwise (NM X NM).
C       IDER    1 to calculate derivatives as well as energies.
C-
      IMPLICIT DOUBLE PRECISION (A-H,O-Z)
      DIMENSION IDER(2)
C
      COMMON/CON/CONST(2,25),ORIGIN
      COMMON/DATA/IP(2,1200),N(2,1200),K(2,1200),X(2,1200),IW(2,1200),
&     OBS(1200)
      COMMON/PRED/ENGY(2,1200),IC(2,1200)
      COMMON/DER/DERIV(2,1200,50),DIFF(1200)
      COMMON/MAT/NM,IPCA(100),NCA(100),KCA(100),XCA(100),IWCA(100),
&     DG(100),EDER(100,24)
C
      DIMENSION H(82,82),PA2(82,82),POD(82,82),
&     POD2(82,82),PASA(82,82)
      DIMENSION PDOTS(82,82),PSOD(82,82),PSAB(82,82),P2(82,82)
      DIMENSION UNIT(82,82),EIVEC(82,82),WRK2(82,82),WRK3(82,82)
      DIMENSION DGN(82),OFDGN(82)
C
C First calculate the size of the matrices to be constructed.
C
      NL=NR
      IF(XR.LT.0) NL=NR-1
      IDIM=2*(NL+1)                    !Total dimensionality of matrix.
C
C We need to find the dimensionality of smaller N matrix (IDS).
C
      IDS=NL+1                         !NL+2,NL if NL+IP even.
      IF(MOD(NL+IPR,2).EQ.1) IDS=NL    !But if NL+IP odd, NL,NL+2.
      IDB=IDIM-IDS
C
C Now call a subroutine to construct the Hamiltonian matrix.
C

      CALL EWORK(IWR,IPR,NL,IDIM,IDS,IDB,KS,KB,H,DGN,OFDGN,PA2,POD,
&     POD2,PASA,PDOTS,PSOD,PSAB,P2,UNIT,EIVEC,WRK2,WRK3)

C Calculate derivatives with respect to each parameter.
C
      IF(IDER(IWR+1).NE.0) CALL HFDER(IDIM,PA2,POD,POD2,PASA,
&     PDOTS,PSOD,PSAB,P2,UNIT,EIVEC,WRK2,WRK3)
C
C Label the calculated energy levels returned in DG.
```

```
C
        NM=IDIM
        DO 100 I=1,IDIM
          IPCA(I)=IPR
          IWCA(I)=IWR
          IF(IWR.EQ.1) DG(I)=DG(I)+ORIGIN
          IF(I.LE.IDS) THEN
            NCA(I)=NL
            KCA(I)=KS+I-1
            XCA(I)=0.5
          ELSE
            NCA(I)=NL+1
            KCA(I)=KB+I-IDS-1
            XCA(I)=-0.5
          ENDIF
 100    CONTINUE
C
        RETURN
        END
C
C-----------------------------------------------------------------------
C

        SUBROUTINE EWORK(IWR,IPR,NL,IDIM,IDS,IDB,KS,KB,H,DGN,OFDGN,
&     PA2,POD,POD2,PASA,PDOTS,PSOD,PSAB,P2,UNIT,WRK1,WRK2,WRK3)
C+
C A subroutine to construct and diagonalize a Watson A-reduction
asymmetric
C   rotor Hamiltonian for a doublet molecule.  The transformation matrix
C   (eigenvectors stored columnwise) is returned in WRK1.
C
C Arguments:
C
C       IWR     0 for lower state, 1 for upper.
C       IPR     Parity of KC.
C       NL      N Rotational quantum number of first (X=0.5) submatrix.
C       IDIM    Total dimensionality of Hamiltonian = IDS + IDB.
C       IDS     Dimension of X=0.5 (small N) submatrix.
C       IDB     Dimension of X=-0.5 (big N) submatrix.
C       KS      Starting KC quantum number of small N submatrix.
C       KB      Starting KC quantum number of big N submatrix.
C       H       Hamiltonian matrix.
C-
        IMPLICIT DOUBLE PRECISION (A-H,O-Z)
C
        COMMON/CON/CONST(2,25),ORIGIN
        COMMON/DATA/IP(2,1200),N(2,1200),K(2,1200),X(2,1200),IW(2,1200),
&     OBS(1200)
        COMMON/PRED/ENGY(2,1200),IC(2,1200)
        COMMON/DER/DERIV(2,1200,50),DIFF(1200)
        COMMON/MAT/NM,IPCA(100),NCA(100),KCA(100),XCA(100),IWCA(100),
&     DG(100),EDER(100,24)
C
        DIMENSION H(IDIM,IDIM),PA2(IDIM,IDIM),POD(IDIM,IDIM)
        DIMENSION PASA(IDIM,IDIM),PDOTS(IDIM,IDIM),PSOD(IDIM,IDIM)
        DIMENSION PSAB(IDIM,IDIM),P2(IDIM,IDIM),UNIT(IDIM,IDIM)
        DIMENSION WRK1(IDIM,IDIM),WRK2(IDIM,IDIM),WRK3(IDIM,IDIM)
```

```
      DIMENSION DGN(IDIM),OFDGN(IDIM),POD2(IDIM,IDIM)
C
C Calculate J quantum number.
C
      JQ=2*NL+1
C
C Then calculate which K values each matrix starts with, K=1 extra
signs,
C and the sign of the contribution to K=1.
C
      IF(MOD(IPR+NL,2).EQ.1) THEN
              KS=1
              KB=0
              ISS=1
              ISB=-1
      ELSE
              KS=0
              KB=1
              ISS=-1
              ISB=1
      ENDIF
C
C Set up the coefficient matrices.
C
      CALL SP2(P2,IDIM,IDS,IDB,NL)
D     WRITE(3,*) 'P2'
D     WRITE(3,*)((P2(J,I),I=1,IDIM),J=1,IDIM)
      CALL SPA2(PA2,IDIM,IDS,IDB,NL,KS,KB)
D     WRITE(3,*) 'PA2'
D     WRITE(3,*)((PA2(J,I),I=1,IDIM),J=1,IDIM)
      CALL SPOD(POD,IDIM,IDS,IDB,NL,KS,KB,ISS,ISB)
D     WRITE(3,*) 'POD'
D     WRITE(3,*)((POD(J,I),I=1,IDIM),J=1,IDIM)
     CALL SPOD2(POD2,IDIM,IDS,IDB,NL,KS,KB,ISS,ISB)
C
C Finished with whats needed for rotation and CD, on to SR.
C
      CALL SPDOTS(PDOTS,IDIM,IDS,IDB,NL)
D     WRITE(3,*) 'PDOTS'
D     WRITE(3,*)((PDOTS(J,I),I=1,IDIM),J=1,IDIM)
      CALL SPASA(PASA,IDIM,IDS,IDB,NL,KS,KB,JQ)
D     WRITE(3,*) 'PASA'
D     WRITE(3,*)((PASA(J,I),I=1,IDIM),J=1,IDIM)
      CALL SPSOD(PSOD,IDIM,IDS,IDB,NL,KS,KB,ISS,ISB,JQ)
D     WRITE(3,*) 'PSOD'
D     WRITE(3,*)((PSOD(J,I),I=1,IDIM),J=1,IDIM)
      CALL SPSAB(PSAB,IDIM,IDS,IDB,NL,KS,KB,JQ)
D     WRITE(3,*) 'PSAB'
D     WRITE(3,*)((PSAB(J,I),I=1,IDIM),J=1,IDIM)
C
C Set up the molecular constants.
C
      ALPHA=CONST(IWR+1,1)
      BETA =CONST(IWR+1,2)
      GAMMA=CONST(IWR+1,3)
      DK   =CONST(IWR+1,4)
      DJK  =CONST(IWR+1,5)
```

```
      DJ   =CONST(IWR+1,6)
      SD1  =CONST(IWR+1,7)
      SD2  =CONST(IWR+1,8)
      HK   =CONST(IWR+1,9)
      HKJ  =CONST(IWR+1,10)
      HJK  =CONST(IWR+1,11)
      HJ   =CONST(IWR+1,12)
      XLK  =CONST(IWR+1,13)
      ALPS =CONST(IWR+1,15)
      BETS =CONST(IWR+1,16)
      EBC  =CONST(IWR+1,17)
      EAB  =CONST(IWR+1,18)
      DKS  =CONST(IWR+1,19)
      DJKS =CONST(IWR+1,20)
      DJS  =CONST(IWR+1,21)
      DKJS =CONST(IWR+1,22)
      SDJS =CONST(IWR+1,23)
      HKS  =CONST(IWR+1,24)
C
      E2ABC=2*ALPS
      EABC=ALPS+3.D0*BETS
C
      DO 1 I=1,IDIM
      DO 1 J=1,IDIM
1     H(I,J)=0.D0
C
C Construct hamiltonian, diagonal rotational part.
C
      CALL IDENT(UNIT,IDIM)
C
      CALL GMSCAL(-1.D0*XLK,PA2,WRK1,IDIM,IDIM)
      CALL GMSCAL(HK,UNIT,WRK2,IDIM,IDIM)
      CALL GMSUM(WRK1,WRK2,IDIM,IDIM)
      CALL GMPRD(WRK1,PA2,WRK2,IDIM,IDIM,IDIM)
      CALL GMSCAL(-1.D0*DK,UNIT,WRK1,IDIM,IDIM)
      CALL GMSUM(WRK1,WRK2,IDIM,IDIM)
      CALL GMSCAL(HKJ,P2,WRK2,IDIM,IDIM)
      CALL GMSUM(WRK1,WRK2,IDIM,IDIM)
      CALL GMPRD(WRK1,PA2,WRK2,IDIM,IDIM,IDIM)
      CALL GMSCAL(ALPHA,UNIT,WRK1,IDIM,IDIM)
      CALL GMSUM(WRK1,WRK2,IDIM,IDIM)
      CALL GMSCAL(-1.D0*DJK,P2,WRK2,IDIM,IDIM)
      CALL GMSUM(WRK1,WRK2,IDIM,IDIM)
      CALL GMPRD(P2,P2,WRK2,IDIM,IDIM,IDIM)
      CALL GMSCAL(HJK,WRK2,WRK2,IDIM,IDIM)
      CALL GMSUM(WRK1,WRK2,IDIM,IDIM)
      CALL GMPRD(WRK1,PA2,H,IDIM,IDIM,IDIM)
D     WRITE(3,*)'Sum of K terms;',H
C
      CALL GMSCAL(HJ,P2,WRK1,IDIM,IDIM)
      CALL GMSCAL(-1.D0*DJ,UNIT,WRK2,IDIM,IDIM)
      CALL GMSUM(WRK1,WRK2,IDIM,IDIM)
      CALL GMPRD(WRK1,P2,WRK2,IDIM,IDIM,IDIM)
      CALL GMSCAL(BETA,UNIT,WRK1,IDIM,IDIM)
      CALL GMSUM(WRK1,WRK2,IDIM,IDIM)
      CALL GMPRD(WRK1,P2,WRK2,IDIM,IDIM,IDIM)
D     WRITE(3,*)'Sum of J-only terms;',WRK1
```

```
        CALL GMSUM(H,WRK2,IDIM,IDIM)
C
C Off-diagonal rotational part.
C
      CALL GMSCAL(SD2,POD2,WRK1,IDIM,IDIM)
      CALL GMSUM(H,WRK1,IDIM,IDIM)
C
        CALL GMSCAL(GAMMA,UNIT,WRK1,IDIM,IDIM)
        CALL GMSCAL(SD1,P2,WRK2,IDIM,IDIM)
        CALL GMSUM(WRK1,WRK2,IDIM,IDIM)
        CALL GMPRD(WRK1,POD,WRK2,IDIM,IDIM,IDIM)
D       WRITE(3,*)'GAMMA and SDJ;',WRK2
        CALL GMSUM(H,WRK2,IDIM,IDIM)
C
C Spin-rotational part:  compute diagonal K-only terms.
C
        CALL GMSCAL(DKS,UNIT,WRK1,IDIM,IDIM)            !1xDKS.
        CALL GMSCAL(HKS,PA2,WRK2,IDIM,IDIM)             !HKSxPA2.
        CALL GMSUM(WRK1,WRK2,IDIM,IDIM)                 !Add them.
        CALL GMPRD(WRK1,PA2,WRK3,IDIM,IDIM,IDIM)        !xPA2.
D       WRITE(3,*)'K-only spin terms;',WRK3
C
C But still have the SDKS term which multiplies NASA not the spherical
C tensor part.  We need to find matrix representing NASA.
C
        CALL GMSCAL(-1/DSQRT(3.D0),PDOTS,WRK1,IDIM,IDIM)
        CALL GMSCAL(2/DSQRT(6.D0),PASA,WRK2,IDIM,IDIM)
        CALL GMSUM(WRK1,WRK2,IDIM,IDIM)                 !WRK1 now
contains
D       WRITE(3,*)'PASA coefficient;',WRK1              ! real PASA.

      CALL GMPRD(WRK1,P2,WRK2,IDIM,IDIM,IDIM)
      CALL GMSCAL(0.5D0*DJKS,WRK2,WRK2,IDIM,IDIM)
      CALL GMSUM(H,WRK2,IDIM,IDIM)
      CALL GMPRD(P2,WRK1,WRK2,IDIM,IDIM,IDIM)
      CALL GMSCAL(0.5D0*DJKS,WRK2,WRK2,IDIM,IDIM)
      CALL GMSUM(H,WRK2,IDIM,IDIM)
C
C Now put together the coefficient of PDOTS (P.S).
C
        CALL GMSCAL(-DSQRT(3.D0)*SDJS,POD,WRK1,IDIM,IDIM)
!SDJSxPOD.
        CALL GMSCAL(-DSQRT(3.D0)*DJS,P2,WRK2,IDIM,IDIM)         !DJSxP2.
        CALL GMSUM(WRK1,WRK2,IDIM,IDIM)                         !Add.
        CALL GMSCAL(-DSQRT(3.D0)*DKJS,PA2,WRK2,IDIM,IDIM)
!DKJSxPA2.
        CALL GMSUM(WRK1,WRK2,IDIM,IDIM)                         !Add.
        CALL GMSCAL(EABC,UNIT,WRK2,IDIM,IDIM)           !Compute T0 term
        CALL GMSUM(WRK2,WRK3,IDIM,IDIM)
        CALL GMSCAL(-1.D0/DSQRT(3.D0),WRK2,WRK2,IDIM,IDIM)
        CALL GMSUM(WRK1,WRK2,IDIM,IDIM)                 !WRK1 has (P.S)
coeff.
        CALL GMPRD(WRK1,PDOTS,WRK2,IDIM,IDIM,IDIM)      !xPDOTS.
        CALL GMSUM(H,WRK2,IDIM,IDIM)                    !Add to H.
D       WRITE(3,*)'P.S term;',WRK2
C
C Now the remaining terms.
```

```
C
        CALL GMSCAL(E2ABC,UNIT,WRK1,IDIM,IDIM)
        CALL GMSCAL(2.D0,WRK3,WRK2,IDIM,IDIM)
        CALL GMSUM(WRK1,WRK2,IDIM,IDIM)
        CALL GMSCAL(1.D0/DSQRT(6.D0),WRK1,WRK2,IDIM,IDIM)
        CALL GMPRD(WRK2,PASA,WRK1,IDIM,IDIM,IDIM)        !T20xPASA.
        CALL GMSUM(H,WRK1,IDIM,IDIM)                     !Add to H.
D       WRITE(3,*)'T20 x PASA;',WRK2
C
        CALL GMSCAL(EBC,PSOD,WRK2,IDIM,IDIM)             !T22xPSOD.
        CALL GMSUM(H,WRK2,IDIM,IDIM)                     !Add to H.
D       WRITE(3,*)'T22 x PSOD;',WRK2
C
        CALL GMSCAL(-EAB,PSAB,WRK2,IDIM,IDIM)            !T21xPSAB.
        CALL GMSUM(H,WRK2,IDIM,IDIM)                     !Add to H.
D       WRITE(3,*)'T21 x PSAB;',WRK2
D       WRITE(3,*)'H before diag;',H
C
C Diagonalize Hamiltonian matrix.
C
        CALL DIAG(H,WRK1,DGN,OFDGN,IDIM)
C
        RETURN
        END
C
C-----------------------------------------------------------------------


        SUBROUTINE SP2(P2,IDIM,IDS,IDB,NL)
C+
C A subroutine to calculate the N(N+1) matrix.
C-
        IMPLICIT DOUBLE PRECISION (A-H,O-Z)
        DIMENSION P2(IDIM,IDIM)
C
        DO 10 I=1,IDIM
        DO 10 J=1,IDIM
 10     P2(I,J)=0.D0
C
        IF(IDS.LE.0) GOTO 30    !Skip if zero.
        DO 20 I=1,IDS
 20     P2(I,I)=NL*1.D0*(NL+1)
C
 30     DO 40 I=1,IDB
 40     P2(I+IDS,I+IDS)=(NL+1)*1.D0*(NL+2)
C
        RETURN
        END
C
C-----------------------------------------------------------------------
C

        SUBROUTINE SPA2(PA2,IDIM,IDS,IDB,NL,KS,KB)
C+
C A subroutine to calculate the PA**2 matrix.
C-
        IMPLICIT DOUBLE PRECISION (A-H,O-Z)
```

```
      DIMENSION PA2(IDIM,IDIM)
C
      DO 10 I=1,IDIM
      DO 10 J=1,IDIM
 10   PA2(I,J)=0.D0
C
      IF(IDS.LE.0) GOTO 30     !Skip if zero.
      DO 20 I=1,IDS
      KW=KS+I-1                !K value as you move down matrix.
 20   PA2(I,I)=KW*1.0D0*KW
C
 30   DO 40 I=1,IDB
      KW=KB+I-1
 40   PA2(I+IDS,I+IDS)=KW*1.0D0*KW
C
      RETURN
      END
C
C-----------------------------------------------------------------------
C

      SUBROUTINE SPASA(PASA,IDIM,IDS,IDB,NL,KS,KB,JQ)
C+
C A subroutine to calculate PASA type SR terms.
C-
      IMPLICIT DOUBLE PRECISION (A-H,O-Z)
      DIMENSION PASA(IDIM,IDIM)
C
      DO 10 I=1,IDIM
      DO 10 J=1,IDIM
 10   PASA(I,J)=0.D0
C
      IF(IDS.LE.0) GOTO 30            !Skip if zero.
      DO 20 I=1,IDS
      KW=KS+I-1
      PASA(I,I)=SR(JQ,NL,KW,NL,KW)
      IF(KW.EQ.0) GOTO 20
      IOD=IDS+KW-KB+1
      WK=SR(JQ,NL+1,KW,NL,KW)
      PASA(I,IOD)=WK
      PASA(IOD,I)=WK
 20   CONTINUE
C
 30   DO 40 I=1,IDB
      KW=KB+I-1
 40   PASA(I+IDS,I+IDS)=SR(JQ,NL+1,KW,NL+1,KW)
C
      RETURN
      END
C
C-----------------------------------------------------------------------
C

      SUBROUTINE SPDOTS(PDOTS,IDIM,IDS,IDB,NL)
C
C A subroutine to calculate the P.S matrix.
C   (diagonal in N and almost same as P2)
```

```
C
        IMPLICIT DOUBLE PRECISION (A-H,O-Z)
        DIMENSION PDOTS(IDIM,IDIM)
C
        DO 10 I=1,IDIM
        DO 10 J=1,IDIM
 10     PDOTS(I,J)=0.D0
C
        IF(IDS.LE.0) GOTO 30            !Skip if zero.
        DO 20 I=1,IDS
 20     PDOTS(I,I)=-0.5D0*NL/DSQRT(3.D0)
C
 30     DO 40 I=1,IDB
 40     PDOTS(I+IDS,I+IDS)=0.5D0*(NL+2)/DSQRT(3.D0)
C
        RETURN
        END

C
C-----------------------------------------------------------------------
C

        SUBROUTINE SPOD2(POD2,IDIM,IDS,IDB,NL,KS,KB,ISS,ISB)
C+
C A subroutine to calculate the off-diagonal part of the rigid rotor.
C-
        IMPLICIT DOUBLE PRECISION (A-H,O-Z)
        DIMENSION POD2(IDIM,IDIM)
C
        C(N,K)=DSQRT(N*1.D0*(N+1)-K*1.D0*(K+1))
C
        DO 10 I=1,IDIM
        DO 10 J=1,IDIM
 10     POD2(I,J)=0.D0
C
        IF(IDS.LE.0) GOTO 30            !Skip if zero.
        DO 20 I=1,IDS
        KW=KS+I-1
        IF(KW.EQ.2) POD2(I,I)=-ISS*NL*1.D0*(NL+1)*(NL*1.D0*(NL+1)-2.D0)
        IF(KW+4.LE.NL) THEN
          WK=C(NL,KW)*C(NL,KW+1)*C(NL,KW+2)*C(NL,KW+3)
          IF(KW.EQ.0) THEN
            POD2(I,I+4)=WK*DSQRT(2.D0)    !K=0 to K=4 special.
            POD2(I+4,I)=WK*DSQRT(2.D0)
          ELSE
            POD2(I,I+4)=WK
            POD2(I+4,I)=WK
          ENDIF
        ENDIF
      IF (KW.EQ.1.AND.KW+2.LE.NL) THEN
       POD2(I,I+2)=ISS*C(NL,-1)*C(NL,0)*C(NL,1)*C(NL,2)
       POD2(I+2,I)=POD2(I,I+2)
      ENDIF
 20     CONTINUE
C
 30     DO 40 I=1,IDB
        KW=KB+I-1
```

```
        IF(KW.EQ.2) POD2(I+IDS,I+IDS)=-ISB*(NL+1)*1.D0*
&      (NL+2)*((NL+1)*1.D0*(NL+2)-2.D0)
        IF(KW+4.LE.NL+1) THEN
          WK=C(NL+1,KW)*C(NL+1,KW+1)*C(NL+1,KW+2)*C(NL+1,KW+3)
          IF(KW.EQ.0) THEN
            POD2(I+IDS,I+IDS+4)=WK*DSQRT(2.D0)
            POD2(I+IDS+4,I+IDS)=WK*DSQRT(2.D0)
          ELSE
            POD2(I+IDS,I+IDS+4)=WK
            POD2(I+IDS+4,I+IDS)=WK
          ENDIF
        ENDIF
      IF (KW.EQ.1.AND.KW+2.LE.NL+1) THEN
        POD2(I,I+2)=ISB*C(NL+1,-1)*C(NL+1,0)*C(NL+1,1)*C(NL+1,2)
        POD2(I+2,I)=POD2(I,I+2)
      ENDIF
 40     CONTINUE
C
        RETURN
        END
C
C-----------------------------------------------------------------------
C

        SUBROUTINE SPOD(POD,IDIM,IDS,IDB,NL,KS,KB,ISS,ISB)
C+
C A subroutine to calculate the off-diagonal part of the rigid rotor.
C-
        IMPLICIT DOUBLE PRECISION (A-H,O-Z)
        DIMENSION POD(IDIM,IDIM)
C
        C(N,K)=DSQRT(N*1.D0*(N+1)-K*1.D0*(K+1))
C
        DO 10 I=1,IDIM
        DO 10 J=1,IDIM
 10     POD(I,J)=0.D0
C
        IF(IDS.LE.0) GOTO 30            !Skip if zero.
        DO 20 I=1,IDS
        KW=KS+I-1
        IF(KW.EQ.1) POD(I,I)=ISS*NL*1.D0*(NL+1)
        IF(KW+2.LE.NL) THEN
          WK=C(NL,KW)*C(NL,KW+1)
          IF(KW.EQ.0) THEN
            POD(I,I+2)=WK*DSQRT(2.D0)   !K=0 to K=2 special.
            POD(I+2,I)=WK*DSQRT(2.D0)
          ELSE
            POD(I,I+2)=WK
            POD(I+2,I)=WK
          ENDIF
        ENDIF
 20     CONTINUE
C
 30     DO 40 I=1,IDB
        KW=KB+I-1
        IF(KW.EQ.1) POD(I+IDS,I+IDS)=ISB*(NL+1)*1.D0*(NL+2)
        IF(KW+2.LE.NL+1) THEN
```

```
          WK=C(NL+1,KW)*C(NL+1,KW+1)
          IF(KW.EQ.0) THEN
            POD(I+IDS,I+IDS+2)=WK*DSQRT(2.D0)
            POD(I+IDS+2,I+IDS)=WK*DSQRT(2.D0)
          ELSE
            POD(I+IDS,I+IDS+2)=WK
            POD(I+IDS+2,I+IDS)=WK
          ENDIF
        ENDIF
 40     CONTINUE
C
        RETURN
        END
C
C-----------------------------------------------------------------------
C

        SUBROUTINE SPSAB(PSAB,IDIM,IDS,IDB,NL,KS,KB,JQ)
C+
C This subroutine calculates the EAB type terms.
C-
        IMPLICIT DOUBLE PRECISION (A-H,O-Z)
        DIMENSION PSAB(IDIM,IDIM)
C
        DO 10 I=1,IDIM
        DO 10 J=1,IDIM
 10     PSAB(I,J)=0.D0
C
        IF(IDS.LE.0) GOTO 30            !Skip if zero.
        DO 20 I=1,IDS
        KW=KS+I-1
        IF(KW+1.LE.NL) THEN
          WK=SR(JQ,NL,KW+1,NL,KW)
          IF(KW.EQ.0) WK=WK*DSQRT(2.D0)
          PSAB(I,I+1)=WK
          PSAB(I+1,I)=WK
        ENDIF
        IOD=IDS+(KW-KB)+1
        WK=SR(JQ,NL+1,KW+1,NL,KW)
        IF(KW.EQ.0) WK=WK*DSQRT(2.D0)
        PSAB(I,IOD+1)=WK
        PSAB(IOD+1,I)=WK
        IF(KW-1.GE.KB) THEN
          WK=SR(JQ,NL+1,KW-1,NL,KW)
          IF(KW-1.EQ.0) WK=WK*DSQRT(2.D0)
          PSAB(I,IOD-1)=WK
          PSAB(IOD-1,I)=WK
        ENDIF
 20     CONTINUE
C
 30     DO 40 I=1,IDB
        KW=KB+I-1
        IF(KW+1.LE.NL+1) THEN
          WK=SR(JQ,NL+1,KW+1,NL+1,KW)
          IF(KW.EQ.0) WK=WK*DSQRT(2.D0)
          PSAB(I+IDS,I+1+IDS)=WK
          PSAB(I+1+IDS,I+IDS)=WK
```

```
      ENDIF
 40   CONTINUE
C
      RETURN
      END
C
C-----------------------------------------------------------------------
C

      SUBROUTINE SPSOD(PSOD,IDIM,IDS,IDB,NL,KS,KB,ISS,ISB,JQ)
C+
C This subroutine calculates the P+S+ type terms.
C-
      IMPLICIT DOUBLE PRECISION (A-H,O-Z)
      DIMENSION PSOD(IDIM,IDIM)
C
      DO 10 I=1,IDIM
      DO 10 J=1,IDIM
 10   PSOD(I,J)=0.D0
C
      IF(IDS.LE.0)GO TO 30     !Skip if zero.
      DO 20 I=1,IDS            !Send through once even if IDS-2<1.
      KW=KS+I-1
      IF(KW.EQ.1) PSOD(I,I)=ISS*SR(JQ,NL,1,NL,-1)
      IF(KW+2.LE.NL) THEN
        WK=SR(JQ,NL,KW+2,NL,KW)
        IF(KW.EQ.0) THEN
          PSOD(I,I+2)=WK*DSQRT(2.D0)          !K=0 to K=2 special.
          PSOD(I+2,I)=WK*DSQRT(2.D0)
        ELSE
          PSOD(I,I+2)=WK
          PSOD(I+2,I)=WK
        ENDIF
      ENDIF
      IF(KW.EQ.1) PSOD(I,IDS-KB+2)=ISS*SR(JQ,NL+1,1,NL,-1)
      PSOD(IDS-KB+2,I)=PSOD(I,IDS-KB+2)
      IF(KW+2.LE.NL+1) THEN
        WK=SR(JQ,NL+1,KW+2,NL,KW)
        IF(KW.EQ.0) WK=WK*DSQRT(2.D0)
        IOD=IDS-KB+KW+1
        PSOD(I,IOD+2)=WK
        PSOD(IOD+2,I)=WK
      ENDIF
      IF(KW-2.GE.KB) THEN
        WK=SR(JQ,NL+1,KW-2,NL,KW)
        IF(KW-2.EQ.0) WK=WK*DSQRT(2.D0)
        IOD=IDS+1+KW-KB
        PSOD(I,IOD-2)=WK
        PSOD(IOD-2,I)=WK
      ENDIF
 20   CONTINUE
C
 30   DO 40 I=1,IDB
      KW=KB+I-1
      IF(KW.EQ.1) PSOD(I+IDS,I+IDS)=ISB*SR(JQ,NL+1,1,NL+1,-1)
      IF(KW+2.LE.NL+1) THEN
        WK=SR(JQ,NL+1,KW+2,NL+1,KW)
```

```
          IF(KW.EQ.0) THEN
            PSOD(I+IDS,I+2+IDS)=WK*DSQRT(2.D0)   !K=0 to K=2 special.
            PSOD(I+2+IDS,I+IDS)=WK*DSQRT(2.D0)
          ELSE
            PSOD(I+IDS,I+2+IDS)=WK
            PSOD(I+2+IDS,I+IDS)=WK
          ENDIF
        ENDIF
 40     CONTINUE
C
        RETURN
        END
C
C-----------------------------------------------------------------------
C

        DOUBLE PRECISION FUNCTION SR(JQ,NP,KP,N,K)
C+
C This function calculates the spin-rotation matrix element.
C-
        IMPLICIT DOUBLE PRECISION (A-H,O-Z)
C
        NPW=2*NP                  !JQ is already double integer.
        NW=2*N
        KPW=2*KP
        KW=2*K
        SR=0.D0
C
C Convert to real arguments.
C
        IS=(-1)**((NPW+1+JQ)/2)
C
C Send back zero if rules not followed.
C
        IF(IABS(NP-N)   .GT.1) GOTO 100
        IF(IABS(KP-K)   .GT.2) GOTO 100
        IF(IABS(JQ-NW)  .GT.2) GOTO 100
        IF(IABS(JQ-NPW).GT.2) GOTO 100
C
C Now calculate SR.
C
        IF((N+NP).GE.2) THEN
          SR=IS*SIXJ(.5D0*NPW,.5D0,.5D0*JQ,.5D0,.5D0*NW,1.D0)
&     *DSQRT(7.5D0)
          WK1=DSQRT(N*(N+1.D0)*(NW+1.D0))
&     *SIXJ(2.D0,.5D0*NW,.5D0*NPW,.5D0*NW,1.D0,1.D0)
          WK2=DSQRT(NP*(NP+1.D0)*(NPW+1.D0))
&     *SIXJ(2.D0,.5D0*NPW,.5D0*NW,.5D0*NPW,1.D0,1.D0)
          SR=SR*(WK1+WK2)*0.5D0
          SR=SR*DSQRT((NW+1.D0)*(NPW+1.D0))
          SR=SR*(-1)**(NP+KP)
        ELSE
          GOTO 100
        ENDIF
        SR=SR*THREJ(0.5D0*NPW,2.D0,0.5D0*NW,-0.5D0*KPW,0.5D0*(KPW-KW),
&     0.5D0*KW)
C
```

```
 100    RETURN
        END
C
C-----------------------------------------------------------------------
C

      DOUBLE PRECISION FUNCTION SIXJ(AA,BB,CC,DD,EE,FF)
C
C ROUTINE TO COMPUTE A SIX-J SYMBOL  A B C
C                                    D E F
C F IS THE ORDER
C D. J. MILTON 1980
      IMPLICIT REAL*8 (A-H,O-Z)
      DATA NOUT/6/
      A = AA
      B = BB
      C = CC
      D = DD
      E = EE
      F = FF
C CHECK TRIANGLE RULE
      Q = DMAX1(A,B,C)
      S = A+B+C-Q
      IF(Q .GT. S) GOTO 21
      Q = DMAX1(D,E,C)
      S = D+E+C-Q
      IF(Q .GT. S) GOTO 21
      Q = DMAX1(D,B,F)
      S = D+B+F-Q
      IF(Q .GT. S) GOTO 21
      Q = DMAX1(A,E,F)
      S = A+E+F-Q
      IF(Q .GT. S) GOTO 21
C
CDUMP IF RANK NOT IN POSITION F
      IF(F .EQ. 1.0D0 .OR. F .EQ. 2.0D0) GOTO 1
      WRITE(NOUT,100) AA,BB,CC,DD,EE,FF
      WRITE(NOUT,103)
      T = 0.0D0
      GOTO  25
C
    1 IDB = NINT(D-B)
C CHECK FOR INTEGER D-B
      IX = IABS(NINT(2.0D0*(D-B)))
      IF(MOD(IX,2) .EQ.1) GOTO 22
      IF(IDB .LE. 0) GOTO 2
C SWAP COLUMNS SO D-B IS NEGATIVE
      T = A
      A = E
      E = T
      T = B
      B = D
      D = T
    2 IAE = NINT(A-E)
      IA = IABS(IAE)
      IB = IABS(IDB)
C CHECK THAT IB IS NOT LESS THAN IA
```

```
      IF(IB .GE. IA) GOTO 5
      T = B
      B = E
      E = T
      T = A
      A = D
      D = T
      GOTO 1
C NOW PICK OUT STANDARD FORM TO BE USED
    5 L = 6*(F-1.)+3*IB+2*IAE+1
      IF(IB .GT. F) L = 3
      S = A+B+C
      PHASE = 1.0
      INDEX = S+0.0001
      IF(MOD(INDEX,2) .EQ. 1) PHASE=-1.0
      GOTO(6,7,8,9,8,10,11,12,13,14,15,16,17,8,18,8,19),L
    8 WRITE(NOUT,101) L
      IF(L .EQ. 3) WRITE(NOUT,104)
      WRITE(NOUT,100) AA,BB,CC,DD,EE,FF
      T = 0.0
      GOTO  25
    6 T=-PHASE*(A*(A+1.)+B*(B+1.)-C*(C+1.))/(2.*DSQRT(A*(A+1.)*
&     (2.*A+1.)*B*(B+1.)*(2.*B+1.)))
      GOTO  25
    7 T=PHASE*DSQRT(((S-2.*A-1.)*(S-2.*A)*(S-2.*B+1.)*(S-2.*B+2.))/
&     (2.*B*(2.*B+1.)*(2.*B-1.)*(2.*A+1.)*(2.*A+2.)*(2.*A+3.)))
      GOTO  25
    9 T=PHASE*DSQRT((S+1.)*(S-2.*C)*(S-2.*A)*(S-2.*B+1)/(
&     4.*A*(A+1.)*(2.*A+1.)*B*(2.*B+1.)*(2.*B-1)))
      GOTO  25
   10 T=PHASE*DSQRT(S*(S+1.)*(S-2.*C)*(S-2.*C-1.)/(4.*(2.*A-1.)*
&     A*(2.*A+1.)*(2.*B-1.)*B*(2.*B+1.)))
      GOTO  25
   11 X = A*(A+1.)+B*(B+1.)-C*(C+1.)
      T=PHASE*(3.*X*(X-1.)-4.*A*(A+1.)*B*(B+1.))/(DSQRT((2.*A-1.)
&     *A*(2.*A+1.)*(A+1.)*(2.*A+3.)*(2.*B-1.)*B*(2.*B+1.)
&     *(B+1.)*(2.*B+3.))*2)
      GOTO  25
   12 T=PHASE*0.5*((C+A+2.)*(C-A-1.)-(B-1.)*(A+B+2.))*
&     DSQRT(((S-2.*A-1.)*(S-2.*A)*(S-2.*B+1.)*(S-2.*B+2.))/(A*(A+1.)*
&(A+2.)*(2.*A+1.)*(2.*A+3.)*B*(B-1.)*(B+1.)*(2.*B-1.)*(2.*B+1.)))
      GOTO  25
   13 T=PHASE*DSQRT((S-2.*A-3.)*(S-2.*A-2.)*(S-2.*A-1.)*(S-2.*A)*
&     (S-2.*B+1.)*(S-2.*B+2.)*(S-2.*B+3.)*(S-2.*B+4.)/((2.*A+1.)*
&     (A+1.)*(2.*A+3.)*(A+2.)*(2.*A+5.)*(2.*B-3.)*(2.*B-1.)*(B-1.)
&     *B*(2.*B+1.)))*0.25D0
      GOTO  25
   14 T=PHASE*((C+A+1.)*(C-A)-B*B+1.)*0.5*DSQRT(3.*(S+1.)*(S-2.
&      *C)*(S-2.*A)*(S-2.*B+1.)/(A*(A+1.)*(2.*A+1.)*(2.*A+3.)*
&     (2.*A-1.)*B*(B+1.)*(B-1.)*(2.*B+1.)*(2.*B-1.)))
      GOTO  25
   15 T=PHASE*DSQRT((S+1.)*(S-2.*C)*(S-2.*A-2.)*(S-2.*A-1.)*
&     (S-2.*A)*(S-2.*B+1.)*(S-2.*B+2.)*(S-2.*B+3.)/(8.*A*(A+1.)*(A+2.)
&      *(2.*A+1.)*(2.*A+3.)*(2.*B-3.)*(2.*B-1.)*(2.*B+1.)*(B-1.)*B))
      GOTO  25
   16 T=PHASE*0.5*((C-A)*(C-A+1.)-(B-1.)*(B-A+1.))*DSQRT(S*(S+1.)*
&     (S-2.*C-1.)*(S-2.*C)/(A*(A+1.)*(A-1.)*(2.*A+1.)*
```

```
&     (2.*A-1.)*B*(B+1.)*(B-1.)*(2.*B+1.)*(2.*B-1.)))
      GOTO  25
   17 T=PHASE*DSQRT(.375D0*S*(S+1.)*(S-2.*C-1.)*(S-2.*A-1.)*
&     (S-2.*C)*(S-2.*A)*(S-2.*B+1.)*(S-2.*B+2.)/((2.*A-1.)*A*
&     (2.*A+1.)*(A+1.)*(2.*A+3.)*(2.*B-3.)*(2.*B-1.)*(2.*B+1.)*
&     (B-1.)*B))
      GOTO  25
   18 T=PHASE*DSQRT(.125D0*(S-1.)*S*(S+1.)*(S-2.*C-2.)*(S-2.*C-1.)
&     *(S-2.*C)*(S-2.*A)*(S-2.*B+1.)/((A-1.)*A*(A+1.)*(2.*A+1.)
&     *(2.*A-1.)*(2.*B-3.)*(B-1.)*(2.*B-1.)*B*(2.*B+1.)))
      GOTO  25
   19 T=PHASE*.25D0*DSQRT((S-2.)*(S-1.)*S*(S+1.)*(S-2.*C-3.)*
&     (S-2.*C-2.)*(S-2.*C-1.)*(S-2.*C)/((2.*A-3.)*(A-1.)*(2.*A-1.)
&     *A*(2.*A+1.)*(2.*B-3.)*(2.*B-1.)*(B-1.)*B*(2.*B+1.)))
      GOTO  25
   21 T = 0.0D0
      GOTO  25
   22 WRITE(NOUT,100) AA,BB,CC,DD,EE,FF
      WRITE(NOUT,105)
      T = 0.0D0
   25 SIXJ = T
      RETURN
  100 FORMAT(//1X,' SIXJ(',6F5.1,') HAS BEEN SET TO ZERO BECAUSE')
  101 FORMAT(1X,' DUMPED SINCE L=',I3,' IS NOT A STANDARD FORM')
  102 FORMAT(1X,' THE TRIANGLE RULE IS NOT SATISFIED')
  103 FORMAT(1X,' RANK (F) IS NOT 1 OR 2 CHANGE ORDER OF ARGUMENTS')
  104 FORMAT(1X,' NOTE THAT L=3 IS A SPECIAL CASE')
  105 FORMAT(1X,' D-B IS HALF INTEGRAL CHECK ARG. ORDER')
      END
C
C-----------------------------------------------------------------------
C

      DOUBLE PRECISION FUNCTION THREJ(BB,CC,AA,YY,ZZ,XX)
C
      IMPLICIT REAL*8 (A-H,O-Z)
C
C 3-J SYMBOL FROM EXPLICIT EXPRESSIONS IN EDMONDS
C D.J.MILTON WITH MINOR MODIFICATIONS
C
      DATA NOUT/6/
C
      A = AA
C C IS THE ORDER Z ITS COMPONENT
C
      B = BB
      C = CC
      X = XX
      Y = YY
      Z = ZZ
      IF(C .GT. 2.1) GOTO 18
      K = 2.0*C
      IF(MOD(K,2) .EQ. 1) GOTO 17
      MZERO = NINT(X+Y+Z)
      IF(MZERO .NE. 0) GOTO 1
      IF(A .LT. DABS(X) .OR. B .LT. DABS(Y) .OR. C .LT. DABS(Z)) GOTO1
      JDEL = A-B
```

```
      IDEL = IABS(JDEL)
      Q = DMAX1(A,B,C)
      S = A+B+C-Q
      IF(Q .GT. S) GOTO 1
      PHASE = 1.0
      SIGN = 1.0
      FAC = 1.0
      IF(IDEL .EQ. JDEL) GOTO 2
      D = A
      W = X
      A = B
      X = Y
      B = D
      Y = W
      INDEX = DABS(A+B+C)+.0001
      IF(MOD(INDEX,2) .EQ. 1) PHASE = -1.0
    2 IF(Z .GE. 0.0) GOTO 3
      X = -X
      Y = -Y
      Z = -Z
      INDEX = DABS(A+B+C)+0.0001
      IF(MOD(INDEX,2) .EQ. 1) SIGN = -1.0
    3 INDEX = DABS(A-X)+0.0001
      IF(MOD(INDEX,2) .EQ. 1) FAC = -1.0
      PHASE = PHASE*FAC*SIGN
      IF(K .EQ. 0) GOTO 21
      I = 5.0D0*Z+2.0D0*C+IDEL-1.0D0
      GOTO(4,5,6,7,8,9,10,11,12,13,1,1,14,15,16),I
    4 THREJ=PHASE*X/DSQRT(A*(A+1.)*(2.*A+1.))
      RETURN
    5 THREJ=PHASE*DSQRT((B+X+1.)*(B-X+1.)/((B+1.)*(2.*B+1.)
&     *(2.*B+3.)))
      RETURN
    6 THREJ=PHASE*(3.*X*X-A*(A+1.))/DSQRT(A*(A+1.)*(2.*A+1.)
&     *(2.*A-1.)*(2.*A+3.))
      RETURN
    7 THREJ=PHASE*X*DSQRT(3.*(B+X+1.)*(B-X+1.)/(B*(B+1.)*(B+2.)
&     *(2.*B+1.)*(2.*B+3.)))
      RETURN
    8 THREJ=PHASE*DSQRT(3.*(B+X+2.)*(B+X+1.)*(B-X+2.)*(B-X+1.)/
&     (2.*(B+1.)*(B+2.)*(2.*B+1.)*(2.*B+3.)*(2.*B+5.)))
      RETURN
    9 THREJ=PHASE*DSQRT((A-X)*(A+X+1.)/(2.*A*(A+1.)*(2.*A+1.)))
      RETURN
   10 THREJ=PHASE*DSQRT((B-X)*(B-X+1.)/(2.*(B+1.)*(2.*B+1.)*(2.*B+3.)))
      RETURN
   11 THREJ=PHASE*(1.+2.*X)*DSQRT(3.*(A-X)*(A+X+1.)/(A*(A+1.)*(2.*A+1.)
&     *(2.*A-1.)*(2.*A+3.)*2.))
      RETURN
   12 THREJ=PHASE*(B+X+X+2.)*DSQRT((B-X)*(B-X+1.)/(B*(B+1.)*(B+2.)
&     *2.*(2.*B+1.)*(2.*B+3.)))
      RETURN
   13 THREJ=PHASE*DSQRT((B-X)*(B-X+1.)*(B-X+2.)*(B+X+2.)/((B+1.)*
&     (B+2.)*(2.*B+1.)*(2.*B+3.)*(2.*B+5.)))
      RETURN
   14 THREJ=PHASE*DSQRT(3.*(A-X-1.)*(A-X)*(A+X+1.)*(A+X+2.)/(A*
&     (A+1.)*(2.*A+1.)*(2.*A+3.)*(2.*A-1.)*2))
```

```
      RETURN
   15 THREJ=PHASE*DSQRT((B-X)*(B-X-1.)*(B-X+1.)*(B+X+2.)/
&     (2.*B*(B+1.)*(B+2.)*(2.*B+1.)*(2.*B+3.)))
      RETURN
   16 THREJ=PHASE*DSQRT((B-X)*(B-X-1.)*(B-X+1.)*(B-X+2.)/((2.*B+1.)
&     *(2.*B+3.)*(2.*B+5.)*(B+1.)*(B+2.)*4.))
      RETURN
   17 WRITE(NOUT,20) BB,CC,AA,YY,ZZ,XX
   20 FORMAT(//1X,' THREEJ(',6F5.1,' HAS HALF INTEGER RANK')
      THREJ=0.0D0
      RETURN
   18 WRITE(NOUT,19) BB,CC,AA,YY,ZZ,XX,CC
   19 FORMAT(//1X,' THREEJ(',6F5.1,' ) HAS RANK',F4.1,
&     ' WHICH IS TOO HIGH FOR CURRENT PROGRAM')
      THREJ = 0.0D0
      RETURN
C SPECIAL CASE WHEN RANK IS ZERO
   21 THREJ=FAC/DSQRT(2.*A+1.D0)
      RETURN
    1 THREJ = 0.0D0
      RETURN
      END
C
C-----------------------------------------------------------------------
C

        SUBROUTINE DIAG(H,EIVEC,DGN,OFDGN,IDIM)
C+
C A subroutine to diagonalize the Hamiltonian matrix and return the
C   properly ordered energies in DG.
C
C Arguments:
C
C       H       Hamiltonian matrix.
C       EIVEC   Eigenvectors stored columnwise.
C       DGN     Diagonal of the tri-diagonalized and diagonalized
matrix.
C       OFDGN   Off-diagonal (by two) of the tri-diagonalized matrix.
C       IDIM    Dimension of matrix to be diagonalized.
C-
        IMPLICIT DOUBLE PRECISION (A-H,O-Z)
C
        COMMON/CON/CONST(2,25),ORIGIN
        COMMON/DATA/IP(2,1200),N(2,1200),K(2,1200),X(2,1200),IW(2,1200),
&     OBS(1200)
        COMMON/PRED/ENGY(2,1200),IC(2,1200)
        COMMON/DER/DERIV(2,1200,50),DIFF(1200)
        COMMON/MAT/NM,IPCA(100),NCA(100),KCA(100),XCA(100),IWCA(100),
&     DG(100),EDER(100,24)
C
        DIMENSION H(IDIM,IDIM),EIVEC(IDIM,IDIM),DGN(IDIM),OFDGN(IDIM)
C
C Diagonalize matrix.
C
        CALL TRED2(IDIM,IDIM,H,DGN,OFDGN,EIVEC)          !Eispack tri-
diag.
        CALL TQL2(IDIM,IDIM,DGN,OFDGN,EIVEC,IER)         !Eispack diag.
```

```
      IF(IER.NE.0) WRITE(6,*) 'Problem in diagonalization...'
C
C Determine new order of eigenvalues.
C
      DO 200 I=1,IDIM
        EMAX=0.D0
        DO 100 J=1,IDIM
          IF(DABS(EIVEC(J,I)).GT.EMAX) THEN
            EMAX=DABS(EIVEC(J,I))
            IPCA(I)=J
          ENDIF
 100    CONTINUE
 200  CONTINUE
C
C Put energies in original order into DG.
C
      DO 300 I=1,IDIM
 300    DG(IPCA(I))=DGN(I)
C
      RETURN
      END
C
C-----------------------------------------------------------------------
C

      SUBROUTINE TRED2(NM,N,A,D,E,Z)
C
      INTEGER I,J,K,L,N,II,NM,JP1
      DOUBLE PRECISION A(NM,N),D(N),E(N),Z(NM,N)
      DOUBLE PRECISION F,G,H,HH,SCALE
C
C     THIS SUBROUTINE IS A TRANSLATION OF THE ALGOL PROCEDURE TRED2,
C     NUM. MATH. 11, 181-195(1968) BY MARTIN, REINSCH, AND WILKINSON.
C     HANDBOOK FOR AUTO. COMP., VOL.II-LINEAR ALGEBRA, 212-226(1971).
C
C     THIS SUBROUTINE REDUCES A REAL SYMMETRIC MATRIX TO A
C     SYMMETRIC TRIDIAGONAL MATRIX USING AND ACCUMULATING
C     ORTHOGONAL SIMILARITY TRANSFORMATIONS.
C
C     ON INPUT
C
C        NM MUST BE SET TO THE ROW DIMENSION OF TWO-DIMENSIONAL
C          ARRAY PARAMETERS AS DECLARED IN THE CALLING PROGRAM
C          DIMENSION STATEMENT.
C
C        N IS THE ORDER OF THE MATRIX.
C
C        A CONTAINS THE REAL SYMMETRIC INPUT MATRIX.  ONLY THE
C          LOWER TRIANGLE OF THE MATRIX NEED BE SUPPLIED.
C
C     ON OUTPUT
C
C        D CONTAINS THE DIAGONAL ELEMENTS OF THE TRIDIAGONAL MATRIX.
C
C        E CONTAINS THE SUBDIAGONAL ELEMENTS OF THE TRIDIAGONAL
C          MATRIX IN ITS LAST N-1 POSITIONS.  E(1) IS SET TO ZERO.
C
```

```
C         Z CONTAINS THE ORTHOGONAL TRANSFORMATION MATRIX
C           PRODUCED IN THE REDUCTION.
C
C         A AND Z MAY COINCIDE.  IF DISTINCT, A IS UNALTERED.
C
C      QUESTIONS AND COMMENTS SHOULD BE DIRECTED TO BURTON S. GARBOW,
C      MATHEMATICS AND COMPUTER SCIENCE DIV, ARGONNE NATIONAL LABORATORY
C
C      THIS VERSION DATED AUGUST 1983.
C
C      ------------------------------------------------------------------
C
       DO 100 I = 1, N
C
          DO 80 J = I, N
   80     Z(J,I) = A(J,I)
C
          D(I) = A(N,I)
  100  CONTINUE
C
       IF (N .EQ. 1) GO TO 510
C      .......... FOR I=N STEP -1 UNTIL 2 DO -- ..........
       DO 300 II = 2, N
          I = N + 2 - II
          L = I - 1
          H = 0.0D0
          SCALE = 0.0D0
          IF (L .LT. 2) GO TO 130
C      .......... SCALE ROW (ALGOL TOL THEN NOT NEEDED) ..........
          DO 120 K = 1, L
  120     SCALE = SCALE + DABS(D(K))
C
          IF (SCALE .NE. 0.0D0) GO TO 140
  130     E(I) = D(L)
C
          DO 135 J = 1, L
             D(J) = Z(L,J)
             Z(I,J) = 0.0D0
             Z(J,I) = 0.0D0
  135     CONTINUE
C
          GO TO 290
C
  140     DO 150 K = 1, L
             D(K) = D(K) / SCALE
             H = H + D(K) * D(K)
  150     CONTINUE
C
          F = D(L)
          G = -DSIGN(DSQRT(H),F)
          E(I) = SCALE * G
          H = H - F * G
          D(L) = F - G
C      .......... FORM A*U ..........
          DO 170 J = 1, L
  170     E(J) = 0.0D0
```

```
C
         DO 240 J = 1, L
            F = D(J)
            Z(J,I) = F
            G = E(J) + Z(J,J) * F
            JP1 = J + 1
            IF (L .LT. JP1) GO TO 220
C
            DO 200 K = JP1, L
               G = G + Z(K,J) * D(K)
               E(K) = E(K) + Z(K,J) * F
  200       CONTINUE
C
  220       E(J) = G
  240    CONTINUE
C     ........... FORM P ..........
         F = 0.0D0
C
         DO 245 J = 1, L
            E(J) = E(J) / H
            F = F + E(J) * D(J)
  245    CONTINUE
C
         HH = F / (H + H)
C     ........... FORM Q ..........
         DO 250 J = 1, L
  250    E(J) = E(J) - HH * D(J)
C     ........... FORM REDUCED A ..........
         DO 280 J = 1, L
            F = D(J)
            G = E(J)
C
            DO 260 K = J, L
  260       Z(K,J) = Z(K,J) - F * E(K) - G * D(K)
C
            D(J) = Z(L,J)
            Z(I,J) = 0.0D0
  280    CONTINUE
C
  290    D(I) = H
  300 CONTINUE
C     ........... ACCUMULATION OF TRANSFORMATION MATRICES ..........
      DO 500 I = 2, N
         L = I - 1
         Z(N,L) = Z(L,L)
         Z(L,L) = 1.0D0
         H = D(I)
         IF (H .EQ. 0.0D0) GO TO 380
C
         DO 330 K = 1, L
  330    D(K) = Z(K,I) / H
C
         DO 360 J = 1, L
            G = 0.0D0
C
            DO 340 K = 1, L
  340       G = G + Z(K,I) * Z(K,J)
```

```
C
            DO 360 K = 1, L
               Z(K,J) = Z(K,J) - G * D(K)
  360     CONTINUE
C
  380     DO 400 K = 1, L
  400     Z(K,I) = 0.0D0
C
  500 CONTINUE
C
  510 DO 520 I = 1, N
         D(I) = Z(N,I)
         Z(N,I) = 0.0D0
  520 CONTINUE
C
      Z(N,N) = 1.0D0
      E(1) = 0.0D0
      RETURN
      END
C
C-----------------------------------------------------------------------
C

      SUBROUTINE TQL2(NM,N,D,E,Z,IERR)
C
      INTEGER I,J,K,L,M,N,II,L1,L2,NM,MML,IERR
      DOUBLE PRECISION D(N),E(N),Z(NM,N)
      DOUBLE PRECISION C,C2,C3,DL1,EL1,F,G,H,P,R,S,S2,TST1,TST2
C
C     THIS SUBROUTINE IS A TRANSLATION OF THE ALGOL PROCEDURE TQL2,
C     NUM. MATH. 11, 293-306(1968) BY BOWDLER, MARTIN, REINSCH, AND
C     WILKINSON.
C     HANDBOOK FOR AUTO. COMP., VOL.II-LINEAR ALGEBRA, 227-240(1971).
C
C     THIS SUBROUTINE FINDS THE EIGENVALUES AND EIGENVECTORS
C     OF A SYMMETRIC TRIDIAGONAL MATRIX BY THE QL METHOD.
C     THE EIGENVECTORS OF A FULL SYMMETRIC MATRIX CAN ALSO
C     BE FOUND IF  TRED2  HAS BEEN USED TO REDUCE THIS
C     FULL MATRIX TO TRIDIAGONAL FORM.
C
C     ON INPUT
C
C        NM MUST BE SET TO THE ROW DIMENSION OF TWO-DIMENSIONAL
C          ARRAY PARAMETERS AS DECLARED IN THE CALLING PROGRAM
C          DIMENSION STATEMENT.
C
C        N IS THE ORDER OF THE MATRIX.
C
C        D CONTAINS THE DIAGONAL ELEMENTS OF THE INPUT MATRIX.
C
C        E CONTAINS THE SUBDIAGONAL ELEMENTS OF THE INPUT MATRIX
C          IN ITS LAST N-1 POSITIONS.  E(1) IS ARBITRARY.
C
C        Z CONTAINS THE TRANSFORMATION MATRIX PRODUCED IN THE
C          REDUCTION BY  TRED2, IF PERFORMED.  IF THE EIGENVECTORS
C          OF THE TRIDIAGONAL MATRIX ARE DESIRED, Z MUST CONTAIN
C          THE IDENTITY MATRIX.
```

```
C
C      ON OUTPUT
C
C        D CONTAINS THE EIGENVALUES IN ASCENDING ORDER.  IF AN
C          ERROR EXIT IS MADE, THE EIGENVALUES ARE CORRECT BUT
C          UNORDERED FOR INDICES 1,2,...,IERR-1.
C
C        E HAS BEEN DESTROYED.
C
C        Z CONTAINS ORTHONORMAL EIGENVECTORS OF THE SYMMETRIC
C          TRIDIAGONAL (OR FULL) MATRIX.  IF AN ERROR EXIT IS MADE,
C          Z CONTAINS THE EIGENVECTORS ASSOCIATED WITH THE STORED
C          EIGENVALUES.
C
C        IERR IS SET TO
C          ZERO       FOR NORMAL RETURN,
C          J          IF THE J-TH EIGENVALUE HAS NOT BEEN
C                     DETERMINED AFTER 30 ITERATIONS.
C
C     CALLS PYTHAG FOR  DSQRT(A*A + B*B) .
C
C     QUESTIONS AND COMMENTS SHOULD BE DIRECTED TO BURTON S. GARBOW,
C     MATHEMATICS AND COMPUTER SCIENCE DIV, ARGONNE NATIONAL LABORATORY
C
C     THIS VERSION DATED AUGUST 1983.
C
C     ------------------------------------------------------------------
C
      IERR = 0
      IF (N .EQ. 1) GO TO 1001
C
      DO 100 I = 2, N
  100 E(I-1) = E(I)
C
      F = 0.0D0
      TST1 = 0.0D0
      E(N) = 0.0D0
C
      DO 240 L = 1, N
         J = 0
         H = DABS(D(L)) + DABS(E(L))
         IF (TST1 .LT. H) TST1 = H
C     .......... LOOK FOR SMALL SUB-DIAGONAL ELEMENT ..........
         DO 110 M = L, N
            TST2 = TST1 + DABS(E(M))
            IF (TST2 .EQ. TST1) GO TO 120
C     .......... E(N) IS ALWAYS ZERO, SO THERE IS NO EXIT
C                THROUGH THE BOTTOM OF THE LOOP ..........
  110    CONTINUE
C
  120    IF (M .EQ. L) GO TO 220
  130    IF (J .EQ. 30) GO TO 1000
         J = J + 1
C     .......... FORM SHIFT ..........
         L1 = L + 1
         L2 = L1 + 1
         G = D(L)
```

```
         P = (D(L1) - G) / (2.0D0 * E(L))
         R = DSQRT(P*P+1.0D0)
         D(L) = E(L) / (P + DSIGN(R,P))
         D(L1) = E(L) * (P + DSIGN(R,P))
         DL1 = D(L1)
         H = G - D(L)
         IF (L2 .GT. N) GO TO 145
C
         DO 140 I = L2, N
  140    D(I) = D(I) - H
C
  145    F = F + H
C     .......... QL TRANSFORMATION ..........
         P = D(M)
         C = 1.0D0
         C2 = C
         EL1 = E(L1)
         S = 0.0D0
         MML = M - L
C     .......... FOR I=M-1 STEP -1 UNTIL L DO -- ..........
         DO 200 II = 1, MML
            C3 = C2
            C2 = C
            S2 = S
            I = M - II
            G = C * E(I)
            H = C * P
            R = DSQRT(P*P+E(I)*E(I))
            E(I+1) = S * R
            S = E(I) / R
            C = P / R
            P = C * D(I) - S * G
            D(I+1) = H + S * (C * G + S * D(I))
C     .......... FORM VECTOR ..........
            DO 180 K = 1, N
               H = Z(K,I+1)
               Z(K,I+1) = S * Z(K,I) + C * H
               Z(K,I) = C * Z(K,I) - S * H
  180       CONTINUE
C
  200    CONTINUE
C
         P = -S * S2 * C3 * EL1 * E(L) / DL1
         E(L) = S * P
         D(L) = C * P
         TST2 = TST1 + DABS(E(L))
         IF (TST2 .GT. TST1) GO TO 130
  220    D(L) = D(L) + F
  240 CONTINUE
C     .......... ORDER EIGENVALUES AND EIGENVECTORS ..........
      DO 300 II = 2, N
         I = II - 1
         K = I
         P = D(I)
C
         DO 260 J = II, N
            IF (D(J) .GE. P) GO TO 260
```

```
            K = J
            P = D(J)
  260     CONTINUE
C
          IF (K .EQ. I) GO TO 300
          D(K) = D(I)
          D(I) = P
C
          DO 280 J = 1, N
            P = Z(J,I)
            Z(J,I) = Z(J,K)
            Z(J,K) = P
  280     CONTINUE
C
  300 CONTINUE
C
      GO TO 1001
C     ........... SET ERROR -- NO CONVERGENCE TO AN
C                 EIGENVALUE AFTER 30 ITERATIONS ..........
 1000 IERR = L
 1001 RETURN
      END
C
C-----------------------------------------------------------------------
C

        SUBROUTINE HFDER (IDIM,PA2,POD,POD2,PASA,PDOTS,PSOD,PSAB,
&     P2,UNIT,EIVEC,WRK1,WRK2)
C+
C A subroutine to calculate energy level derivatives with respect to
C   each molecular parameter using the Helmann-Feinmann theorem.
C-
        IMPLICIT DOUBLE PRECISION (A-H,O-Z)
C
        COMMON/CON/CONST(2,25),ORIGIN
        COMMON/DATA/IP(2,1200),N(2,1200),K(2,1200),X(2,1200),IW(2,1200),
&     OBS(1200)
        COMMON/PRED/ENGY(2,1200),IC(2,1200)
        COMMON/DER/DERIV(2,1200,50),DIFF(1200)
        COMMON/MAT/NM,IPCA(100),NCA(100),KCA(100),XCA(100),IWCA(100),
&     DG(100),EDER(100,24)
C
        DIMENSION PA2(IDIM,IDIM),POD(IDIM,IDIM),PASA(IDIM,IDIM)
        DIMENSION PDOTS(IDIM,IDIM),PSOD(IDIM,IDIM),PSAB(IDIM,IDIM)
        DIMENSION P2(IDIM,IDIM)
        DIMENSION WRK1(IDIM,IDIM),WRK2(IDIM,IDIM)
        DIMENSION UNIT(IDIM,IDIM),EIVEC(IDIM,IDIM)
C
C Transform the coefficient matrices.
C
        CALL XFORM(IDIM,PA2,EIVEC,WRK1,WRK2)
        CALL XFORM(IDIM,POD,EIVEC,WRK1,WRK2)
        CALL XFORM(IDIM,PASA,EIVEC,WRK1,WRK2)
        CALL XFORM(IDIM,PDOTS,EIVEC,WRK1,WRK2)
        CALL XFORM(IDIM,PSOD,EIVEC,WRK1,WRK2)
        CALL XFORM(IDIM,PSAB,EIVEC,WRK1,WRK2)
        CALL XFORM(IDIM,P2,EIVEC,WRK1,WRK2)
```

```
C
C First go through rotational parameters.
C
        CALL GETDER(IDIM,PA2,1,1.D0)                        !Alpha.
C
        CALL GMPRD(P2,PA2,WRK1,IDIM,IDIM,IDIM)
        CALL GETDER(IDIM,WRK1,5,-1.D0)                      !DJK.
C
        CALL GMPRD(P2,WRK1,WRK2,IDIM,IDIM,IDIM)
        CALL GETDER(IDIM,WRK2,11,1.D0)                      !HJK.
C
        CALL GMPRD(PA2,PA2,WRK1,IDIM,IDIM,IDIM)
        CALL GETDER(IDIM,WRK1,4,-1.D0)                      !DK.
C
        CALL GMPRD(P2,WRK1,WRK2,IDIM,IDIM,IDIM)
        CALL GETDER(IDIM,WRK2,10,1.D0)                      !HKJ.
C
        CALL GMPRD(PA2,WRK1,WRK2,IDIM,IDIM,IDIM)
        CALL GETDER(IDIM,WRK2,9,1.D0)                       !HK.
C
        CALL GMPRD(PA2,WRK2,WRK1,IDIM,IDIM,IDIM)
        CALL GETDER(IDIM,WRK1,13,-1.D0)                     !LK.
C
        CALL GETDER(IDIM,P2,2,1.D0)                         !Beta.
C
        CALL GMPRD(P2,P2,WRK1,IDIM,IDIM,IDIM)
        CALL GETDER(IDIM,WRK1,6,-1.D0)                      !DJ.
C
        CALL GMPRD(P2,WRK1,WRK2,IDIM,IDIM,IDIM)
        CALL GETDER(IDIM,WRK2,12,1.D0)                      !HJ.
C
C Off-diagonal rotational parameters.
C
        CALL GETDER(IDIM,POD2,8,1.D0)                       !d2.
C
        CALL GETDER(IDIM,POD,3,1.D0)                        !Gamma.
C
        CALL GMPRD(P2,POD,WRK1,IDIM,IDIM,IDIM)
        CALL GETDER(IDIM,WRK1,7,1.D0)                       !d1.
C
C Spin-rotation coupling parameters.
C
        CALL GMSCAL(2.D0/DSQRT(6.D0),PASA,WRK1,IDIM,IDIM)    !WRK1 NOW
CONTAINS REAL
        CALL GMSCAL(-1.D0/DSQRT(3.D0),PDOTS,WRK2,IDIM,IDIM) !PASA
        CALL GMSUM(WRK1,WRK2,IDIM,IDIM)          !HERE
      CALL GETDER(IDIM,WRK1,15,1.D0)                    !ALPS
        CALL GMPRD(WRK1,P2,WRK2,IDIM,IDIM,IDIM)
        CALL GMPRD(P2,WRK1,EIVEC,IDIM,IDIM,IDIM)            !use EIVEC for
        CALL GMSUM(WRK2,EIVEC,IDIM,IDIM)                    ! work array.
        CALL GETDER(IDIM,WRK2,20,.5D0)                      !DJKS.
C
        CALL GMPRD(PA2,WRK1,WRK2,IDIM,IDIM,IDIM)
        CALL GETDER(IDIM,WRK2,19,1.D0)                      !DKS.
C
        CALL GMPRD(PA2,WRK2,WRK1,IDIM,IDIM,IDIM)
        CALL GETDER(IDIM,WRK1,24,1.D0)                      !HKS.
```

```
C
        CALL GETDER(IDIM,PDOTS,16,-DSQRT(3.D0))     !BETS
C
        CALL GMPRD(POD,PDOTS,WRK1,IDIM,IDIM,IDIM)
        CALL GETDER(IDIM,WRK1,23,1.D0)                  !dJS.
C
        CALL GMPRD(P2,PDOTS,WRK1,IDIM,IDIM,IDIM)
        CALL GETDER(IDIM,WRK1,21,-DSQRT(3.D0))          !DJS.
C
        CALL GMPRD(PA2,PDOTS,WRK1,IDIM,IDIM,IDIM)
        CALL GETDER(IDIM,WRK1,22,-DSQRT(3.D0))          !DKJS.
C
        CALL GETDER(IDIM,PSOD,17,1.D0)                  !Ebc.
C
        CALL GETDER(IDIM,PSAB,18,-1.D0)                 !Eab.
C
        RETURN
        END
C
C-----------------------------------------------------------------------
C

        SUBROUTINE GETDER(IDIM,A,IPRM,SCALE)
C+
C Extracts the diagonal of matrix A and places it in the common block
C   variable EDER(I,IPRM),I=1,IDIM according to the order stored in
IPCA.
C
C Arguments:
C
C       IDIM    Dimension of matrix A.
C       IPRM    Parameter number.
C       SCALE   Scale factor for diagonal.
C-
        IMPLICIT DOUBLE PRECISION (A-H,O-Z)
C
        COMMON/CON/CONST(2,25),ORIGIN
        COMMON/DATA/IP(2,1200),N(2,1200),K(2,1200),X(2,1200),IW(2,1200),
&     OBS(1200)
        COMMON/PRED/ENGY(2,1200),IC(2,1200)
        COMMON/DER/DERIV(2,1200,50),DIFF(1200)
        COMMON/MAT/NM,IPCA(100),NCA(100),KCA(100),XCA(100),IWCA(100),
&     DG(100),EDER(100,24)
C
        DIMENSION A(IDIM,IDIM)
C
        DO 100 I=1,IDIM
          EDER(IPCA(I),IPRM)=A(I,I)*SCALE
 100    CONTINUE
C
        RETURN
        END
C
C-----------------------------------------------------------------------
C

C
```

```
C     ..................................................................
C
C        SUBROUTINE GMPRD
C
C        PURPOSE
C           MULTIPLY TWO GENERAL MATRICES TO FORM A RESULTANT GENERAL
C           MATRIX
C
C        USAGE
C           CALL GMPRD(A,B,R,N,M,L)
C
C        DESCRIPTION OF PARAMETERS
C           A - NAME OF FIRST INPUT MATRIX
C           B - NAME OF SECOND INPUT MATRIX
C           R - NAME OF OUTPUT MATRIX
C           N - NUMBER OF ROWS IN A
C           M - NUMBER OF COLUMNS IN A AND ROWS IN B
C           L - NUMBER OF COLUMNS IN B
C
C        REMARKS
C           ALL MATRICES MUST BE STORED AS GENERAL MATRICES
C           MATRIX R CANNOT BE IN THE SAME LOCATION AS MATRIX A
C           MATRIX R CANNOT BE IN THE SAME LOCATION AS MATRIX B
C           NUMBER OF COLUMNS OF MATRIX A MUST BE EQUAL TO NUMBER OF ROW
C           OF MATRIX B
C
C        SUBROUTINES AND FUNCTION SUBPROGRAMS REQUIRED
C           NONE
C
C        METHOD
C           THE M BY L MATRIX B IS PREMULTIPLIED BY THE N BY M MATRIX A
C           AND THE RESULT IS STORED IN THE N BY L MATRIX R.
C
C     ..................................................................
C
      SUBROUTINE GMPRD(A,B,R,N,M,L)
        REAL*8 A,B,R
      DIMENSION A(N*M),B(M*L),R(N*L)
C
      IR=0
      IK=-M
      DO 10 K=1,L
      IK=IK+M
      DO 10 J=1,N
      IR=IR+1
      JI=J-N
      IB=IK
      R(IR)=0
      DO 10 I=1,M
      JI=JI+N
      IB=IB+1
   10 R(IR)=R(IR)+A(JI)*B(IB)
      RETURN
      END
C
C-----------------------------------------------------------------------
C
```

```
C
C     ..................................................................
C
C        SUBROUTINE GMSUM
C
C        PURPOSE
C           ADD TWO GENERAL MATRICES TO FORM A RESULTANT GENERAL
C           MATRIX
C
C        USAGE
C           CALL GMSUM(A,B,N,M)
C
C        DESCRIPTION OF PARAMETERS
C           A - NAME OF FIRST INPUT MATRIX, SUM PLACED HERE
C           B - NAME OF SECOND INPUT MATRIX
C           N - NUMBER OF ROWS IN MATRICES
C           M - NUMBER OF COLUMNS
C
C        REMARKS
C           ALL MATRICES MUST BE STORED AS GENERAL MATRICES
C           ALL MATRICES MUST BE OF THE SAME DIMENSION
C
C        SUBROUTINES AND FUNCTION SUBPROGRAMS REQUIRED
C           NONE
C
C     ..................................................................
C
      SUBROUTINE GMSUM(A,B,N,M)
        REAL*8 A,B
      DIMENSION A(N,M),B(N,M)
C
        DO 200 I=1,N
                DO 100 J=1,M
                        A(I,J)=A(I,J)+B(I,J)
100             CONTINUE
200     CONTINUE
C
        RETURN
        END
C
C-----------------------------------------------------------------------
C

C
C     ..................................................................
C
C        SUBROUTINE GMSCAL
C
C        PURPOSE
C           MULTIPLY A GENERAL MATRIX BY A REAL SCALAR
C
C        USAGE
C           CALL GMSCAL(X,A,B,N,M)
C
C        DESCRIPTION OF PARAMETERS
C           X - SCALAR
```

```
C           A - NAME OF INPUT MATRIX
C           B - NAME OF OUTPUT MATRIX
C           N - NUMBER OF ROWS IN MATRICES
C           M - NUMBER OF COLUMNS
C
C         REMARKS
C           ALL MATRICES MUST BE STORED AS GENERAL MATRICES
C           ALL MATRICES MUST BE OF THE SAME DIMENSION
C
C         SUBROUTINES AND FUNCTION SUBPROGRAMS REQUIRED
C           NONE
C
C     ..................................................................
C
      SUBROUTINE GMSCAL(X,A,B,N,M)
        REAL*8 A,B,X
      DIMENSION A(N,M),B(N,M)
C
        DO 200 I=1,N
                DO 100 J=1,M
                        B(I,J)=X*A(I,J)
100             CONTINUE
200     CONTINUE
C
        RETURN
        END
C
C-----------------------------------------------------------------------
C

        SUBROUTINE IDENT(A,N)
C+
C Sets up the multiplicative identity in N by N matrix A.
C-
        REAL*8 A(N,N)
C
        DO 200 I=1,N
          DO 100 J=1,N
            IF(I.EQ.J)THEN
              A(I,J)=1.D0
            ELSE
              A(I,J)=0.D0
            ENDIF
 100      CONTINUE
 200    CONTINUE
C
        RETURN
        END
C
C-----------------------------------------------------------------------
C

        SUBROUTINE XPOSE(A,B,N)
C+
C Places the transpose of square NxN matrix A into matrix B.
C-
        IMPLICIT DOUBLE PRECISION (A-H,O-Z)
```

```
      DIMENSION A(N,N),B(N,N)
C
      DO 200 I=1,N
        DO 100 J=1,N
          B(I,J)=A(J,I)
 100    CONTINUE
 200  CONTINUE
C
      RETURN
      END
C
C-----------------------------------------------------------------------
C

      SUBROUTINE XFORM(N,A,T,WRK1,WRK2)
C+
C Transforms NxN square matrix A by the transformation matrix T
returning
C   the result in A.
C
C Arguments:
C
C       N       Dimension of matrices.
C       A       Matrix to be transformed.
C       T       Transformation matrix.
C       WRK     Work matrices.
C-
      IMPLICIT DOUBLE PRECISION (A-H,O-Z)
      DIMENSION A(N,N),T(N,N),WRK1(N,N),WRK2(N,N)
C
      CALL XPOSE(T,WRK1,N)
      CALL GMPRD(WRK1,A,WRK2,N,N,N)
      CALL GMPRD(WRK2,T,A,N,N,N)
C
      RETURN
      END
```

```
      PROGRAM FITDAT
C+
C Fitdat performs a least squares fit using the derivative and
splittings
C   matrices produced by ASYROT for an A-reduced asymmetric rotor.
C
C Required subroutines: NLSQ (and it's subroutines).
C-
      IMPLICIT DOUBLE PRECISION (A-H,O-Z)
      DOUBLE PRECISION A,SC
      DIMENSION IFIT(1200),COR(50)
      DIMENSION DER(1200,50),DIF(1200),WF(1200),VAV(1200)
      DIMENSION CONST(2,24),SC(50)
      DOUBLE PRECISION ORIGIN
C
C Read derivative matrix and observed-calculated from FOR004.DAT.
C
      READ(4,*) NL,NU
      READ(4,*) ((DER(J,L),L=1,50),J=1,NL)
      READ(4,*) (DIF(I),I=1,NL)
C
C Unbiased combination-differences fit?
C
      CALL DZERO(VAV,1200)
      IF(NU.NE.0) READ(4,*) (VAV(I),I=1,NL)
C
C Read parameters and parameter weights from FOR003.DAT.
C
      READ(3,*) ITMP,ORIGIN,SC(49)
      DO 40 I=1,24
 40     READ(3,*) ITMP,CONST(2,I),CONST(1,I),SC(I+24),SC(I)
C
C Read transition weights and fit flags from FOR003.DAT.
C
      DO 50 I=1,NL
 50     READ(3,*) IFIT(I),WF(I)
C
C Delete lines with IFIT=0.
C
      NFIT=0
      DO 200 I=1,NL
        IF (IFIT(I).NE.0) THEN
          NFIT=NFIT+1
          DIF(NFIT)=DIF(I)
          WF(NFIT)=WF(I)
          VAV(NFIT)=VAV(I)
          DO 100 J=1,50
            DER(NFIT,J)=DER(I,J)
 100      CONTINUE
        ENDIF
 200  CONTINUE
      NL=NFIT
C
C Perform least-squares fit.
C
      CALL NLSQ(NL,NU,DER,DIF,WF,SC,VAV,COR)
C
```

```
C Write new constant file to NEW.CON.
C
        OPEN(UNIT=4,NAME='NEW.CON',STATUS='NEW',FORM='FORMATTED')
        DO 300 J=1,2
          DO 250 I=1,24
            WRITE(4,*) (CONST(J,I)+COR(24*(J-1)+I))
 250      CONTINUE
 300    CONTINUE
        WRITE(4,*) (ORIGIN+COR(49))
        WRITE(4,*) (SC(I),I=1,49)
        CLOSE(UNIT=4)
C
        CALL EXIT
        END
C
C-----------------------------------------------------------------------
C

        SUBROUTINE NLSQ(NL,NU,DER,DIF,WF,SC,VAV,XV)
C+
C NLSQ performs a least-squares fit of a set of experimental data using
C   diagnostic least-squares.  The variables are dimensioned for fitting
C   on up to 50 parameters using up to 1200 experimental measurements.
C
C Arguments:
C
C       NL      Number of experimental measurements.
C       NU      If nonzero, indicates an unbiased combination-
differences
C                 fit and is equal to the number of distinct excited
state
C                 energy levels possessing combination-differences.
C       DER     A matrix of derivatives with respect to parameters.
C       DIF     A vector of observed-calculated splittings.
C       WF      Weight for each measurement.
C       SC      Scaling factor for each parameter.
C       VAV     Weighted average transition frequency for all
transitions
C                 sharing a common level (used only in unbiased
combination
C                 differences fits).
C       XV      Correction to each parameter returned by the fit.
C
C Required subroutines:  EIGEN,MSTR,GMTRA,GMPRD,ZERARR.
C-
        IMPLICIT DOUBLE PRECISION (A-H,O-Z)
C
        DIMENSION EIVAL(50),C2(50),BSPLT(50),XV(50),SV(1275)
        DIMENSION STDERR(50),DELTA(1200),EVET(50,50),EIVEC(50,50)
        DIMENSION H(50,50),C3(50,50),D2(50,50)
C
        DIMENSION DER(1200,50),DIF(1200),WF(1200),VAV(1200)
        DIMENSION V(50,50),XTY(50),SC(50)
C
C Open file for output.
C
        OPEN(UNIT=6,NAME='FIT.DAT',STATUS='UNKNOWN',FORM='FORMATTED')
```

```
C
C Weight fit for each line.
C
C       WRITE(5,*) ' Type 1 to weight lines.'
        READ(7,*) NY
        IF(NY.EQ.1) GOTO 20
        DO 10 I=1,NL
 10       WF(I)=1.0
 20     CONTINUE
C
        WTMAX=1.0
        DO 40 J=1,NL
          IF(WF(J).GT.WTMAX) WTMAX=WF(J)
          DIF(J)=DIF(J)*WF(J)
          DO 30 I=1,50
            DER(J,I)=DER(J,I)*WF(J)
 30       CONTINUE
 40     CONTINUE
C
C Parameter scaling.  C
        BIGST=1.0D4
        DO 50 I=1,NL
          DO 50 J=1,50
 50         IF(DER(I,J).GT.BIGST) BIGST=DER(I,J)
C       WRITE(5,*) ' Type 1 for scaling.'
        READ(7,*) NY
        IF(NY.EQ.1) GOTO 70
        DO 60 J=1,50
 60       SC(J)=1.0D4/BIGST
 70     DO 80 I=1,NL
          DO 80 J=1,50
 80         DER(I,J)=DER(I,J)*SC(J)
C
C Form DER transpose * DER, DER transpose * DIF.
C
        CALL DZERO(XTY,50)
        CALL DZERO(V,2500)
        DO 110 I=1,NL
          DO 100 J=1,50
            XTY(J)=DER(I,J)*DIF(I)+XTY(J)
            DO 90 K=1,50
              V(J,K)=DER(I,J)*DER(I,K)+V(J,K)
 90         CONTINUE
 100      CONTINUE
 110    CONTINUE
C
C Diagonalize V.
C
        CALL DZERO(SV,1275)
        CALL MSTR(V,SV,50,0,1)
        CALL EIGEN(SV,EIVEC,50,0)
        CALL MSTR(SV,EIVAL,50,1,2)
        WRITE(6,1000)
1000    FORMAT(' Eigenvalues: '/)
        WRITE(6,1500) EIVAL
C
C Write eigenvectors and eigenvector sums (90% test).
```

```
C
        DO 130 I=0,9
          WRITE(6,1100)5*I+1,5*I+5
1100      FORMAT(/' Eigenvectors (*10) ',I2,' - ',I2,' :'/)
          DO 120 J=1,50
            WRITE(6,1150) J,(10*EIVEC(J,I*5+K),K=1,5)
1150        FORMAT(I3,10X,5(F6.3,5X))
 120      CONTINUE
 130    CONTINUE
C
        WRITE(6,1200)
1200    FORMAT(/' Sum of squares > 0.9 :'/)
        DO 160 I=1,50
          SUM=0.0
          DO 140 J=1,50
            SUM=SUM+EIVEC(I,J)**2
            IF(SUM.GT.0.9) GOTO 150
 140      CONTINUE
 150      WRITE(6,1300)I,J
1300      FORMAT(' Parameter ',I2,' - ',I2)
 160    CONTINUE
C
C Choose number of eigenvalues for fit.
C
 170    CONTINUE
C       WRITE(5,*) ' Input the number of eigenvalues to fit on:'
        READ(7,*) NC
        IF(NC.EQ.0) GOTO 990
        WRITE(6,1400) NC
1400    FORMAT(/' Calculated constants fitting on ',I2,' eigenvalues:'/)
C
C Calculate corrections to constants.
C
        CALL DZERO(DELTA,1200)
        CALL DZERO(C2,50)
        CALL GMTRA(EIVEC,EVET,50,50)
        CALL GMPRD(EVET,XTY,BSPLT,50,50,1)
        DO 180 J=1,NC
          IF(EIVAL(J).EQ.0) GOTO 180
          C2(J)=BSPLT(J)/EIVAL(J)
 180    CONTINUE
        CALL GMPRD(EIVEC,C2,XV,50,50,1)
        CALL GMPRD(DER,XV,DELTA,1200,50,1)
        DO 190 I=1,50
 190      XV(I)=XV(I)*SC(I)
        WRITE(6,1500) XV
1500    FORMAT(5G15.4)
C
C Calculate obs-calc for new constants.
C
        SQ=0.
        SQ2=0.
        DO 200 J=1,NL
          DELTA(J)=DIF(J)-DELTA(J)-VAV(J)
          SQ2=DELTA(J)**2+SQ2
          DELTA(J)=DELTA(J)/WF(J)
          SQ=DELTA(J)**2+SQ
```

```
 200    CONTINUE
C
C Report standard deviation of fit.
C
        WRITE(6,1600) SQ
1600    FORMAT(/' Sum of squares: ',E8.2)
        IF(NL.LE.NC) THEN
          SIGMA2=SQ2
        ELSE
          SIGMA2=SQ2/(NL-NC-NU)
        ENDIF
        SIGMA=DSQRT(SIGMA2)
        WRITE(6,1700) SIGMA
1700    FORMAT(' Standard deviation (expected = 1): ',E8.2)
        SIGMA=DSQRT(SIGMA2)/WTMAX
        WRITE(6,1800) SIGMA
1800    FORMAT(' Standard deviation (largest wt.):  ',E8.2/)
        WRITE(6,1900)
1900    FORMAT(' Projected observed - calculated:'/)
        WRITE(6,1500) (DELTA(I),I=1,NL)
C
C Estimate uncertainties in constants.
C
        DO 210 I=1,50
          DO 210 J=1,50
            C3(I,J)=0.0
 210    CONTINUE
        DO 220 I=1,50
          IF(I.LE.NC) THEN
            C3(I,I)=SIGMA2/EIVAL(I)
          ELSE
            C3(I,I)=1.
          ENDIF
 220    CONTINUE
        CALL GMPRD(EIVEC,C3,D2,50,50,50)
        CALL GMPRD(D2,EVET,H,50,50,50)
        DO 230 I=1,50
 230      STDERR(I)=SQRT(ABS(H(I,I)))*SC(I)
        WRITE(6,2000)
2000    FORMAT(/' Standard errors:'/)
        WRITE(6,1500) STDERR
C
C Write covariance matrix to FOR008.DAT.
C
        DO 250 I=1,50
          DO 240 J=1,50
            H(I,J)=H(I,J)*SC(I)*SC(J)
 240      CONTINUE
 250    CONTINUE
        WRITE(8,*) 'Covariance matrix:'
        WRITE(8,1500) ((H(I,J),I=1,50),J=1,50)
        GOTO 170
C
 990    CLOSE(UNIT=6)
        RETURN
        END
C
```

```
C-----------------------------------------------------------------------
C
C
C     ..................................................................
C
C        SUBROUTINE EIGEN
C
C        PURPOSE
C           COMPUTE EIGENVALUES AND EIGENVECTORS OF A REAL SYMMETRIC
C           MATRIX
C
C        USAGE
C           CALL EIGEN(A,R,N,MV)
C
C        DESCRIPTION OF PARAMETERS
C           A - ORIGINAL MATRIX (SYMMETRIC), DESTROYED IN COMPUTATION.
C               RESULTANT EIGENVALUES ARE DEVELOPED IN DIAGONAL OF
C               MATRIX A IN DESCENDING ORDER.
C           R - RESULTANT MATRIX OF EIGENVECTORS (STORED COLUMNWISE,
C               IN SAME SEQUENCE AS EIGENVALUES)
C           N - ORDER OF MATRICES A AND R
C           MV- INPUT CODE
C                   0   COMPUTE EIGENVALUES AND EIGENVECTORS
C                   1   COMPUTE EIGENVALUES ONLY (R NEED NOT BE
C                       DIMENSIONED BUT MUST STILL APPEAR IN CALLING
C                       SEQUENCE)
C
C        REMARKS
C           ORIGINAL MATRIX A MUST BE REAL SYMMETRIC (STORAGE MODE=1)
C           MATRIX A CANNOT BE IN THE SAME LOCATION AS MATRIX R
C
C        SUBROUTINES AND FUNCTION SUBPROGRAMS REQUIRED
C           NONE
C
C        METHOD
C           DIAGONALIZATION METHOD ORIGINATED BY JACOBI AND ADAPTED
C           BY VON NEUMANN FOR LARGE COMPUTERS AS FOUND IN 'MATHEMATICAL
C           METHODS FOR DIGITAL COMPUTERS', EDITED BY A. RALSTON AND
C           H.S. WILF, JOHN WILEY AND SONS, NEW YORK, 1962, CHAPTER 7
C
C     ..................................................................
C
      SUBROUTINE EIGEN(A,R,N,MV)
      IMPLICIT DOUBLE PRECISION (A-H,O-Z)
      DIMENSION A(1:N*N),R(1:N*N)
C
C     ..................................................................
C
C        IF A DOUBLE PRECISION VERSION OF THIS ROUTINE IS DESIRED, THE
C        C IN COLUMN 1 SHOULD BE REMOVED FROM THE DOUBLE PRECISION
C        STATEMENT WHICH FOLLOWS.
C
      DOUBLE PRECISION A,R,ANORM,ANRMX,THR,X,Y,SINX,SINX2,COSX,
     1                 COSX2,SINCS,RANGE,DSQRT,DABS
C
C        THE C MUST ALSO BE REMOVED FROM DOUBLE PRECISION STATEMENTS
```

```
C         APPEARING IN OTHER ROUTINES USED IN CONJUNCTION WITH THIS
C         ROUTINE.
C
C         THE DOUBLE PRECISION VERSION OF THIS SUBROUTINE MUST ALSO
C         CONTAIN DOUBLE PRECISION FORTRAN FUNCTIONS.  SQRT IN STATEMENTS
C         40, 68, 75, AND 78 MUST BE CHANGED TO DSQRT.  ABS IN STATEMENT
C         62 MUST BE CHANGED TO DABS. THE CONSTANT IN STATEMENT 5 SHOULD
C         BE CHANGED TO 1.0D-12.
C
C         ..............................................................
C
C         GENERATE IDENTITY MATRIX
C
    5 RANGE=1.0D-12
      IF(MV-1) 10,25,10
   10 IQ=-N
      DO 20 J=1,N
      IQ=IQ+N
      DO 20 I=1,N
      IJ=IQ+I
      R(IJ)=0.0
      IF(I-J) 20,15,20
   15 R(IJ)=1.0
   20 CONTINUE
C
C         COMPUTE INITIAL AND FINAL NORMS (ANORM AND ANORMX)
C
   25 ANORM=0.0
      DO 35 I=1,N
      DO 35 J=I,N
      IF(I-J) 30,35,30
   30 IA=I+(J*J-J)/2
      ANORM=ANORM+A(IA)*A(IA)
   35 CONTINUE
      IF(ANORM) 165,165,40
   40 ANORM=1.414*DSQRT(ANORM)
      ANRMX=ANORM*RANGE/FLOAT(N)
C
C         INITIALIZE INDICATORS AND COMPUTE THRESHOLD, THR
C
      IND=0
      THR=ANORM
   45 THR=THR/FLOAT(N)
   50 L=1
   55 M=L+1
C
C         COMPUTE SIN AND COS
C
   60 MQ=(M*M-M)/2
      LQ=(L*L-L)/2
      LM=L+MQ
   62 IF( DABS(A(LM))-THR) 130,65,65
   65 IND=1
      LL=L+LQ
      MM=M+MQ
      X=0.5*(A(LL)-A(MM))
   68 Y=-A(LM)/ DSQRT(A(LM)*A(LM)+X*X)
```

```
      IF(X) 70,75,75
   70 Y=-Y
   75 SINX=Y/ DSQRT(2.0*(1.0+(DSQRT(1.0-Y*Y))))
      SINX2=SINX*SINX
   78 COSX= DSQRT(1.0-SINX2)
      COSX2=COSX*COSX
      SINCS =SINX*COSX
C
C        ROTATE L AND M COLUMNS
C
      ILQ=N*(L-1)
      IMQ=N*(M-1)
      DO 125 I=1,N
      IQ=(I*I-I)/2
      IF(I-L) 80,115,80
   80 IF(I-M) 85,115,90
   85 IM=I+MQ
      GO TO 95
   90 IM=M+IQ
   95 IF(I-L) 100,105,105
  100 IL=I+LQ
      GO TO 110
  105 IL=L+IQ
  110 X=A(IL)*COSX-A(IM)*SINX
      A(IM)=A(IL)*SINX+A(IM)*COSX
      A(IL)=X
  115 IF(MV-1) 120,125,120
  120 ILR=ILQ+I
      IMR=IMQ+I
      X=R(ILR)*COSX-R(IMR)*SINX
      R(IMR)=R(ILR)*SINX+R(IMR)*COSX
      R(ILR)=X
  125 CONTINUE
      X=2.0*A(LM)*SINCS
      Y=A(LL)*COSX2+A(MM)*SINX2-X
      X=A(LL)*SINX2+A(MM)*COSX2+X
      A(LM)=(A(LL)-A(MM))*SINCS+A(LM)*(COSX2-SINX2)
      A(LL)=Y
      A(MM)=X
C
C        TESTS FOR COMPLETION
C
C        TEST FOR M = LAST COLUMN
C
  130 IF(M-N) 135,140,135
  135 M=M+1
      GO TO 60
C
C        TEST FOR L = SECOND FROM LAST COLUMN
C
  140 IF(L-(N-1)) 145,150,145
  145 L=L+1
      GO TO 55
  150 IF(IND-1) 160,155,160
  155 IND=0
      GO TO 50
C
```

```
C        COMPARE THRESHOLD WITH FINAL NORM
C
  160 IF(THR-ANRMX) 165,165,45
C
C        SORT EIGENVALUES AND EIGENVECTORS
C
  165 IQ=-N
      DO 185 I=1,N
      IQ=IQ+N
      LL=I+(I*I-I)/2
      JQ=N*(I-2)
      DO 185 J=I,N
      JQ=JQ+N
      MM=J+(J*J-J)/2
      IF(A(LL)-A(MM)) 170,185,185
  170 X=A(LL)
      A(LL)=A(MM)
      A(MM)=X
      IF(MV-1) 175,185,175
  175 DO 180 K=1,N
      ILR=IQ+K
      IMR=JQ+K
      X=R(ILR)
      R(ILR)=R(IMR)
  180 R(IMR)=X
  185 CONTINUE
      RETURN
      END
C
C-----------------------------------------------------------------------
C

C
C     ..................................................................
C
C        SUBROUTINE MSTR
C
C        PURPOSE
C           CHANGE STORAGE MODE OF A VIRTUAL MATRIX
C
C        USAGE
C           CALL MSTR(A,R,N,MSA,MSR)
C
C        DESCRIPTION OF PARAMETERS
C           A - NAME OF INPUT MATRIX, VIRTUAL
C           R - NAME OF OUTPUT MATRIX
C           N - NUMBER OF ROWS AND COLUMNS IN A AND R
C           MSA - ONE DIGIT NUMBER FOR STORAGE MODE OF MATRIX A
C                 0 - GENERAL
C                 1 - SYMMETRIC
C                 2 - DIAGONAL
C           MSR - SAME AS MSA EXCEPT FOR MATRIX R
C
C        REMARKS
C           MATRIX R CANNOT BE IN THE SAME LOCATION AS MATRIX A
C           MATRIX A MUST BE A SQUARE MATRIX
C
```

```
C         SUBROUTINES AND FUNCTION SUBPROGRAMS REQUIRED
C            LOCE
C
C         METHOD
C            MATRIX A IS RESTRUCTURED TO FORM MATRIX R.
C             MSA MSR
C              0   0  MATRIX A IS MOVED TO MATRIX R
C              0   1  THE UPPER TRIANGLE ELEMENTS OF A GENERAL MATRIX
C                     ARE USED TO FORM A SYMMETRIC MATRIX
C              0   2  THE DIAGONAL ELEMENTS OF A GENERAL MATRIX ARE USED
C                     TO FORM A DIAGONAL MATRIX
C              1   0  A SYMMETRIC MATRIX IS EXPANDED TO FORM A GENERAL
C                     MATRIX
C              1   1  MATRIX A IS MOVED TO MATRIX R
C              1   2  THE DIAGONAL ELEMENTS OF A SYMMETRIC MATRIX ARE
C                     USED TO FORM A DIAGONAL MATRIX
C              2   0  A DIAGONAL MATRIX IS EXPANDED BY INSERTING MISSING
C                     ZERO ELEMENTS TO FORM A GENERAL MATRIX
C              2   1  A DIAGONAL MATRIX IS EXPANDED BY INSERTING MISSING
C                     ZERO ELEMENTS TO FORM A SYMMETRIC MATRIX
C              2   2  MATRIX A IS MOVED TO MATRIX R
C
C     ..............................................................
C
      SUBROUTINE MSTR(A,R,N,MSA,MSR)
        DOUBLE PRECISION A,R
      DIMENSION R(N*N),A(N*N)
C
      DO 20 I=1,N
      DO 20 J=1,N
C
C        IF R IS GENERAL, FORM ELEMENT
C
      IF(MSR) 5,10,5
C
C        IF IN LOWER TRIANGLE OF SYMMETRIC OR DIAGONAL R, BYPASS
C
    5 IF(I-J) 10,10,20
   10 CALL LOCE(I,J,IR,N,N,MSR)
C
C        IF IN UPPER AND OFF DIAGONAL  OF DIAGONAL R, BYPASS
C
      IF(IR) 20,20,15
C
C        OTHERWISE, FORM R(I,J)
C
   15 R(IR)=0.0
      CALL LOCE(I,J,IA,N,N,MSA)
C
C        IF THERE IS NO A(I,J), LEAVE R(I,J) AT 0.0
C
      IF(IA) 20,20,18
   18 R(IR)=A(IA)
   20 CONTINUE
      RETURN
      END
C
```

```
C-----------------------------------------------------------------------
C

C
C     ..................................................................
C
C        SUBROUTINE GMTRA
C
C        PURPOSE
C           TRANSPOSE A GENERAL MATRIX
C
C        USAGE
C           CALL GMTRA(A,R,N,M)
C
C        DESCRIPTION OF PARAMETERS
C           A - NAME OF MATRIX TO BE TRANSPOSED
C           R - NAME OF RESULTANT MATRIX
C           N - NUMBER OF ROWS OF A AND COLUMNS OF R
C           M - NUMBER OF COLUMNS OF A AND ROWS OF R
C
C        REMARKS
C           MATRIX R CANNOT BE IN THE SAME LOCATION AS MATRIX A
C           MATRICES A AND R MUST BE STORED AS GENERAL MATRICES
C
C        SUBROUTINES AND FUNCTION SUBPROGRAMS REQUIRED
C           NONE
C
C        METHOD
C           TRANSPOSE N BY M MATRIX A TO FORM M BY N MATRIX R
C
C     ..................................................................
C
      SUBROUTINE GMTRA(A,R,N,M)
        DOUBLE PRECISION A,R
      DIMENSION A(N*M),R(N*M)
C
      IR=0
      DO 10 I=1,N
      IJ=I-N
      DO 10 J=1,M
      IJ=IJ+N
      IR=IR+1
   10 R(IR)=A(IJ)
      RETURN
      END
C
C-----------------------------------------------------------------------
C

C
C     ..................................................................
C
C        SUBROUTINE GMPRD
C
C        PURPOSE
C           MULTIPLY TWO GENERAL MATRICES TO FORM A RESULTANT GENERAL
C           MATRIX
```

```
C
C        USAGE
C           CALL GMPRD(A,B,R,N,M,L)
C
C        DESCRIPTION OF PARAMETERS
C           A - NAME OF FIRST INPUT MATRIX
C           B - NAME OF SECOND INPUT MATRIX
C           R - NAME OF OUTPUT MATRIX
C           N - NUMBER OF ROWS IN A
C           M - NUMBER OF COLUMNS IN A AND ROWS IN B
C           L - NUMBER OF COLUMNS IN B
C
C        REMARKS
C           ALL MATRICES MUST BE STORED AS GENERAL MATRICES
C           MATRIX R CANNOT BE IN THE SAME LOCATION AS MATRIX A
C           MATRIX R CANNOT BE IN THE SAME LOCATION AS MATRIX B
C           NUMBER OF COLUMNS OF MATRIX A MUST BE EQUAL TO NUMBER OF ROW
C           OF MATRIX B
C
C        SUBROUTINES AND FUNCTION SUBPROGRAMS REQUIRED
C           NONE
C
C        METHOD
C           THE M BY L MATRIX B IS PREMULTIPLIED BY THE N BY M MATRIX A
C           AND THE RESULT IS STORED IN THE N BY L MATRIX R.
C
C     ..................................................................
C
      SUBROUTINE GMPRD(A,B,R,N,M,L)
        DOUBLE PRECISION A,B,R
      DIMENSION A(N*M),B(M*L),R(N*L)
C
      IR=0
      IK=-M
      DO 10 K=1,L
      IK=IK+M
      DO 10 J=1,N
      IR=IR+1
      JI=J-N
      IB=IK
      R(IR)=0.
      DO 10 I=1,M
      JI=JI+N
      IB=IB+1
   10 R(IR)=R(IR)+A(JI)*B(IB)
      RETURN
      END
C
C-----------------------------------------------------------------------
C

C
C     ..................................................................
C
C        SUBROUTINE LOCE
C
C        PURPOSE
```

```
C           COMPUTE A VECTOR SUBSCRIPT FOR AN ELEMENT IN A MATRIX OF
C           SPECIFIED STORAGE MODE
C
C        USAGE
C           CALL LOCE (I,J,IR,N,M,MS)
C
C        DESCRIPTION OF PARAMETERS
C           I   - ROW NUMBER OF ELEMENT
C           J   - COLUMN NUMBER  OF ELEMENT
C           IR  - RESULTANT VECTOR SUBSCRIPT
C           N   - NUMBER OF ROWS IN MATRIX
C           M   - NUMBER OF COLUMNS IN MATRIX
C           MS  - ONE DIGIT NUMBER FOR STORAGE MODE OF MATRIX
C                 0 - GENERAL
C                 1 - SYMMETRIC
C                 2 - DIAGONAL
C
C        REMARKS
C           NONE
C
C        SUBROUTINES AND FUNCTION SUBPROGRAMS REQUIRED
C           NONE
C
C        METHOD
C           MS=0   SUBSCRIPT IS COMPUTED FOR A MATRIX WITH N*M ELEMENTS
C                  IN STORAGE (GENERAL MATRIX)
C           MS=1   SUBSCRIPT IS COMPUTED FOR A MATRIX WITH N*(N+1)/2 IN
C                  STORAGE (UPPER TRIANGLE OF SYMMETRIC MATRIX). IF
C                  ELEMENT IS IN LOWER TRIANGULAR PORTION, SUBSCRIPT IS
C                  CORRESPONDING ELEMENT IN UPPER TRIANGLE.
C           MS=2   SUBSCRIPT IS COMPUTED FOR A MATRIX WITH N ELEMENTS
C                  IN STORAGE (DIAGONAL ELEMENTS OF DIAGONAL MATRIX).
C                  IF ELEMENT IS NOT ON DIAGONAL (AND THEREFORE NOT IN
C                  STORAGE), IR IS SET TO ZERO.
C
C     ..................................................................
C
      SUBROUTINE LOCE(I,J,IR,N,M,MS)
C
      IX=I
      JX=J
      IF(MS-1) 10,20,30
   10 IRX=N*(JX-1)+IX
      GO TO 36
   20 IF(IX-JX) 22,24,24
   22 IRX=IX+(JX*JX-JX)/2
      GO TO 36
   24 IRX=JX+(IX*IX-IX)/2
      GO TO 36
   30 IRX=0
      IF(IX-JX) 36,32,36
   32 IRX=IX
   36 IR=IRX
      RETURN
      END
C
C-----------------------------------------------------------------------
```

```
C
      SUBROUTINE IZERO(IMAT,N)
C
      INTEGER IMAT(N)
C
      DO 100 I=1,N
 100  IMAT(I)=0
C
      RETURN
      END
C
C-----------------------------------------------------------------------
C
      SUBROUTINE DZERO(XMAT,N)
C
      DOUBLE PRECISION XMAT(N)
C
      DO 200 I=1,N
 200  XMAT(I)=0.0
C
      RETURN
      END
```